ABSTRACT

A Multigrid Krylov Method for Eigenvalue Problems

Zhao Yang, Ph.D.

Advisors: Ronald B. Morgan, Ph.D.and Jonatan Lenells, Ph.D.

We are interested in computing eigenvalues and eigenvectors of matrices derived from differential equations. They are often large sparse matrices, including both symmetric and non-symmetric cases.

Restarted Arnoldi methods are iterative methods for eigenvalue problems based on Krylov subspaces. Multigrid methods solve differential equations by taking advantage of the hierarchy of discretizations. A multigrid Krylov method is proposed by combining Arnoldi and multigrid methods. We compare the new approach with other methods, and explore the theory to explain its efficiency.

A Multigrid Krylov Method for Eigenvalue Problems

by

Zhao Yang, B.S., M.S.

A Dissertation

Approved by the Department of Mathematics

_____

Lance L. Littlejohn, Ph.D., Chairperson

Submitted to the Graduate Faculty of
Baylor University in Partial Fulfillment of the
Requirements for the Degree
of
Doctor of Philosophy

Approved by the Dissertation Committee

_____

Ronald B. Morgan, Ph.D., Chairperson

_____

Robert Kirby, Ph.D.

_____

Mark R. Sepanski, Ph.D.

_____

Qin Sheng, Ph.D.

_____

Walter Wilcox, Ph.D.

Accepted by the Graduate School
August 2015

_____

J. Larry Lyon, Ph.D., Dean

Page bearing signatures is kept on file in the Graduate School.

TABLE OF CONTENTS

ACKNOWLEDGMENTS

I want to thank Baylor University for giving me the opportunity to study here. This enabled me to touch a world that I had known little about before. I have learned different things, and I also started to think outside the box. I know that it is just a beginning, since there is still a lot for me to see and to do.

I am grateful for doing research and teaching at Baylor. I would like to thank my advisor Dr. Ronald Morgan for guiding me all the way along. He gives me tons of advice on how to do research and teach, especially when I have difficulties and confusions. My brain has been sharpened through constant discussions with him, which will be most memorable for me. I would like to thank my advisor Dr. Jonatan Lenells for his profound encouragement and trust in me. I was greatly honored by the chance he offered me to work on his project after I took his class. I want to thank Dr. Qin Sheng and Dr. Lance Littlejohn for their huge support in my academic career. Dr. Sheng is always inspiring, and he impacts my professional life significantly. Special thanks to Dr. Littlejohn for his enduring effort to help international students to study and work better at Baylor. One of my favorite classes was taught by Dr. Robert Kirby, and I appreciate his professionalism in numerical analysis which broadened my perspective. I also want to thank the other members of my committee-Dr. Mark Sepanski, and Dr. Walter Wilcox of Baylor physics, for their kindness and time, as well as other professors in the math department.

Finally, I want to thank my family and friends. I received all the hope from my parents and my grandparents, and I thank their long-time effort and support. I thank my husband Li Guo for supporting me with his heart and actions. I am grateful for having my son Andy, who motivates me to be a good parent. I can not list all the names here, but I appreciate the love that all my colleagues and friends

have brought me so that I am able to have a comfortable and colorful life in the last six years.

After all, I am grateful to have become a better person at Baylor. The pride and love will be always in my heart.

To my parents

CHAPTER ONE

Introduction

We are interested in large eigenvalue problems $Ax = \lambda x$, where A is often a sparse matrice. Many of these problems are obtained by discretizing linear differential operators, which arise in a variety of areas of science and engineering. Eigenvalues and eigenvectors are very important in these applications, and they are also very helpful in the iterative solution of systems of linear equations. In this thesis, our goal is to find a few eigenvectors corresponding to the eigenvalues with smallest magnitudes for a large sparse matrix A. We use finite difference discretization. A can be either a symmetric or a non-symmetric sparse matrix.

There are two types of methods for eigenvalue problems, direct and iterative. For dense matrices, the most popular direct method is the QR iteration, which is the main idea used in the LAPACK software package [5] [6]. The QR iteration uses a series of orthogonal similarity transforms and converges to a Schur decomposition. For large sparse matrices, direct methods are too expensive, and in practice usually only a few of the eigenpairs are desired. Therefore iterative methods are more efficient. The Lanczos method [14] is a iterative method for symmetric matrices, and the Arnoldi method [2] is a general procedure for non-symmetric case. In both methods only a matrix-vector product is needed in each iteration to generate a Krylov subspace. These methods use the Rayleigh-Ritz procedure to extract eigenvalue information from the Krylov subspace.

Arnoldi and Lanczos methods have several difficulties. The Arnoldi method computes the orthogonal projection of A onto an m dimensional Krylov subspace after m steps. Sometimes m has to be large to get the desired eigenpairs, so the computational and storage requirements grow dramatically. Several restarted Arnoldi

methods have been developed to overcome such difficulties. Sorensen's Implicitly Restarted Arnoldi method (IRAM) is a big success, and it was implemented in the ARPACK package [16] [25]. It can be viewed as a truncation of the implicitly shifted QR iteration. Morgan proposed another restated Arnoldi with approximate eigenvectors (Arnoldi-E) method [18], where the Ritz eigenvectors are attached to a Krylov subspace. It is proved to be mathematically equivalent to IRAM, but it also has some other applications.

For a large sparse problem generated by a differential operator, another group of efficient algorithms are multigrid methods. Multigrid methods can tackle the original operator and exploit discretizations with different mesh sizes. The information from coarse grids, especially the smooth eigenvectors, can help the computation on the fine grid. In this thesis, we explore a multigrid Arnoldi method which combines restarted Arnoldi methods and multigrid methods.

The dissertation is organized as follows. Chapter Two introduces variant Arnoldi methods as well as Multigrid methods. A Multigrid Arnoldi method will be presented in Chapter Three, followed by some comparisons with other methods and details of implementation. We mainly discuss the Two-grid Arnoldi method in this thesis. We first run restarted Arnoldi method on the coarse grid, and then Arnoldi-E is applied on the fine grid with the approximations obtained from the coarse grid. Chapter Four studies the relations of eigenpairs on coarse and fine grids, in order to analyze the convergence for the symmetric case. Chapter Five gives theory for Arnoldi-E on the fine grid. Near Krylov decomposition is explored and analyzed. Chapter Six explores a more general Multiple-grid Arnoldi method. Lastly, Chapter Seven discusses future work.

CHAPTER TWO

Preliminaries

The Arnoldi method is a very well-known Krylov subspace method for non-symmetric eigenvalue problems. It is an iterative method based on projection methods, which transform a matrix into a smaller matrix with nicer structure. However, the expense and the storage increase as the method proceeds. Hence restarted Arnoldi methods were invented, including explicit and implicit restarted methods. In this thesis, we are interested in eigenvalue problems derived from differential operators. We aim to explore a new restarted Arnoldi method combined with multigrid techniques. Chapter Two is organized as follows: we start with general projection methods(2.1) and Krylov subspaces(2.2). The basic Arnoldi method is given(2.3), followed by explicitly restarted Arnoldi method(2.4) and implicitly restarted Arnoldi methods(2.5)(2.6). We discuss the ideas of Krylov decompositions and near Krylov decompositions(2.7)(2.8) for the analysis of our method later, as well as the Schur decomposition(2.9). Then we turn to differential operators and introduce finite difference discretizations(2.10). Lastly we look at the multigrid method(2.11).

2.1 Orthogonal Projection Methods

Arnoldi methods are orthogonal projection methods [29] for solving eigenvalue problems $Ax = \lambda x$. An orthogonal projection method finds an approximate solution in some subspace $\mathcal{K}$ by letting the residual be orthogonal to the same subspace $\mathcal{K}$.

For an eigenvalue problem, we seek an approximate eigenpair (θ, y) in $\mathcal{K}$, such that the so-called Galerkin condition is satisfied:

$$Ay - \theta y \perp \mathcal{K}.$$

Assume the columns of a matrix V are an orthonormal basis of $\mathcal{K}$, then y can be

written as $y = Vg$. The Galerkin condition becomes:

$$V^H(Ay - \theta y) = 0,$$
$$V^H(AVg - \theta Vg) = 0,$$
$$V^H AVg = \theta g.$$

So (θ, g) is an eigenpair of $B = V^H AV$. We have the following Rayleigh-Ritz procedure to implement the above orthogonal projection idea.

Algorithm 2.1 Rayleigh-Ritz procedure

1. Compute an orthonormal basis $\{q_i\}_{i=1,\cdots,m}$ of the m dimensional subspace $\mathcal{K}$. Let $Q = [q_1, q_2, \cdots, q_m]$.
2. Compute $B_m = Q^H AQ$.
3. Find the desired eigenvalues θ_i of B_m.
4. Compute the eigenvectors g_i of B_m associated with the θ_i's, and the corresponding approximate eigenvectors of A are $y_i = Qg_i$.

The θ_i's are called Ritz values, and $y_i = Qg_i$ are Ritz vectors. The residual of y_i is computed by $r_i = Ay_i - \theta y_i$. If the subspace $\mathcal{K}$ used in step 1 is a Krylov subspace, which will be introduced in the next section, Algorithm 2.1 becomes the Arnoldi method.

2.2 Krylov Subspaces

Given an $n \times n$ matrix A and a starting vector v, an m dimensional Krylov subspace is spanned by a sequence of vectors, which are obtained by repeatedly calculating matrix-vector multiplications:

$$\mathcal{K}_m(A, v) = Span\{v, Av, A^2v, \cdots, \mathcal{A}^{m-1}v\}.$$

All vectors in the subspace $\mathcal{K}_m(A, v)$ can be written as $y = p(A)v$, where p is a polynomial of degree $m - 1$ or less. If A has a full set of eigenvectors $z_1, z_2, \cdots, z_n$,

and v can always be expressed as $v = \sum_{i=1}^{n} \alpha_i z_i$, then

$$y = p(A)v = \sum_{i=1}^{n} \alpha_i p(A) z_i = \sum_{i=1}^{n} \alpha_i p(\lambda_i) z_i.$$

If we want y to be a good approximation to an eigenvector, say z_j, then p has to be large at λ_j and small at other eigenvalues. It is easy to find such p if λ_j is well separated from the rest of the spectrum. The Krylov subspace is best at approximating eigenvectors associated with eigenvalues on the periphery of the spectrum and not close to another.

If the desired eigenvalues are in the interior close to some value τ, then the shift-and-invert strategy [33] can be used. The corresponding Krylov subspace is:

$$\mathcal{K}_m((A-\tau I)^{-1}, v) = Span\{v, (A-\tau I)^{-1}v, (A-\tau I)^{-2}v, \cdots, (A-\tau I)^{-(m-1)}v\}.$$

If (λ, x) is an eigenpair of A, then $((\lambda-\tau)^{-1}, x)$ is an eigenpair of $(A-\tau I)^{-1}$. The eigenvalues of A that are closest to τ are the eigenvalues of $(A-\tau I)^{-1}$ that are of the greatest modulus, and hence $\mathcal{K}_m((A-\tau I)^{-1}, v)$ obtains good approximations to x. To implement the shift-and-invert Arnoldi method, we do not calculate $(A-\tau I)^{-1}v$ explicitly. Instead, we solve $(A-\tau I)u = v$ for u.

2.3 Arnoldi Decomposition and Parallel Property

The Arnoldi method was introduced by Arnoldi [2] in 1951. It builds an orthonormal basis of the Krylov subspace using modified Gram-Schmidt and reduces a dense matrix into a Hessenberg form. The following is the Arnoldi method with modified Gram-Schmidt algorithm [29].

Algorithm 2.2 Arnoldi with modified Gram-Schmidt algorithm

1. Start. Choose a vector v_1 of norm 1.

2. Iterate. For $j = 1, 2, \cdots, m$ do:

   (a) $w := Av_j$

(b) For $i = 1, 2, \cdots, j$ do:

$h_{i,j} = (w, v_i)$

$w := w - h_{i,j} v_i$

(c) $h_{j+1,j} = \|w\|_2$

(d) $v_{j+1} = w / h_{j+1,j}$

The algorithm stops if $\|w\|_2$ becomes zero, that means Av_j is a combination of $v_1, \cdots, v_j$. Otherwise, the vectors $v_1, v_2, \cdots, v_m$ are orthogonal to each other and of unit length by construction, and they form a basis for the Krylov subspace.

$$Span\{v_1, v_2, \cdots, v_m\} = Span\{v_1, Av_1, A^2 v_1, \cdots, \mathcal{A}^{m-1} v_1\} = \mathcal{K}_m(A, v_1). \qquad (2.1)$$

Equation (2.1) can be proved by induction. Suppose

$$Span\{v_1, v_2, \cdots, v_k\} = Span\{v_1, Av_1, A^2 v_1, \cdots, \mathcal{A}^{k-1} v_1\},$$
$$\text{and for every } j, Av_j = \sum_{i=1}^{j+1} h_{i,j} v_i.$$

Then

$$\begin{aligned} A^k v_1 &\in ASpan\{v_1, Av_1, A^2 v_1, \cdots, \mathcal{A}^{k-1} v_1\} = ASpan\{v_1, v_2, \cdots, v_k\} \\ &= Span\{Av_1, Av_2, \cdots, Av_k\} = Span\{\sum_{i=1}^{2} h_{i,1} v_i, \sum_{i=1}^{3} h_{i,2} v_i, \cdots, \sum_{i=1}^{k+1} h_{i,k} v_i\} \\ &= Span\{v_1, v_2, \cdots, v_k, v_{k+1}\}. \end{aligned}$$

So

$$Span\{v_1, Av_1, A^2 v_1, \cdots, A^{k-1} v_1, A^k v_1\} \subset Span\{v_1, v_2, \cdots, v_k, v_{k+1}\}.$$

The above two subspaces are of the same dimension, so they are the same subspace and (2.1) holds.

There is an Arnoldi decomposition based on Algorithm 2.2, which is an important relation in the study of Krylov methods. Let $V_m = [v_1, v_2, \cdots, v_m]$ and H_m

be the matrix whose entries $h_{i,j}$ are defined by the algorithm. From the algorithm, we have $h_{i,j} = 0$ for $i > j + 1$. H_m has zero entries below the first subdiagonal, and we call it an upper Hessenberg matrix. The following relations hold:

$$AV_m = V_m H_m + h_{m+1,m} v_{m+1} e_m^H, \tag{2.2}$$

$$V_m^H A V_m = H_m. \tag{2.3}$$

Equation (2.2) is the Arnoldi decomposition. The following implicit Q-theorem [25] indicates that the Arnoldi decomposition is determined by the first column of V. Therefore Arnoldi decompositions are essentially unique, and the Krylov subspace corresponding to an Arnoldi decomposition has a unique starting vector.

Theorem 2.1. *(Implicit Q-theorem) Suppose*

$$AV = VH + re_m^T,$$

$$AQ = QG + fe_m^T,$$

where Q, V have orthonormal columns and G, H are both upper Hessenberg with positive subdiagonal elements. If $Qe_1 = Ve_1$ and $Q^T f = V^T r = 0$, then $Q = V$, $G = H$, and $f = r$.

We can get the parallel property for residuals of Ritz vectors from the Arnoldi decomposition. Suppose (θ_i, g_i) are eigenpairs of H_m, then θ_i are Ritz values of A, and $y_i = V_m g_i$ are Ritz vectors. A well known formula for the residual of an Ritz vector by using (2.2) is:

$$\begin{aligned} r_i &:= Ay_i - \theta_i y_i = AV_m g_i - \theta_i V_m g_i \\ &= V_m H_m g_i + h_{m+1,m} v_{m+1} e_m^T g_i - \theta_i V_m g_i \\ &= V_m (H_m g_i - \theta_i g_i) + h_{m+1,m} v_{m+1} e_m^T g_i \\ &= (h_{m+1,m} e_m^T g_i) v_{m+1}. \end{aligned} \tag{2.4}$$

According to (2.4), we can calculate the norm of the residual by

$$\|r_i\| = |h_{m+1,m} e_m^T g_i|,$$

and residuals of all Ritz vectors are multiples of the last Arnoldi vector v_{m+1}.

2.4 Explicitly Restarted Arnoldi Methods

In Algorithm 2.2, the approximations of Ritz vectors will usually improve as m gets bigger, but the cost of computation and storage increase, as well as the cost of computing the eigenpairs of a Hessenberg matrix of order m. One way to avoid large m is to restart the algorithm.

For restarted Arnoldi methods [29], the dimension of the subspace m is chosen and fixed. After running basic Arnoldi iteration, residuals are computed to check the convergence. If the approximations are not accurate enough, a new starting vector is needed and another Arnoldi iteration proceeds until approximations converge.

Algorithm 2.3 Explicitly restarted Arnoldi method

1. Start. Choose a starting vector v_1 with norm 1 and a dimension m.
2. Iterate. Perform m steps of Arnoldi Iteration (Algorithm 2.2).
3. Find approximate eigenvalues and eigenvectors. If desired, compute Ritz values θ_i and Ritz vectors y_i. Compute the residual norms for desired eigenvectors, if satisfied stop, else go to 4.
4. Restart. Choose a new starting vector. Normalize for v_1 and go to 2.

A natural idea for the new starting vector is some linear combination of approximate eigenvectors obtained from the previous iteration. But it turns out that the combination has to be determined in a certain way, otherwise such an approach can be ineffective. The reasons were given by Morgan [18]. One efficient way to construct the new starting vector is to use polynomial filters: take the new starting vector to be $v_1^{new} = \psi(A)v_1$, where $\psi(A)$ is a polynomial determined from the knowledge of the approximate spectrum. ψ can be chosen in different ways, one option

has the form:

$$\psi(t) = (t - \theta_1)(t - \theta_2) \cdots (t - \theta_p), \tag{2.5}$$

where θ_i are so-called unwanted values among the computed Ritz values.

2.5 Implicitly Restarted Arnoldi Methods (IRAM)

It is sometimes difficult and expensive to calculate the starting vector in explicitly restarted Arnoldi method, hence there is a lot of research about the implicitly restarted Arnoldi approach. The implicitly restarted Arnoldi (IRAM) was proposed by Sorensen [25] [29], and is more stable than most explictly restarted approaches. This method exploits the QR algorithm within the Arnoldi iteration, but it is equivalent to applying a polynomial filter to the initial starting vector.

Algorithm2.4 The p-step shift QR

For $j = 1, \cdots, p$ do:

$(H - \mu_j I) = Q_j R_j$

$H := R_j Q_j + \mu_j I$

End For

Algorithm2.5 Implicitly Resarted Arnoldi method (IRAM)

1. Choose $m = k + p$. Perform Arnoldi iteration to get $AV_m = V_m H_m + h_{m+1,m} v_{m+1} e_m^T$.
2. Select the p shifts $\mu_1, \cdots, \mu_p$ from the eigenvalues of H_m.
3. Perform p-step shift QR: $[H_m^+, Q] := QR(H_m, \mu_1, \cdots, \mu_p)$
4. Compute $V_m^+ = V_m Q$. Let $V_k = V_m^+(:, 1:k)$ and $H_k = H_m^+(1:k, 1:k)$.
5. Compute $v = V_m^+(:, k+1) H_m^+(k+1, k) + h_{m+1,m} v_{m+1} Q(m, k)$. Let $h_{k+1,k} = \|v\|_2$, $v_{k+1} = v / h_{k+1,k}$. Now $AV_k = V_k H_k + h_{k+1,k} v_{k+1} e_k^T$, go to 1.

Q is the unitary matrix such that $H_m^+ = Q^H H_m Q$ in step 3. In step 4, The first column of V_m^+ is updated by $v_1^+ = \phi(A) v_1$ after the implicit p-step shift QR process, where $\phi(t) = (1/\tau)(t - \mu_1)(t - \mu_2) \cdots (t - \mu_p)$ with τ a normalization factor.

There are various choices for μ_i's, but one immediate option is to take $\mu_i = \theta_i$, where θ_i are unwanted Ritz values. We call θ_i's exact shifts with respect to H, and in this case $\phi(t)$ is the same as $\psi(t)$ in (2.5). So when exact shifts are chosen, the implicitly restarted Arnoldi is equivalent to restarting the Arnoldi with the updating $v_1^+ = \psi(A)v_1$, and v_1^+ is a combination of desired Ritz vectors.

2.6 Restarted Arnoldi Methods with Eigenvectors (Arn-E)

In Algorithm 2.5, we always have an Arnoldi decomposition $AV_k = V_k H_k + h_{k+1,k} v_{k+1} e_k^T$ of order k from the last cycle, then we expand the decomposition to order m. It means that in every cycle we implicitly restart Arnoldi with the subspace $Span\{v_1, v_2, \cdots, v_k, v_{k+1}\}$, and expand it to the m dimensional subspace $Span\{v_1, v_2, \cdots, v_k, v_{k+1}, Av_{k+1}, A^2 v_{k+1}, \cdots, A^{m-k-1} v_{k+1}\}$. If the exact shifts are used, i.e, shits in step 2 are unwanted eigenvalues of H_m. There are some nice theorems, which are proven by Sorensen, Lehoucq and Morgan [15] [18] [25].

Theorem 2.2. *Suppose there is an Arnoldi decomposition* $AV_m = V_m H_m + h_{m+1,m} v_{m+1} e_m^T$, *and Sorensen restarting is used with exact shifts. Let the desired Ritz vectors be* $y_1, y_2, \cdots, y_k$. *Then during the next Arnoldi run, the subspace of degree k is* $Span\{y_1, y_2, \cdots, y_k\} = Span\{v_1^+, v_2^+, \cdots, v_k^+\}$ *and* $v_{k+1}^+ = v_{m+1}$, *where* v_i^+*'s are Arnoldi vectors in the decomposition* $AV_k^+ = V_k^+ H_k + h_{k+1,k} v_{k+1}^+ e_k^T$ *for restarting.*

Theorem 2.3. *Let* $y_1, y_2, \cdots, y_k$ *be the desired Ritz vectors from an Arnoldi decomposition* $AV_m = V_m H_m + h_{m+1,m} v_{m+1} e_m^T$, *and* $Ay_i = \theta_i y_i + (h_{m+1,m} e_m^T g_i) v_{m+1}$ *as shown in (2.4). Then* $Span\{y_1, y_2, \cdots, y_k, v_{m+1}, Av_{m+1}, \cdots, A^{p-1} v_{m+1}\} = Span\{y_1, y_2, \cdots, y_k, Ay_i, A^2 y_i, \cdots, A^p y_i\}$.

Theorem 2.4. *Let* $m = k + p$. *The subspace generated during a run of the Sorensen method after restarting is* $Span\{y_1, y_2, \cdots, y_k, Ay_i, A^2 y_i, \cdots, A^p y_i\}$ *for any i such that* $1 \le i \le k$.

Theorem 2.4 is based on Theorem 2.2 and 2.3. Let v_{m+1} be the last Arnoldi vector from the previous cycle and v_i^+ be updated Arnoldi vectors for the next run. The updated subspace with exact shifts is:

$$
\begin{aligned}
& Span\{v_1^+, v_2^+, \cdots, v_m^+\} \\
=& Span\{v_1^+, v_2^+, \cdots, v_k^+, v_{k+1}^+, Av_{k+1}^+, \cdots, A^{p-1}v_{k+1}^+\} && (2.6) \\
=& Span\{y_1, y_2, \cdots, y_k, v_{k+1}^+, Av_{k+1}^+, \cdots, A^{p-1}v_{k+1}^+\} && \text{(use Thorem 2.2)} \\
=& Span\{y_1, y_2, \cdots, y_k, v_{m+1}, Av_{m+1}, \cdots, A^{p-1}v_{m+1}\} && \text{(use Thorem 2.2)} \\
=& Span\{y_1, y_2, \cdots, y_k, Ay_i, A^2y_i, \cdots, A^py_i\} && \text{(use Thorem 2.3)} \quad (2.7)
\end{aligned}
$$

According to Theorem 2.4, the following restarted Arnoldi with Ritz vectors, which generates subspace (2.7), is equivalent to IRAM, which generates the subspace (2.6). Both methods improve all approximations at the same time.

Algorithm 2.6 Restarted Arnoldi with Ritz vectors

1. Choose $m = k + p$ and the target τ. Perform Arnoldi iteration to get $AV_m = V_m H_m + h_{m+1,m} v_{m+1} e_m^T$.
2. Small eigenvalue problem. Compute eigenpairs (θ_i, g_i) of H_m nearest τ. If satisfied stop, otherwise let G be a real orthonormal matrix whose columns span $[g_1, \cdots, g_k]$.
3. Let $V_k = V_m G$, $H_k = G^H H_m G$ and $v_{k+1} = v_{m+1}$, such that $AV_k = V_k H_k + hv_{k+1}(e_m^T G)$. Go to 1.

If some good approximations are known beforehand, such information can be used at the beginning, and we have another way to restart Arnoldi with eigenvector approximations (Arn-E).

Algorithm 2.7 Restarted Arnoldi with eigenvector approximations (Arn-E)

1. Choose $m = k + p$. Let $y_1, y_2, \cdots, y_k$ be approximate eigenvectors, or the real and imaginary parts of approximate eigenvectors. Let $v_1 = y_1/\|y_1\|$.
2. Perform Arnoldi iteration. Get $AV_p = V_p H_p + h_{p+1,p} v_{p+1} e_p^T$ of order p.

3. Addition of other approximate eigenvectors. Orthogonalize $y_2, \cdots, y_k$ against previous v_i to get $v_{p+2}, \cdots, v_m$. Compute $H(:, p+1:m) = V^T A[v_{p+1}, v_{p+2}, \cdots, v_m]$ and $H(p+1:m, 1:p) = [v_{p+1}, v_{p+2}, \cdots, v_m]^T A V_p$.
4. Small eigenvalue problem. Compute eigenpairs (θ_i, g_i) of H_m nearest τ. If satisfied stop, otherwise go to 5.
5. Restart. Let y_1 through y_k be Ritz vectors, or the real and imaginary parts of Ritz vectors.

2.7 Krylov Decomposition

The Arnoldi decomposition (2.2) is

$$AV_m = V_m H_m + h_{m+1,m} v_{m+1} e_m^T.$$

Where H_m is upper Hessenberg and columns of V_m are orthonormal vectors. Stewart [26] introduced a less constraining decomposition named Krylov decomposition as the following:

Definition 2.5. A Krylov decomposition of order m is a relation of the form

$$AU_m = U_m B_m + u_{m+1} b_{m+1}^T,$$

where B_m is arbitrary and (U_m, u_{m+1}) has independent columns. The columns of (U_m, u_{m+1}) are called the basis for the decomposition, and they span the space of the decomposition. If the basis is orthonormal, we say the decomposition is orthonormal.

This definition removes restrictions imposed on an Arnoldi decomposition (2.2), but we have the following theorem.

Theorem 2.6. *[26] let $AU = UB + ub^T$ be a Krylov decomposition of order k. Then it is equivalent to an Arnoldi decomposition. If the Hessenberg part of the Arnoldi decomposition is unreduced, the Arnoldi decomposition is essentially unique.*

This theorem allows us to explore new methods and theory since the Krylov decomposition is much easier to maintain than the Arnoldi decomposition. Actually, the relation $AV_k = V_k H_k + hv_{k+1}(e_m^T G)$ in step 3 of Algorithm 2.6 (restart Arnoldi with Ritz vectors) is a Krylov decomposition, since H_k is not a strict upper Hessenberg.

2.8 Near Krylov Decomposition and Krylov Residual

In this section we discuss approximate Krylov subspaces, since sometimes bases for Krylov subspaces are inaccurate. There can be different approaches to assess the quality of an approximate Krylov subspace. We adopt Stewart's idea [27] to give the definition of a near Krylov decomposition.

Definition 2.7. Assume (U_m, u_{m+1}) has independent columns and (B_m, b_{m+1}) is arbitrary, then

$$AU_m = U_m B_m + u_{m+1} b_{m+1}^T + R. \tag{2.8}$$

is a near Krylov decomposition, and R is called the Krylov residual of the decomposition.

We assume $\|R\|$ is small in (2.8). If a near Krylov subspace $\mathcal{U}$ is given, there is a way to construct an orthogonal basis U for $\mathcal{U}$ so that the norm of the Krylov residual $\|R\|$ is minimal.

Theorem 2.8. *[27] Let A be of dimension n and let $W \in C^{n\times m}$ be orthonormal. Let $S = AW - W(W^H AW)$ and $\sigma_1 \geq \cdots \geq \sigma_m \geq 0$ be the singular values of S. Let $V = (V_{m-1}, v_m) \in C^{m\times m}$ be unitary with the columns V_{m-1} being the right singular vectors of S corresponding to $\sigma_2, \cdots, \sigma_m$. Set $U = WV = (U_{m-1}, u_m)$ and $R = SV_{m-1}$. Then the near Krylov decomposition $AU_{m-1} = U_{m-1}B_{m-1} + u_m b_m^T + R$ has the minimal residual norm $\|R\| = \sigma_2$.*

We can project the Krylov residual R in (2.8) back on A. The following theorem shows that a near Krylov decomposition is an exact decomposition of matrix A with a perturbation.

Theorem 2.9. *[26] Let $AU = UB + ub^T + R$ and assume that U is of full rank. Let $E = -RU^\dagger$, where $U^\dagger = (U^H U)^{-1} U^H$ is the pseudoinverse of U. Then*

$$(A + E)U = UB + ub^T,$$

and

$$\frac{\|R\|}{\|U\|} \leq \|E\| \leq \|R\|\|U^\dagger\|.$$

When U is an orthonormal matrix, $U^\dagger = U^T$ and $\|E\| = \|R\|$.

2.9 Schur Decomposition

We have the following real Schur decomposition [9] [15] which will be used to prove theorems later.

Theorem 2.10. *Real Schur Decomposition If $A \in R^{n\times n}$ then there exists an orthogonal $Q \in R^{n\times n}$ such that*

$$Q^T A Q = \begin{bmatrix} R_{11} & R_{12} & \cdots & R_{1m} \\ 0 & R_{22} & \cdots & R_{2m} \\ \vdots & \vdots & \ddots & \vdots \\ 0 & 0 & \cdots & R_{mm} \end{bmatrix} = R,$$

where each R_{ii} is a square block of order one or two. The blocks of order two contain the complex conjugate eigenvalues of A. The matrix R is said to be in upper quasi-triangular matrix form.

2.10 Discretization of Differential Operators

In this thesis, we solve eigenvalue problems from discretizing differential operators, and we mainly use finite difference discretization [2] [7].

2.10.1 Discretization of a 1D Differential Problem

Consider the following eigenvalue problem of a second order ordinary differential operator:

$$-u''(x) + \beta u'(x) = \lambda u(x), 0 \leq u \leq 1, \tag{2.9}$$
$$u(0) = u(1) = 0.$$

The domain $[0, 1]$ is partitioned into n subintervals with the same step length $h = 1/n$. Let u_j be a finite difference approximation to the exact solution $u(x_j)$, where $x_j = jh$ is an interior grid point, for $j = 1, \cdots, n-1$.

$$\frac{-u_{j-1} + 2u_j - u_{j+1}}{h^2} + \beta \frac{u_{j+1} - u_{j-1}}{2h} = \lambda u_j,$$
$$(-\frac{1}{h^2} - \frac{\beta}{2h})u_{j-1} + \frac{2}{h^2}u_j + (-\frac{1}{h^2} + \frac{\beta}{2h})u_{j+1} = \lambda u_j,$$

$$\frac{1}{h^2}\begin{bmatrix} 2 & -1+\frac{\beta h}{2} & & & & & \\ -1-\frac{\beta h}{2} & 2 & -1+\frac{\beta h}{2} & & & & \\ & \cdot & \cdot & \cdot & & & \\ & & \cdot & \cdot & \cdot & & \\ & & & -1-\frac{\beta h}{2} & 2 & -1+\frac{\beta h}{2} & \\ & & & & -1-\frac{\beta h}{2} & 2 & \end{bmatrix} \begin{bmatrix} u_1 \\ u_2 \\ \cdot \\ \cdot \\ \cdot \\ u_{n-1} \end{bmatrix} = \lambda \begin{bmatrix} u_1 \\ u_2 \\ \cdot \\ \cdot \\ \cdot \\ u_{n-1} \end{bmatrix}. \tag{2.10}$$

We denote (2.10) by

$$A\vec{u} = \lambda \vec{u},$$

which is the matrix eigenvalue problem we want to solve.

The stencil representation of the matrix A is

$$A = \frac{1}{h^2}\begin{pmatrix} -1-\frac{\beta h}{2} & 2 & -1+\frac{\beta h}{2} \end{pmatrix}. \tag{2.11}$$

When $\beta = 0$,

$$A = \frac{1}{h^2}\begin{pmatrix} -1 & 2 & -1 \end{pmatrix}, \tag{2.12}$$

and A is a symmetric matrix.

2.10.2 Discretization of a 2D Differential Problem

For a 2D Laplace problem

$$-\Delta u = -u_{xx} - u_{yy} = \lambda u,$$

or a more general diffusion-convection problem

$$\begin{aligned} -\Delta u + \beta \cdot \bigtriangledown u &= \lambda u, \\ -\Delta u + a u_x + b u_y &= \lambda u, \text{ assume } \beta = [a, b]^T \end{aligned} \tag{2.13}$$

on the domain $[0, 1] \times [0, 1]$, with Dirichlet boundary condition

$$u(x, y) = 0, \text{ for } x = 0, \text{or } y = 0.$$

We partition each direction into n subintervals with the same step length $h = 1/n$. Let $u_{i,j}$ be a finite difference approximation to the exact solution $u(x_i, y_j)$, where $(x_i, y_j) = (ih, jh)$ for $j = 1, \cdots, n-1$. Then (2.13) is discretized as

$$\frac{-u_{i-1,j} + 2u_{i,j} - u_{i+1,j}}{h^2} + \frac{-u_{i,j-1} + 2u_{i,j} - u_{i,j+1}}{h^2} + a\frac{u_{i+1,j} - u_{i-1,j}}{2h} + b\frac{u_{i,j+1} - u_{i,j-1}}{2h} = \lambda u_{i,j}.$$

Let

$$\vec{u} = [u_{1,1}, u_{1,2}, \cdots, u_{1,n-1}, u_{2,1}, \cdots, u_{2,n-1}, \cdots, u_{n-1,1}, \cdots u_{n-1,n-1}]^T,$$

then we have the matrix form

$$A\vec{u} = \begin{bmatrix} B & a_1 I & & & & \\ a_2 I & B & a_1 I & & & \\ & \cdot & \cdot & \cdot & & \\ & & \cdot & \cdot & \cdot & \\ & & & a_2 I & B & a_1 I \\ & & & & a_2 I & B \end{bmatrix} \vec{u} = \lambda \vec{u}, \tag{2.14}$$

where

$$a_1 = -\frac{1}{h^2} + \frac{a}{2h},$$
$$a_2 = -\frac{1}{h^2} - \frac{a}{2h}.$$

And if we use the same representation as (2.11), the block matrix B can be written as

$$B = \frac{1}{h^2}\begin{pmatrix} -1 - \frac{bh}{2} & 4 & -1 + \frac{bh}{2} \end{pmatrix}.$$

2.11 Eigenpairs of Symmetric Matrices from Discretization

We discuss eigenpairs of the symmetric matrix (2.12) for 1D and 2D differential operators [7]. They will help us do some analysis later.

2.11.1 Eigenpairs of the Symmetric Matrix from 1D Problem

The eigenvectors of

$$A = \frac{1}{h^2}\begin{pmatrix} -1 & 2 & -1 \end{pmatrix}$$

are

$$\omega_{k,j} = \sin\big(\frac{jk\pi}{n}\big), 1 \le k \le n-1, 1 \le j \le n-1, \tag{2.15}$$

and the eigenvalues are

$$\lambda_k(A) = \frac{4}{h^2}\sin^2\big(\frac{k\pi}{2n}\big). \tag{2.16}$$

2.11.2 Eigenpairs of the Symmetric Matrix from 2D Problems

For the 2D problem on the unit square $\Omega = [0,1] \times [0,1]$

$$-\Delta u = \lambda u, u = 0 \text{ on } \partial\Omega.$$

The matrix problem $A\vec{u} = \lambda\vec{u}$ is (2.14) with

$$a_1 = -\frac{1}{h^2}\ ,\ a_2 = -\frac{1}{h^2},$$
$$B = \frac{1}{h^2}\begin{pmatrix} -1 & 4 & -1 \end{pmatrix}.$$

The eigenvalues of A are

$$\lambda_{kl} = \frac{4}{h^2}\Big[\sin^2\big(\frac{k\pi}{2n}\big) + \sin^2\big(\frac{l\pi}{2n}\big)\Big], \tag{2.17}$$
$$1 \le k, l \le n-1.$$

The eigenvectors for $\lambda_{kl}, 1 \le k, l \le n-1$ are

$$w_{ij} = \big(\sin\frac{ik\pi}{n}\big)\big(\sin\frac{jl\pi}{n}\big),$$

where w_{ij} is the value at each interior node (x_i, y_i),

$$w_{ij} = w(x_i, y_j) = w(ih, jh).$$

A significant difference from the 1D eigenvalue problem is that there are repeated eigenvalues for the 2D problem. Since from (2.17),

$$\lambda_{kl} = \lambda_{lk},$$

when $k \neq l$, there would be at least two repeated eigenvalues. This property makes the 2D eigenvalue problem harder than the 1D case.

2.12 Multigrid Methods

Multigrid methods [7] are used to solve linear systems obtained from differential equations. They take advantage of a hierarchy of discretizations. The idea of

multigrid methods is to go back and forth among different grids to improve numerical approximations. There are three important steps:

1. Iteratively relax on a grid to smooth the error;
2. Restrict the residual error from a finer grid to a coarser grid;
3. Interpolate a correction from a coarser grid to a finer grid.

Let us first define the notation.

Fine grid: Ω^h is the grid with step length h. A^h is the matrix using discretization on Ω^h. r^h is the residual $r^h = f^h - A^h u^h$.

Coarse grid: Ω^{2h} is the grid with step length h. A^{2h} is the matrix using discretization on Ω^{2h}. r^{2h} is the residual $r^{2h} = f^{2h} - A^{2h} u^{2h}$.

Interpolation: I_{2h}^h maps a vector on coarse grid to fine grid

Restriction: I_h^{2h} maps a vector on fine grid to coarse grid

The two-grid scheme (Algorithm 2.8) is the basic algorithm for multigrid V-cycle scheme (Algorithm 2.9). The details of iterative relaxation, interpolation and restriction operators will be discussed in the following subsections.

Algorithm 2.8 Two-grid Correction Scheme

1. Relax υ_1 times on $A^h u^h = f^h$ on Ω^h with arbitrary initial guess v^h.
2. Compute $r^h = f^h - A^h v^h$.
3. Compute $r^{2h} = I_h^{2h} r^h$.
4. Solve $A^{2h} e^{2h} = r^{2h}$ on Ω^{2h}.
5. Correct fine-grid solution $v^h \leftarrow v^h + I_{2h}^h e^{2h}$.
6. Relax υ_2 times on Ω^h with initial guess v^h.

Algorithm 2.9 V-cycle Scheme

1. Relax υ_1 times on $A^h u^h = f^h$ on Ω^h with a given initial guess v^h.

2. If Ω^h = coarsest grid, then go to step 4. Else.

$$f^{2h} \leftarrow I_h^{2h}(f^h - A^h v^h)$$
$$v^{2h} \leftarrow 0$$
$$v^{2h} \leftarrow V^{2h}(v^{2h}, f^{2h})$$

3. Correct $v^h \leftarrow v^h + I_{2h}^h e^{2h}$.
4. Relax υ_2 times on Ω^h with initial guess v^h.

2.12.1 Weighted Jacobi

There are several relaxation methods which can be used on each grid. One of the simplest schemes is the Jacobi method. For an equation $Au = f$, we split the matrix A in the form

$$A = D - L - U,$$

where D is the diagonal of A, and $-L$ and $-U$ are the strictly lower and upper triangular parts of A. Then the equation becomes

$$(D - L - U)u = f,$$

and then

$$Du = (L + U)u + f,$$
$$u = D^{-1}(L + U)u + D^{-1}f.$$

Let the Jacobi iteration matrix be

$$R_J = D^{-1}(L + U),$$

the solution is obtained iteratively via

$$u^{(1)} = R_J u^{(0)} + D^{-1}f.$$

The weighted Jacobi is

$$u^{(1)} = [(1-\omega)I + \omega R_J]u^{(0)} + D^{-1}f,$$

where $\omega \in R$.

2.12.2 1D Linear Interpolation

Interpolation is a technique to construct new data points from a set of known data points. In multigrid, linear interpolation is used in step 5 of Algorithm 2.8 and step 3 of Algorithm 2.9. We use I_{2h}^h to denote the map from the coarse grid to the fine grid.

$$I_{2h}^h : \Omega^{2h} \to \Omega^h.$$

Let v^h and v^{2h} be defined on Ω^h and Ω^{2h}. Then

$$I_{2h}^h v^{2h} = v^h,$$

where for $0 \le i \le \dfrac{N}{2} - 1$,

$$\begin{aligned} v_{2i}^h &= v_i^{2h}, \\ v_{2i+1}^h &= \frac{1}{2}(v_i^{2h} + v_{i+1}^{2h}). \end{aligned} \tag{2.18}$$

So I_{2h}^h can be written as

$$I_{2h}^h = \frac{1}{2}\begin{bmatrix} 1 & & & & \\ 2 & & & & \\ 1 & 1 & & & \\ & 2 & & & \\ & 1 & & & \\ & & \ddots & & \\ & & & 1 & \\ & & & 2 & \\ & & & 1 & \end{bmatrix}_{(\frac{N}{2}-1)\times(N-1)} . \tag{2.19}$$

2.12.3 1D Cubic Spline Interpolation

In the multigrid Arnoldi method we will propose later, we use the spline interpolation [11], because it gives more accurate and smooth approximations on the fine grid.

Suppose we have n intervals and $n+1$ points, including the two endpoints of the interval. The cubic spline interpolation is a piecewise continuous curve, passing through all given points $(x_i, y_i), i = 0, 1, \cdots, n+1$. On each interval $[x_i, x_{i+1}]$, there is a cubic polynomial

$$S_i(x) = a_i(x - x_i)^3 + b_i(x - x_i)^2 + c_i(x - x_i) + d_i.$$

All these polynomials S_i together are denoted $S(x)$. The spline $S(x)$ satisfies

$$S_i(x_i) = y_i, S_i(x_{i+1}) = y_{i+1},$$
$$S'_{i-1}(x_i) = S'_i(x_i), S''_{i-1} = S''_i(x_i).$$

2.12.4 1D Restriction

We use I_h^{2h} to denote the restriction operator from the fine grid to the coarse grid:

$$I_h^{2h} : \Omega^h \to \Omega^{2h}$$
$$I_h^{2h} u^h = u^{2h},$$

where

$$u_i^{2h} = \frac{1}{4}(u_{2i-1}^h + 2u_{2i}^h + u_{2i+1}^h).$$

I_h^{2h} can be written as

$$I_h^{2h} = \frac{1}{4}\begin{bmatrix} 1 & 2 & 1 & & & & & \\ & & 1 & 2 & 1 & & & \\ & & & & \cdots & & & \\ & & & & & & 1 & 2 & 1 \end{bmatrix}_{(n-1)\times(n/2-1)} \tag{2.20}$$

2.12.5 Important Conditions

For 1D problems, if linear interpolation and restriction operators are defined as (2.19) and (2.20), there is a relation:

$$I_{2h}^{h} = 2(I_{h}^{2h})^{T}. \tag{2.21}$$

The coarse grid matrix A^{2h} can be identified as

$$A^{2h} = I_{h}^{2h} A^{h} I_{2h}^{h}. \tag{2.22}$$

If A^{h} is symmetric as in (2.4), then

$$A^{2h} = I_{h}^{2h} A^{h} I_{2h}^{h} = \frac{1}{(2h)^2} \begin{pmatrix} -1 & 2 & -1 \end{pmatrix},$$

which is the same as we do discretization on Ω^{2h}. (2.22) is called the Galerkin condition for multigrid.

CHAPTER THREE

Multigrid Arnoldi Method

3.1 Motivation

Eigenvalue problems can be very difficult and matrices obtained from discretizations are very large in some situations. Even with the restarted Arnoldi method, the convergence of all desired eigenvectors can be slow, and the storage and computation are very expensive. Here is one example.

Example 3.1. We want to find the 10 smallest numerical eigenvalues and corresponding eigenvectors of Laplacian operator on the unit square.

$$-\Delta u = \lambda u$$

$$u = 0 \text{ on the boundary}$$

Matrix A has the form (2.14). We use the restarted Arnoldi method (Algorithm 2.6). The Krylov subspace is of dimension 30, and 15 eigenvector approximations are retained from previous Arnoldi iteration. We denote this by Arn(30,15).

In order to find more accurate eigenpairs, we need finer discretizations. But finer discretizations lead to larger matrices and smaller eigenvalues, which make it harder for the Arnoldi method.

Figure 3.1 and 3.2 illustrate the difficulty of having a large matrix. Both figures show the residuals of 10 desired eigenvectors after each Arnoldi cycle. In Figure 3.1 the matrix A is of size 65025×65025, where there are $2^8 = 256$ intervals and hence 255 interior nodes on each direction. In Figure 3.2 the matrix A is of size 261121×261121, where there are $2^9 = 512$ intervals and 511 interior nodes on each direction.

It takes 555 cycles to get all desired eigenvectors to converge to 1e-8, and 647 cycles to 1e-10 for the matrix of size 65025. From Table 3.1, we see that if the matrix

size goes four times larger, the numbers of cycles needed becomes almost four times more. Furthermore, one cycle on the fine grid is about four times more expensive than one cycle on the coarse grid. The mvp in Table 3.1 shows the total number of matrix-vector products for each matrix during the Arnoldi iteration.

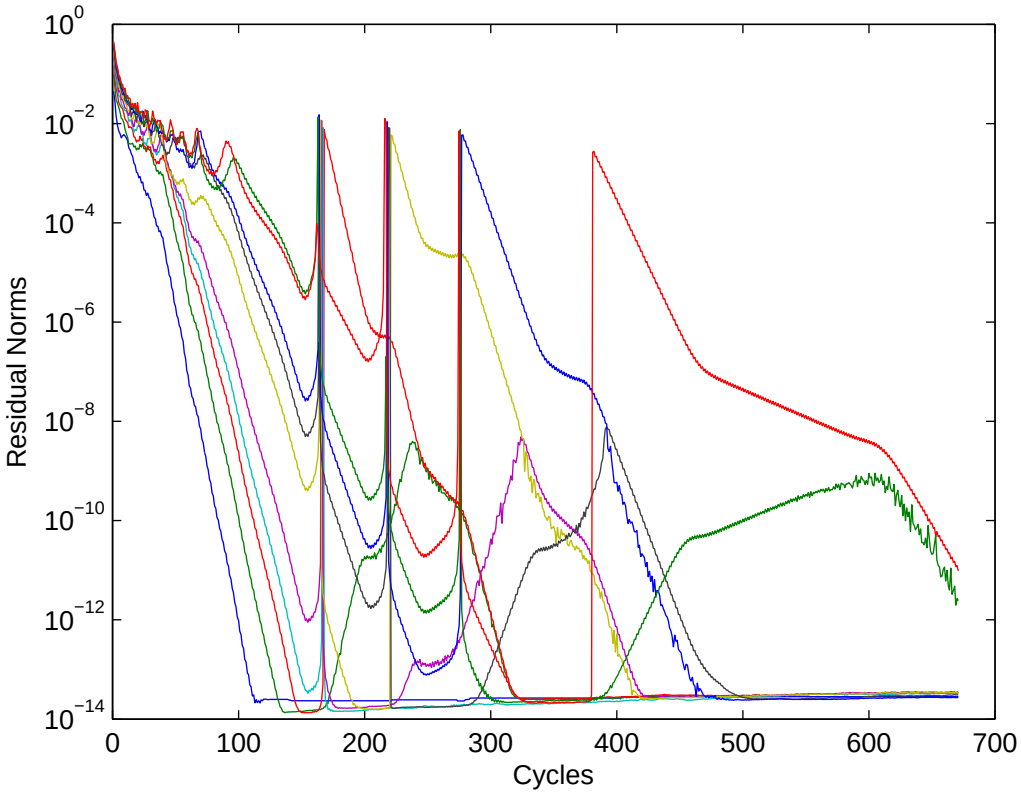

Figure 3.1: Restarted Arnoldi (30,15) for 2D problem with size 65025.

Table 3.1: Convergence for two matrices.

matrix size	discretization size	tolorance 1e-8		tolerance 1e-10	
		cycles	mvp	cycles	mvp
65025	1/256	555	8340	647	9720
261121	1/512	1283	19260	2469	37050

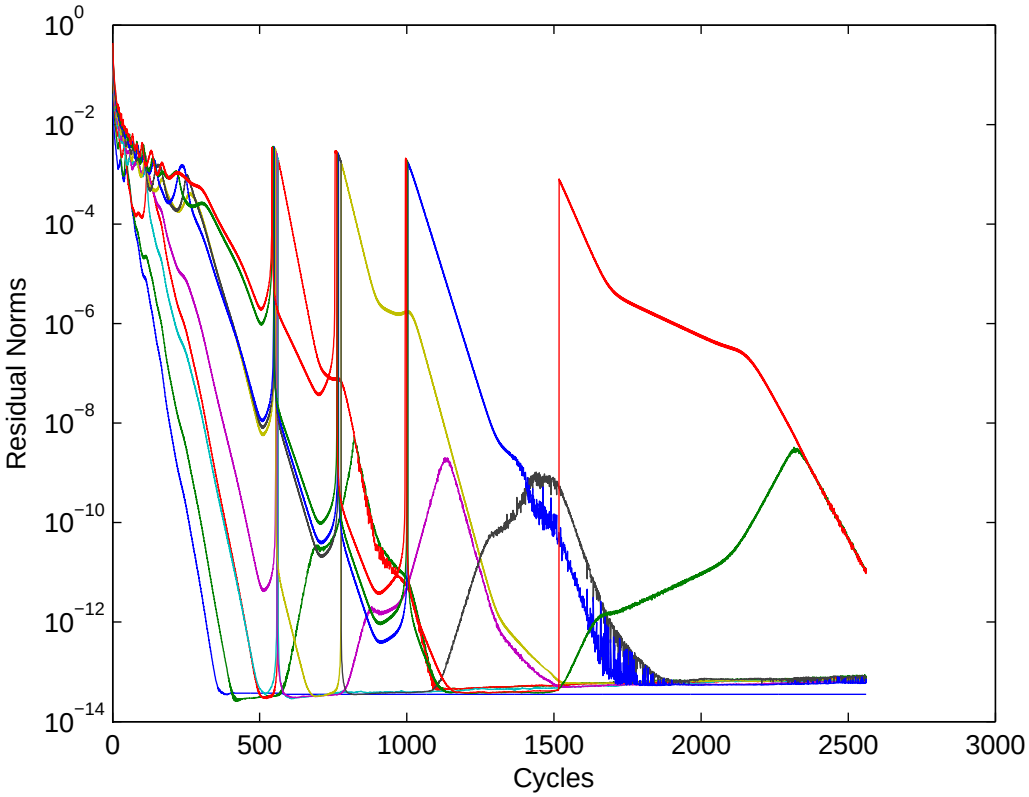

Figure 3.2: Restarted Arnoldi (30,15) for 2D problem with size 261121.

For higher-dimensional problems, one difficulty is that there are many repeated eigenvalues. Arnoldi methods may miss the repeated ones at first and then find them when round off error occurs. We see some jump-ups in both two figures, which happens when new eigenpairs are found. If we set up the tolerance larger, we may miss some repeated eigenpair. Actually, in the table it shows 1283 cycles are needed for the tolerance 1e-8 on the fine grid, but we do not have all 10 smallest eigenvalues at this point. We need 2295 cycles to get the missed one. So sometimes certain accuracy is needed in order to find missed ones. At the same time, as the size of the matrix gets bigger, the computational cost and storage requirement increase dramatically. This motivates us to find a new method to improve the restarted Arnoldi method.

Figure 3.1 and 3.2 have different convergence rates but similar pattern, which inspires us to use the information of eigenpairs from a coarser grid. We propose the multigrid Arnoldi method by combining restarted Arnoldi methods and multigrid techniques. We present the method on two grids. First, approximations of eigenvectors on a coarse grid are calculated. Then we interpolate them and get the initial vectors on the fine grid. Lastly, we take the advantage of already known approximations and improve them by using Arnoldi-E. The three steps are:

1. Run restarted Arnoldi on the coarse grid.
2. Use coarse grid eigenvectors to create approximate eigenvectors on the fine grid (we use spline interpolation).
3. improve approximate eigenvectors on the fine grid with the Arnoldi-E method.

The starting vector in step 3 is taken by alternating through all desired eigenvectors. In Section 3.3, a more detailed algorithm will be given. Here we apply the new method to the same problem in Example 3.1 and see if it can improve the existing methods

Example 3.1 (continuing from p. 24). We apply the Two-grid Arnoldi to the 2D problem in Example 3.1. A^f on the fine grid is of size $n^f = 511^2 = 261121$ with 511 nodes on each direction. A^c on the coarse grid discretization size is half of the fine grid, and we get the matrix of size $n^c = 255^2 = 65025$.

We run Arnoldi(30,15) with 555 cycles until 10 desired eigenvectors converge to 1e-8 on the coarse grid. We use spline interpolation to get approximations on the fine grid, and then we run Arnoldi-E(30,15). It turns out that only 10 cycles are needed on the fine grid to make residuals of 10 desired eigenvectors be below 1e-8, and 25 cycles for them to be below 1e-10.

Figure 3.3 shows the convergence with Two-grid Arnoldi. The x-axis represents the number of equivalent cycles, which is approximately the cost of a cycle on the fine grid.

$$\text{Equivalent cycle } = \frac{1}{\text{grid factor}} \times \text{cg cycle} + \text{fg cycle}.$$

With the concept of equivalent cycle, we are able to compare the Two-grid Arnoldi method with the standard Arnoldi method.

In this example, the grid factor is considered to be 4. And if there are 555 cycles on the coarse grid and 10 cycles on the fine grid, the equavalent cycles are $\frac{1}{4} \times 555 + 10 \approx 149$. So there are approximately 149 equivalent cycles to get all eigenvectors converge to 1e-8. Similarly there are $\frac{1}{4} \times 555 + 25 \approx 164$ equivalent cycles to get them to 1e-10.

On Figure 3.3, the residuals of eigenvectors on the coarse grid are plotted for the first $\frac{555}{4} = 139$ cycles, next we plot the residuals of eigenvectors on the fine grid, which corresponds to 140-160 cycles.

Let us compare Two-grid Arnoldi with standard Arnoldi by plotting the convergence of the two methods on the same figure.

We list the equivalent cycles for two methods in Table 3.2.

Table 3.2: Comparison between Two-grid Arnoldi and restarted Arnoldi.

Methods	1e-8	1e-10
Two-grid Arnoldi	149	164
Restarted Arnoldi	2295	2469

We list 2295 instead of 1283 cycles (as in Table 3.1) for standard Arnoldi with tolerance 1e-8 to make sure all desired eigenpairs are found. Two-grid Arnoldi is as about 15 times faster as the restarted Arnoldi in this example, which is a significant improvement.

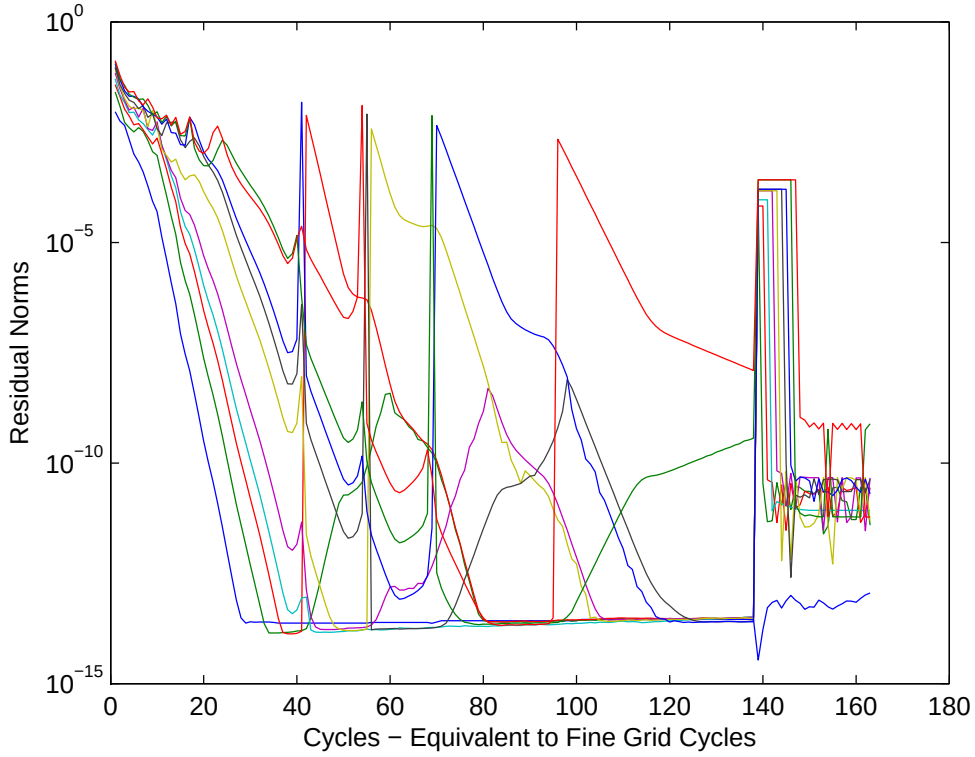

Figure 3.3: Two-grid Arnoldi for 2D problem. Fine grid matrix size is 261121 and coarse grid matrix size is 65025.

3.3 Implementation

We discuss details about the implementation of the Two-grid Arnoldi method.

Algorithm 3.1 Two-grid Arnoldi

1. Choose sizes of fine grid n^f and coarse grid n^c. Fix the dimension of subspace m, the number of eigenvectors retained from previous cycle k, and the number of wanted eigenvectors *numev*. Fix the tolerance *tol*.
2. Do finite difference discretization and get A^c on the coarse grid, A^f on the fine grid.
3. Run restarted Arnoldi(m,k) with Ritz vectors (Algorithm 2.6) on the coarse grid until residuals of desired *numev* vectors are below *tol*.
4. Interpolation. Let y_i^c be approximate Ritz vectors on the coarse grid. Interpolate y_i^c to the fine grid.

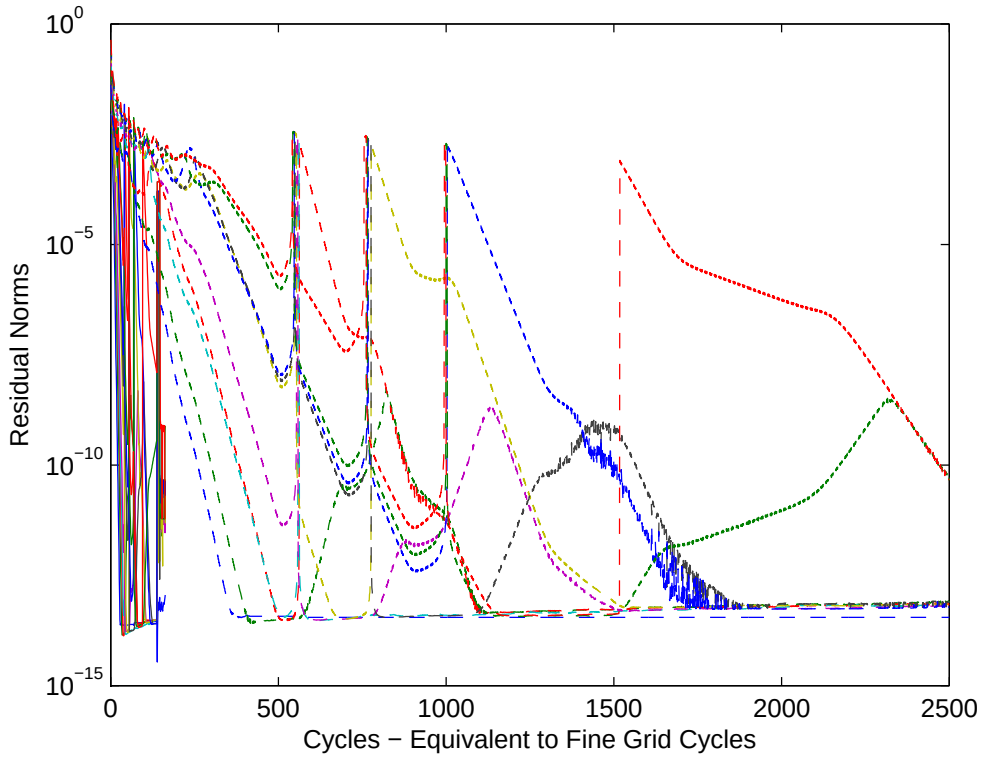

Figure 3.4: Standard restarted Arnoldi compared to Two-grid Arnoldi. 2D problem. Fine grid matrix size is 261121 and coarse grid matrix size is 65025.

5. Run restarted Arnoldi-E(m,k) with approximate eigenvectors (Algorithm 2.7) on the fine grid until residuals of desired *numev* vectors are below *tol*.

In step 5 of Algorithm 3.1, we restart Arnoldi-E for every cycle. The k vectors $y_1, y_2, \cdots, y_k$ are obtained from the previous cycle, and one of them is taken as the starting vector to generate the Krylov subspace $\{y_i, Ay_i, A^2y_i, \cdots, A^{m-k}y_i\}$. Then other vectors are attached, so we will have the subspace.

$$\{y_i, Ay_i, \cdots, A^{m-k}y_i, y_1, \cdots, y_{i-1}, y_{i+1}, \cdots, y_k\}$$

We discuss how to choose the starting vector in step 5. In 3.3.1 we compare different ways to pick the starting vector, and in 3.3.2 we study the case when the approximate eigenvectors happen to be complex.

3.3.1 Starting Vector and the Size of Krylov Subspace

A natural way to choose the starting vector is alternating through all desired vectors. It means that the first cycle has y_1 as the starting vector, the second cycle y_2 is the starting vector, and so on. After y_{numev} is used as the starting vector, we come back and restart with y_1 again.

When the starting vectors for the fine grid are very accurate, alternating through all vectors is very effective as we saw in Example 3.1. In the next example, we discuss the situation that the starting vectors are not good enough and many more cycles are needed. This may happen when the coarse grid is too coarse or the eigenvectors have not converged to certain degree on the coarse grid.

Example 3.2. 1D Problem: $-u'' = \lambda u$. The matrix A has the form (2.12) of size 1023, and the coarse grid is 256. We run to accuracy of only 1e-3 for the smallest 10 eigenpairs on coarse grid. Then we do the following four tests and show the results.

1. Figure 3.5 shows the convergence when we alternate through all 15 vectors with Arnoldi(30,15).

2. Figure 3.6 shows the convergence when we alternate through all 15 vectors with Arnoldi(30,15). If the residual norm of one vector is below 1e-14, we will not take it as the starting vector but move and check the next one.

3. Figure 3.7 shows the convergence when we alternate through the desired 10 vectors with Arnoldi(30,15). Converged to 1e-14 Ritz pairs are skipped.

4. Figure 3.8 shows the convergence when we fix the starting vectors until it converges to some degree with Arnoldi(30,15).

5. Figure 3.9 shows the convergence when we alternate through all 15 vectors with Arnoldi(40,15). Converged Ritz pairs are skipped.

The convergence slows down when some Ritz vectors get very accurate in Figure 3.5. It is because if a Ritz vector has reached very high accuracy (about 1e-14), starting with this vector can not improve the approximations much. So in

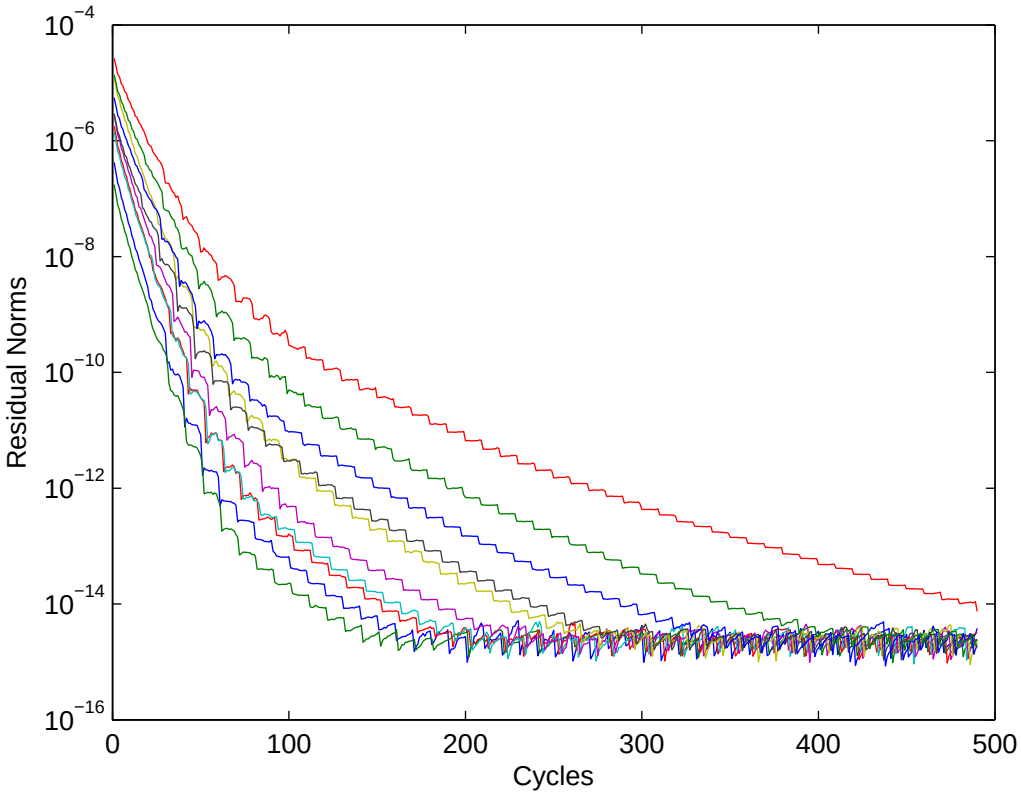

Figure 3.5: Alternate through 15 vectors with Arn(30,15).

the later experiments, if one vector has the residual norm below 1e-14, we skip this vector and move to the next one. In this way we can work more on those vectors which are not converged yet.

It takes 345 cycles in Figure 3.6, but only 266 cycles in Figure 3.7 for all desired eigenvectors to converge below 1e-14. One reason is that the latter algorithm focuses even more on the ten desired vectors. For example, the 10th vectors is taken as the starting vector for 55 times in Figure 3.7, but only 31 times in Figure 3.6.

In Figure 3.8, we fix the starting vector until it converges to some degree. More specially, we use the first vector as the starting vector until the residual converges below 1e-6, then we restart Arnoldi-E with the second vector until it converges below 1e-6, and so on. After all desired vectors have the accuracy of 1e-6, we come back to the first vector and work on it until it converges to 1e-7 and so on. It takes

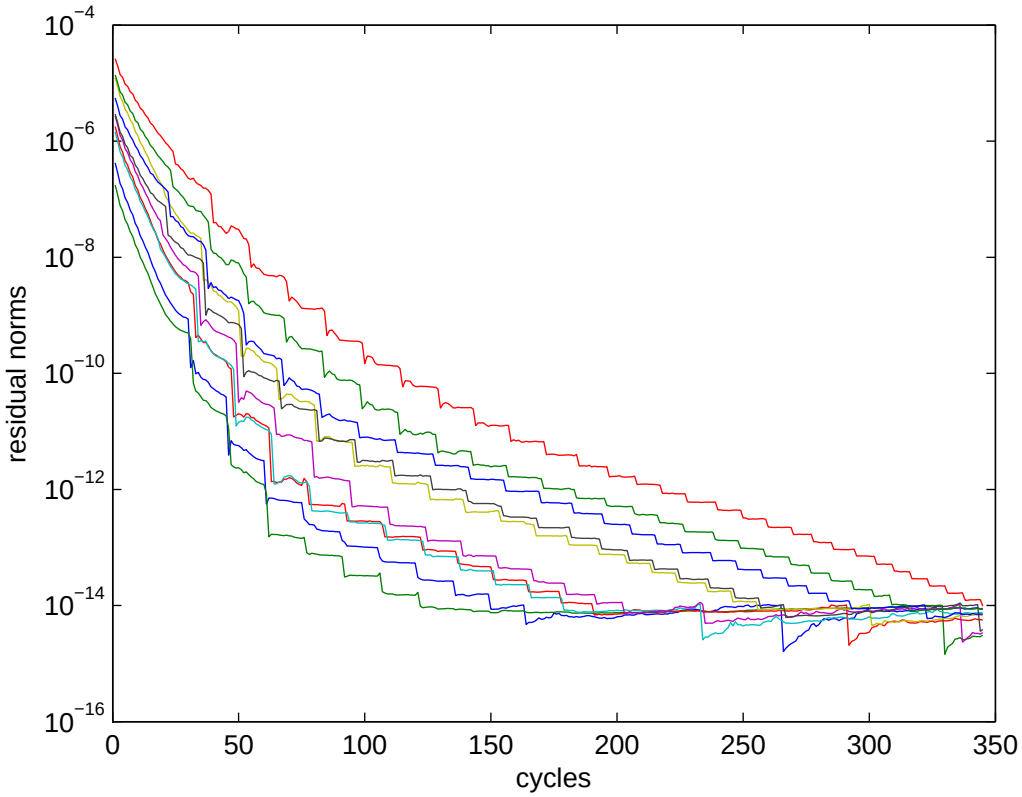

Figure 3.6: Alternate through 15 vectors with Arn(30,15). Skip the converged ones.

263 cycles to make residuals of the first 10 approximate eigenvectors to be less than 1e-14, almost the same as Figure 3.7.

In Figure 3.9 we apply Arn(40,15) instead of Arn(30,15) on the fine grid. We alternate through 10 desired eigenvectors but skip converged ones. It takes 109 cycles with 2834 mvp's on the fine grid, which is less than 266 cycles with 4256 mvp's with Arn(30,15) in Figure 3.6.

We have the following conclusions of Example 3.5. If we emphasize more the eigenvectors which are hard to converge, the overall convergence can be better. So for the experiments we do later, we usually alternate through all desired eigenvectors. When some eigenvectors are already very accurate (1e-14), we do not take them as the starting vector.

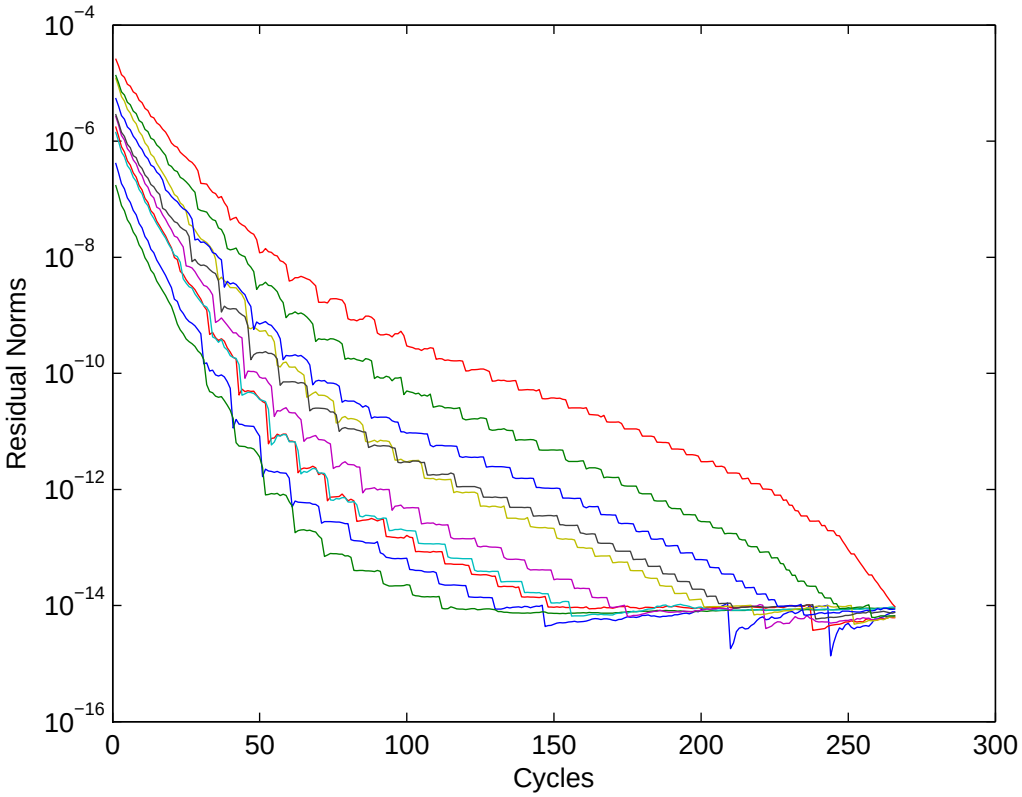

Figure 3.7: Alternate through 10 desired vectors with Arn(30,15). Skip the converged ones.

3.3.2 Non-symmetric Matrices

Sometimes we need to deal with complex vectors, for instance when the matrix is non-symmetric. In order to reduce the computational cost, we split a complex vector into its real and imaginary parts. If we have y_1 and y_2 as a conjugate pair with $y_i = x_1 \pm x_2$, we replace $\{y_1, y_2\}$ by $\{x_1, x_2\}$.

Suppose we have $\{y_1, y_2, \cdots, y_k\}$ from the previous cycle, and suppose y_1 is the starting vector, then for the next cycle, the subspace is

$$span\{y_1, y_2, \cdots, y_k, Ay_1, A^2y_1, \cdots, A^{m-k}y_1\}. \tag{3.1}$$

Suppose we can split complex vectors as

$$y_1 = x_1 + ix_2, y_2 = x_1 - ix_2, \cdots, y_i = x_i + ix_{i+1}, y_{i+1} = x_i - ix_{i+1},$$

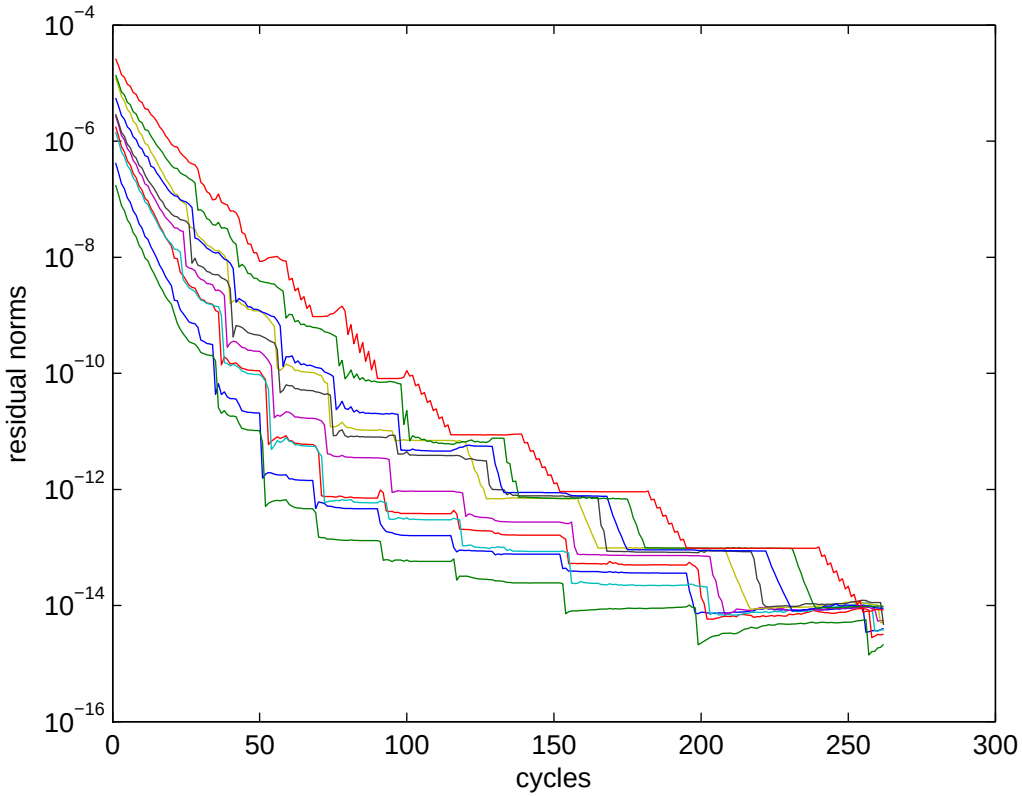

Figure 3.8: Fix starting vector until it converges to some degree with Arn(30,15).

and we replace complex vectors by real vectors, then the subspace would be

$$span\{x_1, x_2, \cdots, x_{k-1}, x_k, Ax_1, A^2x_1, \cdots, A^{m-k}x_1\}. \tag{3.2}$$

If the last vector y_k is a complex vector but it is not a conjugate of other vectors, k is decreased by 1 so that all complex vectors appear in pairs.

Splitting reduces the computation expense, because it keeps the subspace real instead of complex. The next example shows that splitting complex vectors can work as well as using complex vectors.

Example 3.3. We consider a more general 1D differential operator

$$-u'' + \beta u' = \lambda u, \text{where } u(0) = u(1) = 0.$$

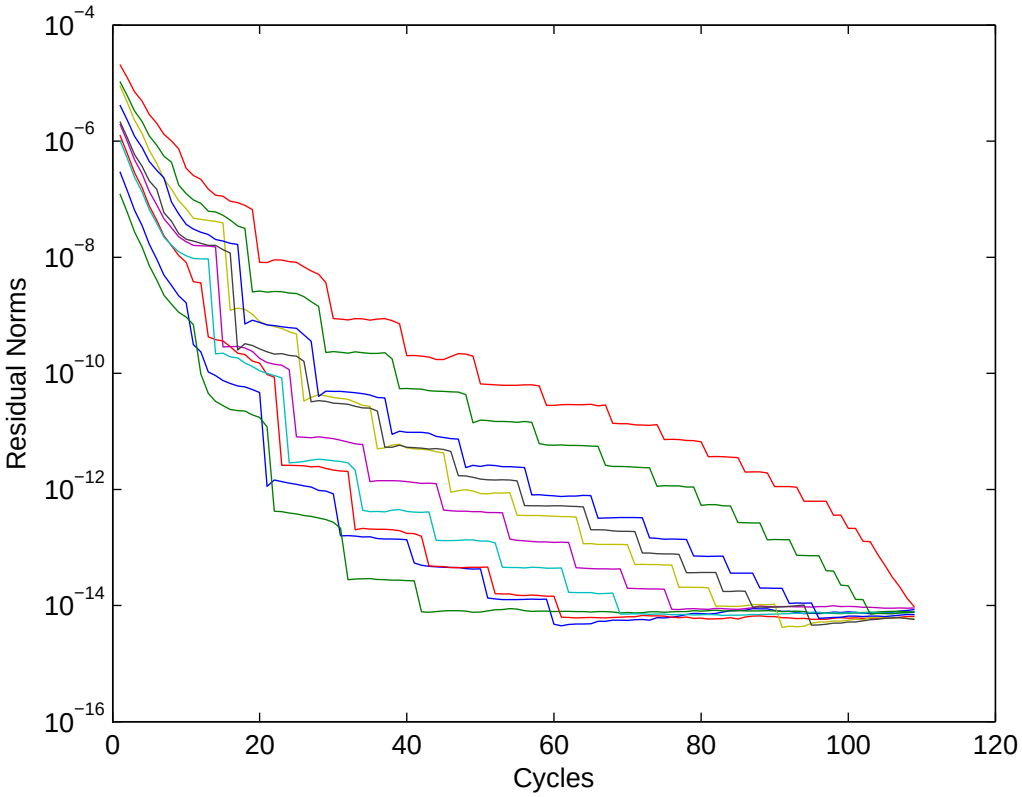

Figure 3.9: Alternate through 10 desired vectors with Arn(40,15). Skip the converged ones.

The matrix from finite discretization can be expressed as (2.11).

$$A = \begin{pmatrix} -1 - \dfrac{\beta h}{2} & 2 & -1 + \dfrac{\beta h}{2} \end{pmatrix}.$$

Let $\beta = 100$, we want to find the 10 smallest eigenvalues and corresponding eigenvectors of A. The matrix size is 1023, and the coarse grid is 256. We run 36 cycles of restarted Arnoldi(30,15) on the coarse grid until all 15 eigenvectors are converged to 1e-8. Then we run Arnoldi-E(30,15) on the fine grid where we alternate through desired eigenvectors.

Figure 3.10 shows the convergence of residuals when we restart Arnoldi-E with original Ritz vectors (use subspace (3.1) for each cycle). Figure 3.11 shows the convergence when we split complex Ritz vectors (use subspace (3.2) for each cycle).

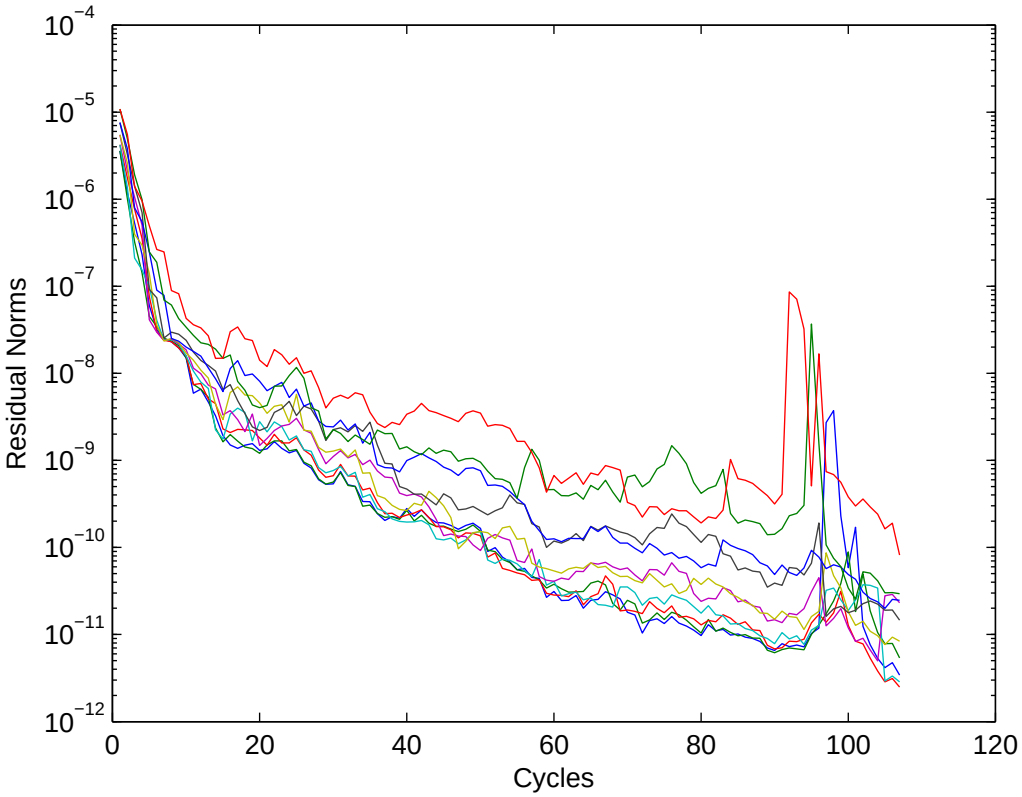

Figure 3.10: Restart with eigenvectors, 15 vectors have residuals below 1e-8 on the coarse grid.

It takes 28 cycles for all vectors to converge to 1e-8, and 116 cycles to 1e-10 when we split complex vectors. It takes 28 cycles for all vectors to converge to 1e-8 and 107 cycles to 1e-10 when we do not split complex vectors.

There is one comment about the implemention with a non-symmetric matrix. For the symmetric case, we only require all desired eigenvectors to converge to the tolerance. But for non-symmetric case, experiments show that it may be better to make all k vectors converge to the same degree on the coarse grid. Figure 3.12 shows if only 10 eigenvectors converge to 1e-8 on the coarse grid. It takes 147 cycles on the fine grid, which is more than Figure 3.11.

Therefore, for non-symmetric matrices, we run implicit Arnoldi(m,k) on the coarse grid until all k eigenvectors converge to the tolarance, then we run Arnoldi-

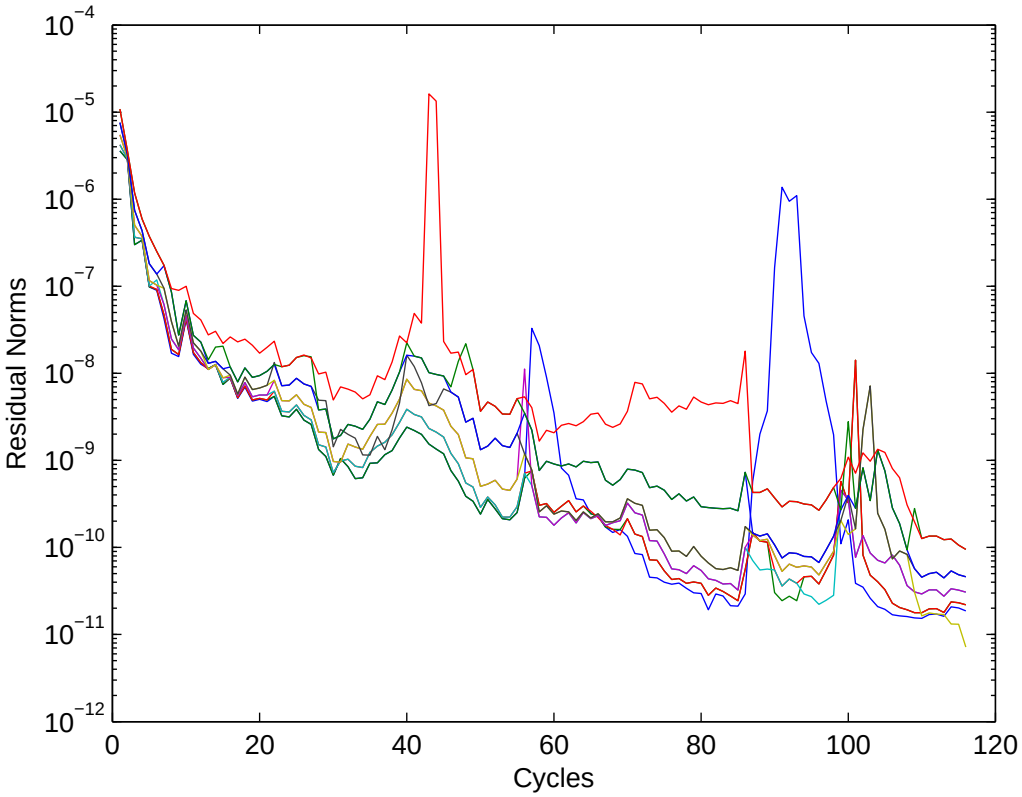

Figure 3.11: Restart with real and imaginary parts of eigenvectors, 15 vectors have residuals below 1e-8 on the coarse grid.

E(m,k) on the fine grid, alternating through desired eigenvectors. In order to save computational cost, we always split complex vectors into its real and imaginary parts in our experiments. More study is needed of why this is effective.

3.4 Experiments and Comparisons

We test more examples with our new method in this section, and we also compare the method with the shift-and-invert Arnoldi.

3.4.1 Test Different Coarse Grids

In the following example, the fine grid is fixed, but different coarse grids are changed and tested.

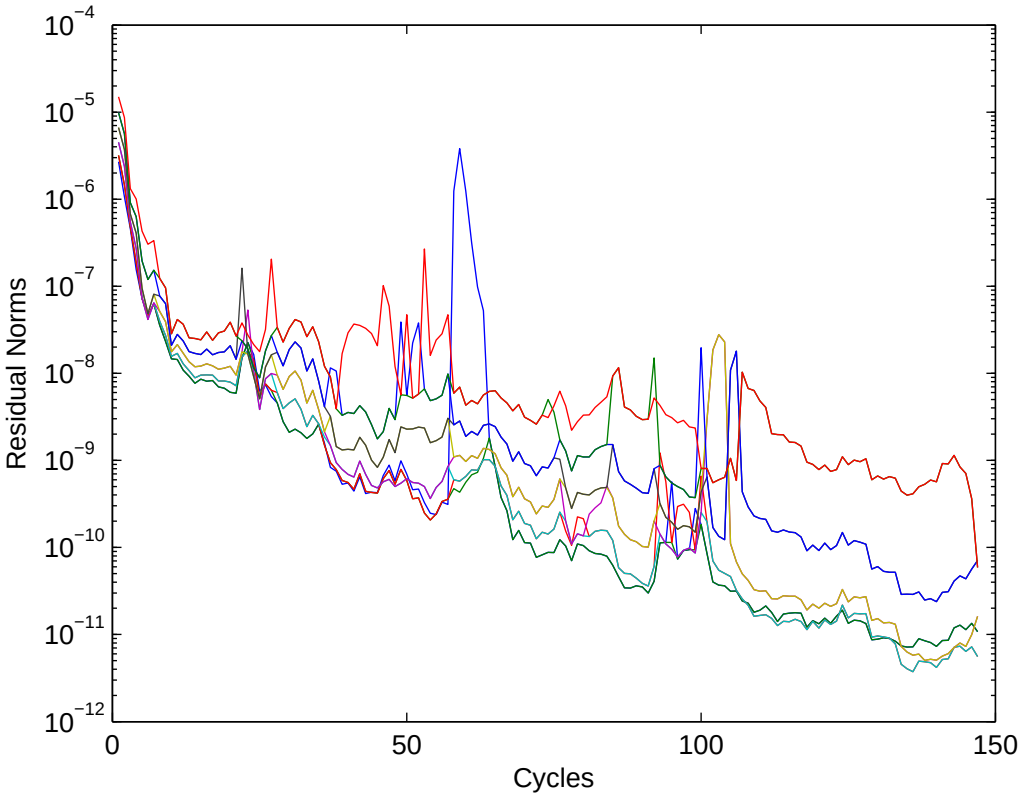

Figure 3.12: Restart with real and imaginary parts of eigenvectors. Only 10 vectors have residuals below 1e-8 on the coarse grid.

Example 3.4. The symmetric matrix A has the form (2.12) of size 1023, and we want to find 10 smallest numerical eigenvalues and corresponding eigenvectors.

We test different coarse grids of size 511, 255, 127, 63, or 31. Table 3.3 shows the results. On both grids, the tolerance is 1e-8. The convergence is checked by calculating the residual of the 10th Ritz vector. We alternate through all desired eigenvectors on the fine grid. In Table 3.3, the equivalent matrix-vector multiplication is calculated as

$$\text{equivalent mvp} = \frac{\text{cg cycles} * 15 + 15}{\text{grid factor}} + \text{fg cycles} * 31 + 9.$$

On the coarse grid, there are 15 matrix-vector multiplications for each cycle, except that the first cycle needs 30 multiplications. This number is divided by the grid factor to get the equivalent mvp on the fine grid. On the fine grid, there are 30

matrix vector multiplications, plus one more for calculating the residual of the 10th eigenvector for each cycle. The last 9 is from calculating the residual of the rest of the eigenvectors as a final check.

Table 3.3: Experiments with different coarse grids.

coarse grid	grid factor	cg cycles	fg cycles	equivalent mvp's	time
31	32	2	170	5280	0.90
63	16	5	40	1255	0.28
127	8	11	10	342	0.15
255	4	25	10	417	0.22
511	2	63	10	799	0.46

The Two-grid Arnoldi works very well when the coarse grid is one quarter or one eighth of the fine grid. But when the coarse grid goes too coarse, the interpolation does not give very accurate approximations for the fine grid.

3.4.2 Comparisions with Shift-and-invert Arnoldi

We compare the Two-grid Arnoldi method with shift-and-invert Arnoldi where multigrid is used as a linear solver. Both the symmetric case (Example 3.5) and non-symmetric case (Example 3.6) are discussed.

Example 3.5. We deal with the same problem as in Example 3.4. A has the form (2.12) of size 1023, and we want to find the 10 smallest numerical eigenvalues and corresponding eigenvectors.

The shift-and-invert Arnoldi method is introduced in Section 2.2. If we are interested in the smallest eigenvalues and corresponding eigenvectors, we just take

$\tau = 0$. The Krylov subspace is

$$\begin{aligned} \mathcal{K}_m(A^{-1}, v) &= Span\{v, A^{-1}v, A^{-2}v, \cdots, A^{-(m-1)}v\} \\ &= Span\{v_1, v_2, \cdots, v_m\}. \end{aligned} \tag{3.3}$$

We solve $Aw = v$ by using multigrid (Algorithm 2.9), so that $w = A^{-1}v$, where one Jacobi relaxation weighted by $\frac{2}{3}$ is done on each grid.

The shift-and-invert Arnoldi with multigrid as a linear solver is basically an inner-outer Krylov method. The unrestarted Arnoldi (Algorithm 2.2) is the outer iteration. The size of the Krylov subspace m increases at each iteration when one more vector is added in the subspace. Then at the mth iteration, there is the relation

$$BV_{n\times m} = V_{n\times m}H_{m\times m} + v_{n+1}e_m^T, \text{where } B = A^{-1}.$$

We calculate the 10 largest eigenvalues each iteration since the eigenvalues are reciprocals of those of the original problems.

Table 3.4 shows the number of equivalent matrix-vector products and total time to run shift-and-invert Arnoldi. There are two rows in the table since we find the solution of $Aw = v_m$ to the tolerance of 1e-6 and 1e-8 respectively. It takes about 12 V-cycles for multigrid to solve $Aw = v$ to get the accuracy of 1e-6 and about 17 V-cycles to 1e-8. It works well even when the linear solver is not as accurate as the tolerance. Some inner-outer Krylov method theory has an explanations for that [10].

The equivalent matrix-vector products is the sum of equivalent products for solving equations with multigrid, the mvp needed for checking the residual of 10th vector each cycle, and the mvp for the final check for all other vectors.

Table 3.4: Results of shift-and-invert Arnoldi.

m	rtol for lin. eq's	equivalent mvp's	time
29	1e-6	1139	0.38
29	1e-8	1537	0.48

Let us compare the mvp and time with the two methods. From Table 3.3 and Table 3.4, we see that Two-grid Arnoldi is fairly competitive. It runs fast when the coarse grid is not too coarse, and it can be even faster sometimes. The corresponding numbers of equivalent matrix-vector products are also less.

The next example compares Two-grid Arnoldi with shift-and-invert Arnoldi for non-symmetric case. We will see problems that shift-and-invert Arnoldi has trouble with, but Two-grid Arnoldi can still work well.

Example 3.6. Consider the 1D differential operator

$$-u'' + \beta u' = \lambda u, \text{where } u(0) = u(1) = 0.$$

The matrix can be expressed as

$$A = \begin{pmatrix} -1 - \frac{\beta h}{2} & 2 & -1 + \frac{\beta h}{2} \end{pmatrix}$$

of size 1023. We want to find the 10 smallest eigenvalues and corresponding eigenvectors of A.

A is not symmetric. Standard multigrid methods does not work very well when the coefficient β gets bigger. We fix the maximum V-cycle number to be 100, which means there will be at most 100 V-cycles to solve the linear equation $Aw = v$ and get $A^{-1}v$. When $\beta = 17$ or less, the linear equations can be solved to the accuracy 1e-8 at each iteration. When $\beta = 18$, the linear equations can not be solved to even 1e-4 each time. Then not all eigenvectors converge to 1e-8. When $\beta = 22$ or larger, the linear equations can not get good solutions in 100 V-cycles, shift-and-invert Arnoldi fails. Table 3.5 gives more details.

However, Two-grid Arnoldi can work very well for a bigger β. Figure 3.9 and 3.10 showed the convergence when $\beta = 100$ for the same problem. Let the coarse grid be 255, and we change the value of β. We split complex Ritz vectors into real and imaginary parts. The tolerance is 1e-8 on both grids. We run implicit Arnoldi(m,k)

on the coarse grid until all k eigenvectors converge to the tolarance, then we run Arnoldi-E(m,k) on the fine grid, alternating through desired eigenvectors. Results are listed in Table 3.6.

Table 3.5: Results of shift-and-invert Arnoldi.

β	m	rtol for lin eq's	eqivalent mvp's	time
16	26	1e-8	5562	1.51
17	26	1e-8	7793	1.88
18-21	not all eigenvectors converge to 1e-8			
22	diverge			

Since k is decreased by 1 if the last Ritz vector is complex, we use matlab to count the matrix vector multiplications on the coarse grid, and then calculate

$$\text{equivalent mvp } = \frac{\text{cg mvp}}{\text{grid factor}} + \text{fg cycles} * 31 + 9.$$

Table 3.6: Results of Two-grid Arnoldi.

β	coarse grid	cg cycles	fg cycles	cg mvp	equivalent mvp's	time
100	255	36	28	571	1020	0.45
150	255	39	81	616	2674	0.76
200	255	62	80	969	2731	0.86

Example 3.5 shows Two-grid Arnoldi can work as well as shift-and-invert Arnoldi with multigrid as a linear solver for the symmetric case. Two-grid Arnoldi is more useful for non-symmetric matrices as we saw in Example 3.6.

3.4.3 Helmholtz Problem

We next consider a problem with an indefinite matrix. Standard multigrid methods do not work for this matrix, but Two-grid Arnoldi does work.

Example 3.7. We consider a one-dimensional Helmholtz problem $-u'' - 40,000u = \lambda u$. For simplicity, we use zero boundary conditions. The fine grid matrix is of size $n^f = nfg = 1023$ and it has 63 negative eigenvalues. Our goal is to compute the 10 eigenvalues closest to the origin, so this is an interior eigenvalue problem. Therefore we switch to harmonic restarted Arnoldi [19] in the first phase of Two-grid Arnoldi. For the second phase, we use harmonic Arnoldi-E [20]. These methods use harmonic Rayleigh-Ritz [17] [23] which makes convergence more reliable for interior eigenvalues. Figure 3.13 has harmonic Arnoldi compared to two tests of Two-grid Arnoldi. Figure 3.14 has a close-up of Two-grid Arnoldi with $n^c = ncg = 511$. Harmonic Arnoldi uses 1148 cycles for 10 eigenvalues to converge to residual norms below 10^{-8}. However, it misses one of the 10 smallest eigenvalues in magnitude (non-Harmonic takes 3058 cycles and misses two of the 10 smallest). Harmonic Two-grid Arnoldi needs 124 fine-grid-equivalent cycles with $n^c = 511$ and 217 for $n^c = 255$. Both find all of the 10 smallest eigenvalues. As mentioned earlier, Two-grid Arnoldi can do much of its work on the coarse grid where the problem is easier. This makes it more reliable.

We also tried a larger fine grid matrix with $n^f = 2047$, and the harmonic Two-grid approach with $n^c = 511$ improves by a factor of almost 100 (59 fine-grid-equivalent cycles compared to 5636 for harmonic Arnoldi).

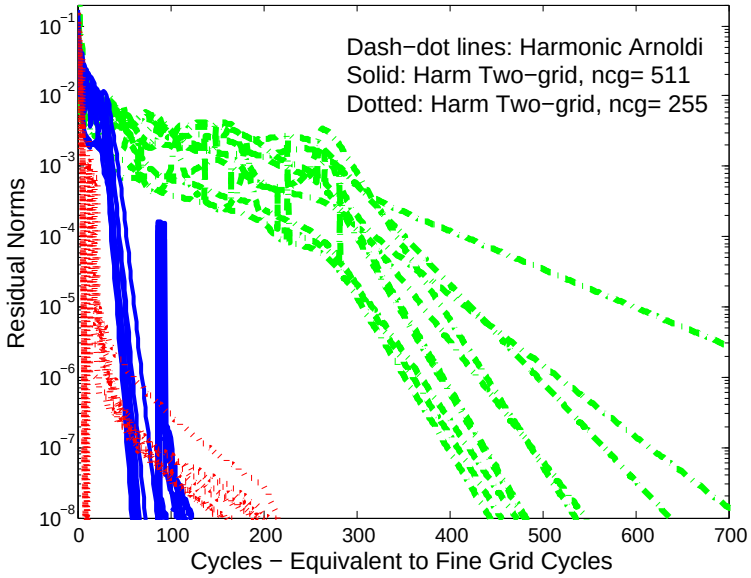

Figure 3.13: Standard Arnoldi compared to Two-grid Arnoldi for a 1-D simple Helholtz matrix. Fine grid matrix size is $nfg = 1023$ and coarse grid matrix sizes are $ncg = 511$ and $ncg = 255$.

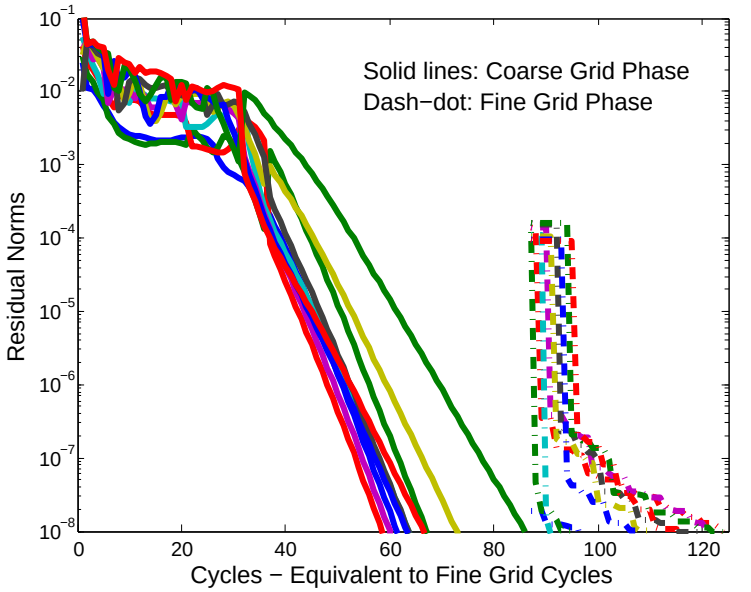

Figure 3.14: Two-grid Arnoldi for a 1-D simple Helholtz matrix. Fine grid matrix size is $nfg = 1023$ and coarse grid matrix size is $ncg = 511$.

CHAPTER FOUR

Eigenvalue Analysis for Symmetric Case

We notice in Example 3.2 that when the matrix is symmetric, the approximations from the coarse grid can be very good initial guesses for the fine grid, especially when the coarse grid is not too coarse. The main goal in this chapter is to explore the reasons.

We study the symmetric problem $-u'' = \lambda u$, and let the coarse grid size be exactly one half as the fine grid. Let n be the number of subintervals and $h = \dfrac{1}{n}$ be the step length on the fine grid, and then $2h$ is the step length on the coarse grid. We use the same notation introduced in Section 2.11. We prove that after the linear interpolation I_{2h}^h, the Ritz value of $I_{2h}^h w^{2h}$ has the accuracy of $O(h)$, while w^{2h} is an exact eigenvector of A^{2h}. Section 4.1 studies eigenvalues on two grids, and section 4.2 discusses eigenvectors.

4.1 Analysis of Eigenvalues

Proposition 4.1 gives the relation of eigenvalues on the coarse and the fine grids.

Proposition 4.1. *Let* $A^h = \dfrac{1}{h^2}\begin{bmatrix} -1 & 2 & -1 \end{bmatrix}$ *and* $A^{2h} = \dfrac{1}{(2h)^2}\begin{bmatrix} -1 & 2 & -1 \end{bmatrix}$ *be the matrices on the fine grid and the coarse grid respectively. Let* $\{\lambda_k^h\}_{k=1,\cdots,n}$ *and* $\{\lambda_k^{2h}\}_{k=1,\cdots,\frac{n}{2}}$ *be corresponding eigenvalues. For the first* $\frac{n}{2}$ *eigenvalues,* $\lambda_k^h = \lambda_k^{2h} + O(h^2)$ *when* h *is very small.*

Proof. According to (2.16), the eigenvalues of A^h are

$$\lambda_k^h = \frac{4}{h^2}\sin^2(\frac{k\pi}{2n}),$$

and the eigenvalues of A^{2h} are

$$\lambda_k^{2h} = \frac{4}{(2h)^2}\sin^2(\frac{k\pi}{2\frac{n}{2}}) = \frac{4}{(2h)^2}\sin^2(\frac{k\pi}{n}).$$

Since

$$\sin x = x - \frac{x^3}{3!} + \frac{x^5}{5!} - \frac{x^7}{7!} + \cdots = x + O(x^3),$$

when x is very small. So when n is very big, and $h = \frac{1}{n}$ is very small,

$$\begin{aligned}\lambda_k^h &= \frac{4}{h^2}\sin^2(\frac{k\pi}{2n}) = \frac{4}{h^2}\sin^2(\frac{k\pi h}{2}) = \frac{4}{h^2}(\frac{k\pi h}{2} + O((\frac{k\pi h}{2})^3))^2 \\ &= \frac{4}{h^2}(\frac{k\pi h}{2} + O(h^3))^2 = \frac{4}{h^2}(\frac{k^2\pi^2 h^2}{4} + O(h^4)) = k^2\pi^2 + O(h^2),\end{aligned}$$

and

$$\begin{aligned}\lambda_k^{2h} &= \frac{4}{(2h)^2}\sin^2(\frac{k\pi}{n}) = \frac{4}{(2h)^2}\sin^2(k\pi h) = \frac{4}{(2h)^2}(k\pi h + O(h^3))^2 \\ &= \frac{4}{4h^2}(k^2\pi^2 h^2 + O(h^4)) = k^2\pi^2 + O(h^2).\end{aligned}$$

So

$$\lambda_k^h = \lambda_k^{2h} + O(h^2).$$

□

Proposition 4.1 implies that if we find an eigenvalue on the coarse grid with the accuracy $O(h^2)$, then it is also an approximate eigenvalue on the fine grid with the accuracy $O(h^2)$.

4.2 Analysis of Eigenvectors

We are also interested in how accurate an approximate eigenvector from the coarse grid could be. Since the procedure involves interpolations, the norm of the linear interpolation operator is discussed. Proposition 4.2 and 4.3 discuss the norm of the interpolation operator I_{2h}^h. Then we use these results and relations from multigrid (Section 2.11.5) to prove Theorem 4.4.

Proposition 4.2. *Let*

$$P = I_{2h}^{h} = \frac{1}{2}\begin{bmatrix} 1 & & & & \\ 2 & & & & \\ 1 & 1 & & & \\ & 2 & & & \\ & 1 & \ddots & & \\ & & & 1 & \\ & & & 2 & \\ & & & 1 & \end{bmatrix}_{(n-1)\times(\frac{n}{2}-1)}$$

be the linear interpolation matrix, then

$$\|I_{2h}^{h}\|^2 = \|P\|^2 = 2 + O(h), \text{where } h = \frac{1}{n}.$$

Proof. We use P to represent I_{2h}^{h} for convenience. Let

$$u = \begin{bmatrix} x_1, x_2, \cdots, x_{\frac{n}{2}-1} \end{bmatrix}^T \in R^{\frac{n}{2}-1}, \text{ then}$$

$$Pu = \begin{bmatrix} \frac{1}{2}x_1, x_1, \frac{1}{2}x_1 + \frac{1}{2}x_2, x_2, \frac{1}{2}x_2 + \frac{1}{x}x_3, x_3, \cdots, \frac{1}{2}x_{\frac{n}{2}-2} + \frac{1}{2}x_{\frac{n}{2}-1}, x_{\frac{n}{2}-1}, \frac{1}{2}x_{\frac{n}{2}-1} \end{bmatrix}^T$$
$$\in R^{n-1}.$$

We want to find the norm of P, first we have

$$\begin{aligned}
\|Pu\|^2 &= \frac{1}{4}x_1^2 + x_1^2 + \frac{1}{4}(x_1+x_2)^2 + x_2^2 + \frac{1}{4}(x_2+x_3)^2 + \cdots \\
&+ \frac{1}{4}(x_{\frac{n}{2}-2} + x_{\frac{n}{2}-1})^2 + x_{\frac{n}{2}-1}^2 + \frac{1}{4}x_{\frac{n}{2}-1}^2 \\
&= \frac{1}{4}x_1^2 + x_1^2 + \frac{1}{4}x_1^2 + \frac{1}{2}x_1x_2 + \frac{1}{4}x_2^2 + x_2^2 + \frac{1}{4}x_2^2 + \frac{1}{2}x_2x_3 + \frac{1}{4}x_3^2 + \cdots \\
&+ \frac{1}{4}x_{\frac{n}{2}-2}^2 + \frac{1}{2}x_{\frac{n}{2}-2}x_{\frac{n}{2}-1} + \frac{1}{4}x_{\frac{n}{2}-1}^2 + x_{\frac{n}{2}-1}^2 + \frac{1}{4}x_{\frac{n}{2}-1}^2 \\
&= \frac{3}{2}(x_1^2 + x_2^2 + \cdots + x_{\frac{n}{2}-1}^2) + \frac{1}{2}(x_1x_2 + x_2x_3 + \cdots + x_{\frac{n}{2}-2}x_{\frac{n}{2}-1}) \\
&= \frac{3}{2}\|u\|^2 + \frac{1}{2}(x_1x_2 + x_2x_3 + \cdots + x_{\frac{n}{2}-2}x_{\frac{n}{2}-1}) \qquad (4.1) \\
&\le \frac{3}{2}\|u\|^2 + \frac{1}{4}(x_1^2 + x_2^2 + x_2^2 + x_3^2 + \cdots + x_{\frac{n}{2}-2}^2 + x_{\frac{n}{2}-1}^2) \\
&\le \frac{3}{2}\|u\|^2 + \frac{1}{4}(x_1^2 + x_1^2 + x_2^2 + x_2^2 + x_3^2 + \cdots + x_{\frac{n}{2}-2}^2 + x_{\frac{n}{2}-1}^2 + x_{\frac{n}{2}-1}^2) \\
&\le \frac{3}{2}\|u\|^2 + \frac{1}{2}(x_1^2 + x_2^2 + \cdots + x_{\frac{n}{2}-1}^2) = \frac{3}{2}\|u\|^2 + \frac{1}{2}\|u\|^2 \\
&= 2\|u\|^2.
\end{aligned}$$

So

$$\|Pu\|^2 \leq 2\|u\|^2,$$
$$\|Pu\| \leq \sqrt{2}\|u\| \text{ for all } u \in R^{\frac{n}{2}-1}.$$

Therefore,

$$\|P\| = \max \frac{\|Pu\|}{\|u\|} \leq \sqrt{2}. \tag{4.2}$$

On the other hand, let us pick a particular vector

$$x_0 = \begin{bmatrix} 1 & 1 & 1 & \cdots & 1 \end{bmatrix}^T \in R^{\frac{n}{2}-1},$$

then

$$Px_0 = \begin{bmatrix} \frac{1}{2} & 1 & 1 & \cdots & 1 & \frac{1}{2} \end{bmatrix}^T \in R^{n-1}.$$

We can calculate that

$$\frac{\|Px_0\|^2}{\|x_0\|^2} = \frac{\frac{1}{4} + (n-3) + \frac{1}{4}}{\frac{n}{2}-1} = \frac{n - \frac{5}{2}}{\frac{n}{2}-1} = \frac{2n-5}{n-2}$$
$$= 2 - \frac{1}{n-2} \geq 2 - \frac{1}{n} = 2 - h.$$

Since $\|P\| \geq \dfrac{\|Px_0\|}{\|x_0\|}$, so

$$\|P\|^2 \geq \frac{\|Px_0\|^2}{\|x_0\|^2} \geq 2 - h. \tag{4.3}$$

Combine (4.2) and (4.3),

$$2 - h \leq \|P\|^2 \leq 2.$$

We can say that

$$\|P\|^2 = 2 + O(h),$$

which proves the proposition. □

From (2.15) the eigenvectors of matrix A corresponding to n subintervals are

$$\omega_{k,j}^h = \sin\big(\frac{jk\pi}{n}\big), 1 \le k \le n-1, 1 \le j \le n-1.$$

So let $m = \frac{n}{2}$, eigenvectors of A^{2h} are

$$\omega_{k,j}^{2h} = \sin\big(\frac{jk\pi}{m}\big), 1 \le k \le m-1, 1 \le j \le m-1.$$

Proposition 4.3 finds the relation between the norm of an eigenvector ω_k^{2h} and the vector $P\omega_k^{2h}$ after linear interpolation.

Proposition 4.3. *Let $P = I_{2h}^h$ as defined in the above proposition, where $h = \frac{1}{n}$. Let $m = \dfrac{n}{2}$ and $w = \left[\sin\big(\frac{k\pi}{m}\big) \quad \sin\big(\frac{2k\pi}{m}\big) \quad \sin\big(\frac{3k\pi}{m}\big) \quad \cdots \quad \sin\big(\frac{(m-1)k\pi}{m}\big)\right]^T \in R^{\frac{n}{2}-1}$. Then $Pw \in R^{n-1}$, and*

$$\|I_{2h}^h w\|^2 = \|Pw\|^2 = 2\|w\|^2 + O(h).$$

Proof. Substitute w in equation (4.1) we get

$$\begin{aligned}\|Pw\|^2 = \frac{3}{2}\|w\|^2 + \frac{1}{2}\Big(&\sin\big(\frac{k\pi}{m}\big)\sin\big(\frac{2k\pi}{m}\big) + \sin\big(\frac{2k\pi}{m}\big)\sin\big(\frac{3k\pi}{m}\big) + \cdots \\ &+ \sin\big(\frac{(m-2)k\pi}{m}\big)\sin\big(\frac{(m-1)k\pi}{m}\big)\Big). \end{aligned} \tag{4.4}$$

By Taylor expansion,

$$\sin(x+h) = \sin x + h\cos x + O(h^2),$$

and since $\dfrac{1}{m} = \dfrac{2}{n} = 2h$,

$$\sin\big(\frac{(j+1)k\pi}{m}\big) = \sin\big(\frac{jk\pi}{m} + \frac{k\pi}{m}\big) = \sin\big(\frac{jk\pi}{m}\big) + O(\frac{k\pi}{m}) = \sin\big(\frac{jk\pi}{m}\big) + O(h).$$

Then

$$\sin\big(\frac{jk\pi}{m}\big)\sin\big(\frac{(j+1)k\pi}{m}\big) = \sin\big(\frac{jk\pi}{m}\big)\Big(\sin\big(\frac{jk\pi}{m}\big) + O(h)\Big) = \sin^2\big(\frac{jk\pi}{m}\big) + O(h).$$

Then (4.4) becomes

$$\begin{aligned}\|Pw\|^2 &= \frac{3}{2}\|w\|^2 + \frac{1}{2}\Big(\sin^2\big(\frac{k\pi}{m}\big) + \sin^2\big(\frac{2k\pi}{m}\big) + \cdots + \sin^2\big(\frac{(m-2)k\pi}{m}\big) + O(h)\Big) \\ &= \frac{3}{2}\|w\|^2 + \frac{1}{2}\Big(\|w\|^2 - \sin^2\big(\frac{(m-1)k\pi}{m}\big) + O(h)\Big) \\ &= 2\|w\|^2 - \frac{1}{2}\sin^2\big(\frac{(m-1)k\pi}{m}\big) + O(h). \end{aligned} \tag{4.5}$$

Again use Taylor expansion,

$$\sin\big(\frac{(m-1)k\pi}{m}\big) = \sin\big(k\pi - \frac{k\pi}{m}\big) = \sin(k\pi) + O(h) = O(h).$$

Finally, we have

$$\|Pw\|^2 = 2\|w\|^2 + O(h).$$

□

There are two important properties for multigrid method introduced in Section 2.11.5, $I_{2h}^h = 2(I_h^{2h})^T$ (when the coarse grid is one half as the fine grid) and $A^{2h} = I_h^{2h}A^hI_{2h}^h$. They are very useful in the following analysis. Theorem 4.4 shows the Rayleigh quotient of an approximate eigenvector from the coarse grid is of accuracy $O(h)$ to the exact eigenvalue.

Theorem 4.4. *Let* $A^h = \frac{1}{h^2}\begin{bmatrix}-1 & 2 & -1\end{bmatrix}$ *and* $A^{2h} = \frac{1}{(2h)^2}\begin{bmatrix}-1 & 2 & -1\end{bmatrix}$. *The interpolation* I_{2h}^h *and restriction* I_h^{2h} *are defined as (2.19) and (2.20). Suppose*

$$A^{2h}w^{2h} = \lambda^{2h}w^{2h},$$

$$\textit{and } u^h = I_{2h}^h w^{2h}.$$

Then the Rayleigh quotient of u^h *would be*

$$\rho^h = \frac{(u^h)^TA^hu^h}{(u^h)^Tu^h} = \lambda^h + O(h).$$

Proof. The numerator of ρ^h is

$$\begin{aligned}(u^h)^T A^h u^h &= (I_{2h}^h w^{2h})^T A^h (I_{2h}^h w^{2h}) \\ &= (w^{2h})^T (I_{2h}^h)^T A^h I_{2h}^h w^{2h}.\end{aligned}$$

Apply (2.21) $I_{2h}^h = 2(I_h^{2h})^T$ and (2.22) $A^{2h} = I_h^{2h} A^h I_{2h}^h$,

$$\begin{aligned}(u^h)^T A^h u^h &= (w^{2h})^T 2(I_h^{2h}) A^h I_{2h}^h w^{2h} = (w^{2h})^T 2A^{2h} w^{2h} \\ &= 2(w^{2h})^T A^{2h} w^{2h} = 2(w^{2h})^T \lambda^{2h} w^{2h} \\ &= 2\lambda^{2h} \|w^{2h}\|^2. \end{aligned} \tag{4.6}$$

On the other hand, the denominator of ρ^h is

$$\begin{aligned}(u^h)^T u^h &= (I_{2h}^h w^{2h})^T (I_{2h}^h w^{2h}) \\ &= (Pw)^T (Pw) \text{ (use the notation in Proposition (4.3))} \\ &= \|Pw\|^2 = \|w\|^2 + O(h) \text{ (use Proposition (4.3))} \\ &= 2\|w^{2h}\|^2 + O(h).\end{aligned}$$

So the Rayleigh quotient is

$$\rho^h = \frac{(u^h)^T A^h u^h}{(u^h)^T u^h} = \frac{2\lambda^{2h}\|w\|^2}{2\|w\|^2 + O(h)} = \frac{\lambda^{2h}}{1 + O(h)} = (1 + O(h))\lambda^{2h}. \tag{4.7}$$

From Proposition (4.1)

$$\lambda^h = \lambda^{2h} + O(h^2).$$

Then (4.7) becomes

$$\begin{aligned}\rho^h &= (1 + O(h))(\lambda^h + O(h^2)) \\ &= (1 + O(h))\lambda^h + O(h^2) \\ &= \lambda^h + O(h).\end{aligned}$$

□

CHAPTER FIVE

Near Krylov Property Theory

In this chapter, we study how having subspaces that are nearly Krylov is key to the success of our methods. For a different look at near Krylov for linear equations, see [8] [31].

5.1 Observation

With Restarted Arnoldi on the coarse grid, it generally is the case that the eigenvectors converge together. One does not wait for other ones to finish converging before it starts to converge. We observe that the same thing can happen on the fine grid with all eigenvectors converging together. This phenomena gives us a hint that the approximations from the coarse grid may have some property that random vectors do not have. In order to illustrate this point, we conduct the following comparison.

Example 5.1. We are looking for the 10 smallest eigenvalues and corresponding eigenvectors of $-u'' = \lambda u$. The matrix A has the form as (2.12) with size 1023. We test two sets of starting vectors, one is the set we get from a coarser grid but solved to low accuracy, and the other is from perturbing exact eigenvectors.

(1) Two-grid Arnoldi. The coarse grid is 256. After 18 cycles, we get the accuracy of 1e-3 for the smallest 10 eigenpairs on the coarse grid. Then we move to the fine grid of size 1023 and use Arnoldi-E.

(2) Arnoldi-E with perturbed eigenvectors. We find the 10 exact eigenvectors of the matrix A and denote them together as a 1023×10 matrix, then we perturb them by adding a random matrix with norm 1e-5. Then we apply Arnoldi-E to these perturbed vectors.

Now we have two different sets of starting vectors. If we fix the starting vector to be y_1 to generate the Krylov subspace for Arnoldi-E, and we run 10 cycles for each set, we get Figure 5.1 and 5.2. If we alternate 10 vectors as starting vectors for Arnoldi-E, we get Figure 5.3 and 5.4 with the two sets.

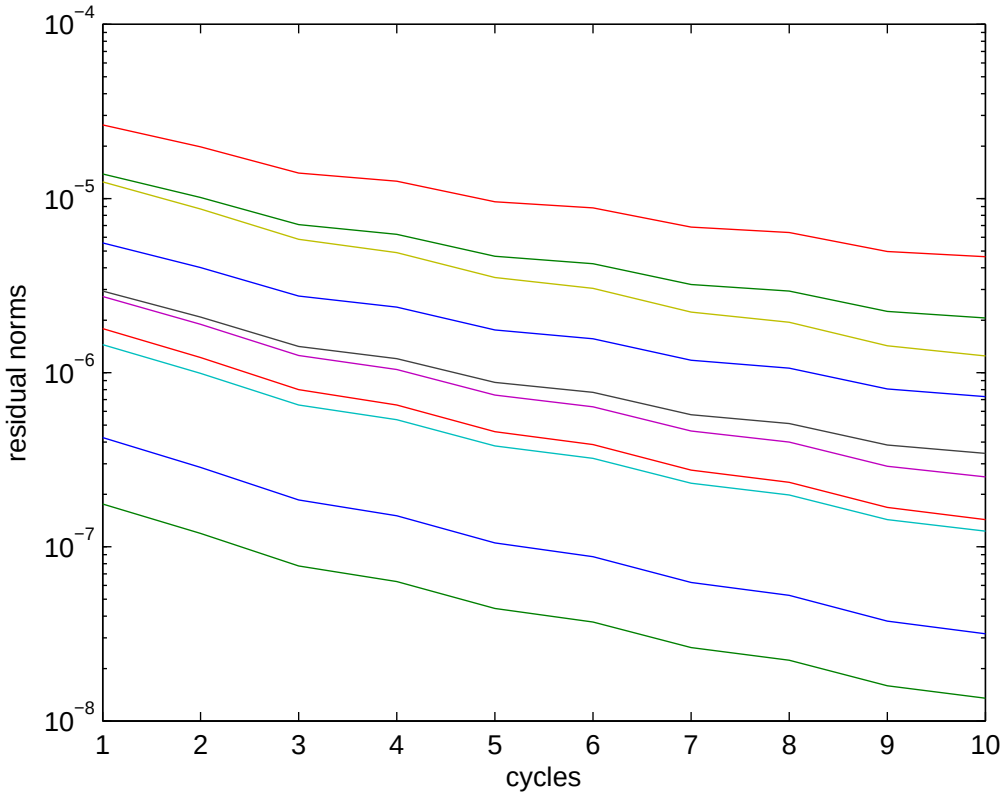

Figure 5.1: Arnoldi-E, using approximations from the coarse grid. Starting vector is fixed as y_1.

Figure 5.1 and 5.3 are almost the same, and this means that no matter which vector is the starting vector, all the vectors converge together. Figure 5.2 and 5.4 show that a vector can converge only when it is the starting vector for Arnoldi-E.

We are interested in this behavior of eigenvectors converging together, since this property can make the convergence of all desired eigenvectors fast.

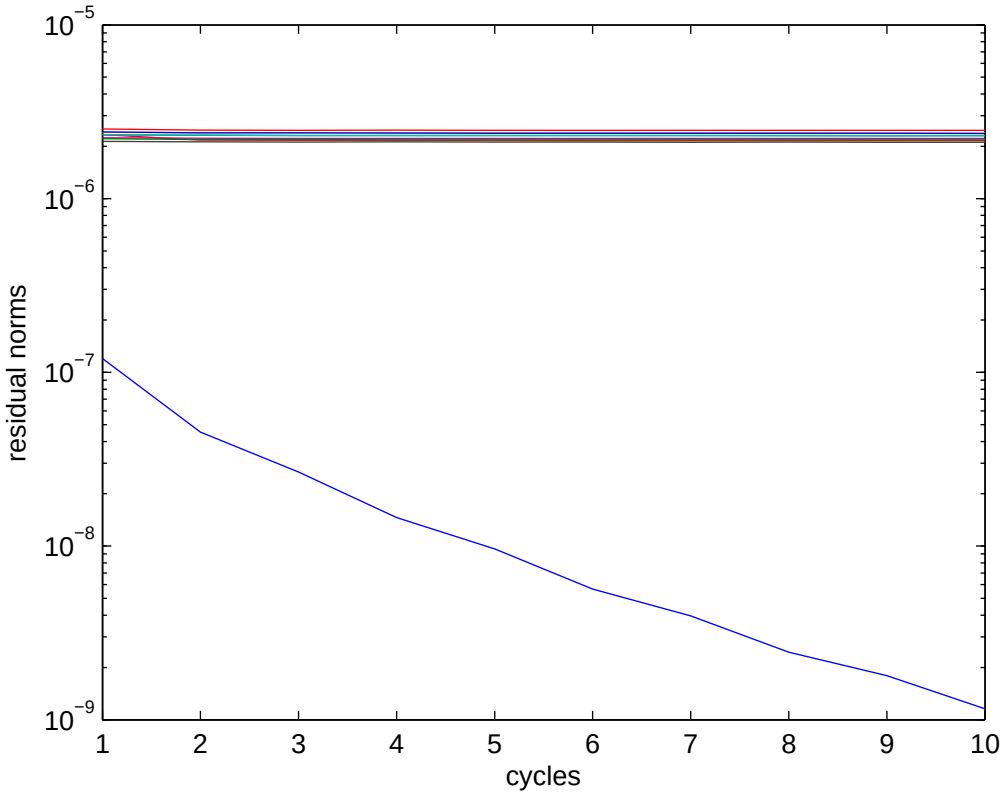

Figure 5.2: Arnoldi-E, using perturbed eigenvectors. Starting vector is fixed as y_1.

5.2 Parallel Property and Krylov Decomposition.

We study the relation between the parallel residuals property and the Krylov decomposition, and then we get the conclusion that the parallel property is a necessary and sufficient condition for having a Krylov decomposition. Suppose there is a Krylov decomposition

$$AU_{n\times m} = U_{n\times m}B_{m\times m} + u_{m+1}b_{m+1}^T, \tag{5.1}$$

where $(U_{n\times m}, u_{m+1})$ is a linear independent basis. Suppose $(\theta_i, g_i), i = 1, \cdots, k$ are eigenpairs of $B_{m\times m}$, i.e

$$\begin{aligned} AU_{n\times m}g_i &= U_{n\times m}B_{m\times m}g_i + u_{m+1}b_{m+1}^T g_i, \\ Ay_i &= \theta_i y_i + (b_{m+1}^T g_i)u, \\ Ay_i &= \theta_i y_i + a_i u, \text{where } a_i = b_{m+1}^T g_i. \end{aligned} \tag{5.2}$$

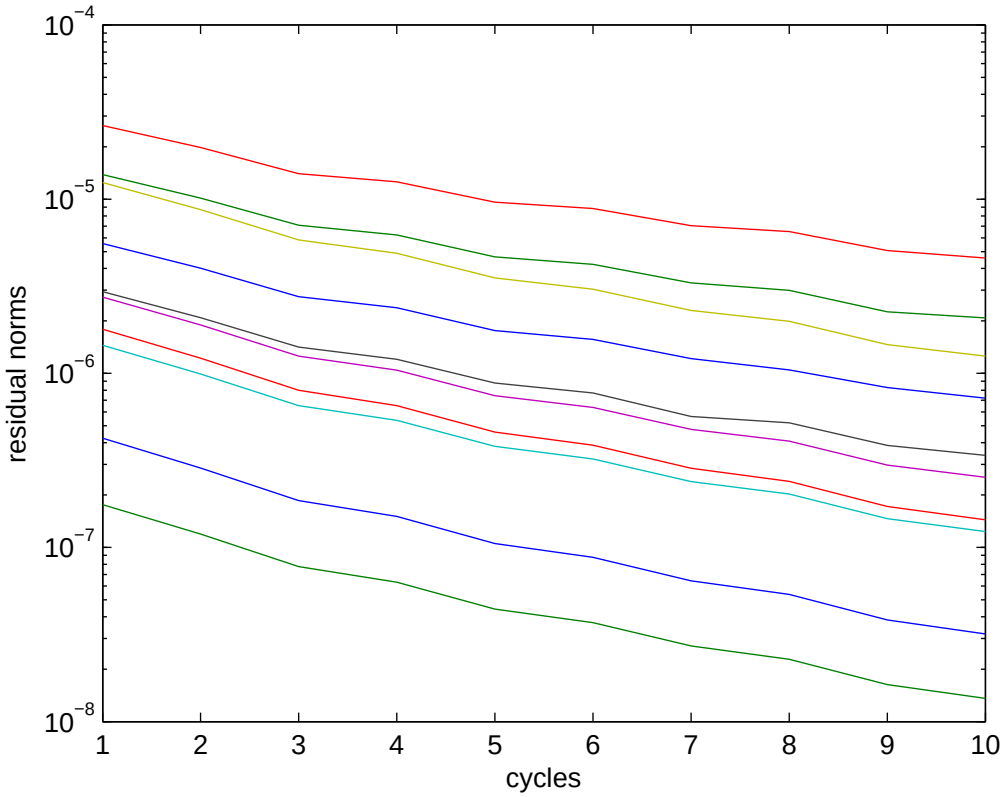

Figure 5.3: Arnoldi-E, using approximations from the coarse grid. Alternate starting vectors.

Equation (5.2) shows the parallel property of all residuals, and it comes from the Krylov decomposition (5.1).

On the other side, The parallel property of all residuals (5.2) implies there is a Krylov decomposition (5.1).

$$AY = Y\Theta + ua^T,$$

where $Y = [y_1, y_2, \cdots, y_k]$, Θ is a diagonal matrix with corresponding θ_i on the diagonal, and $a = [a_1, a_2, \cdots, a_k]^T$.

Theorem 2.6 indicates that any Krylov decomposition corresponds to a Krylov subspace. Hence from the above analysis, we can say the parallel property can also determine a Krylov subspace.

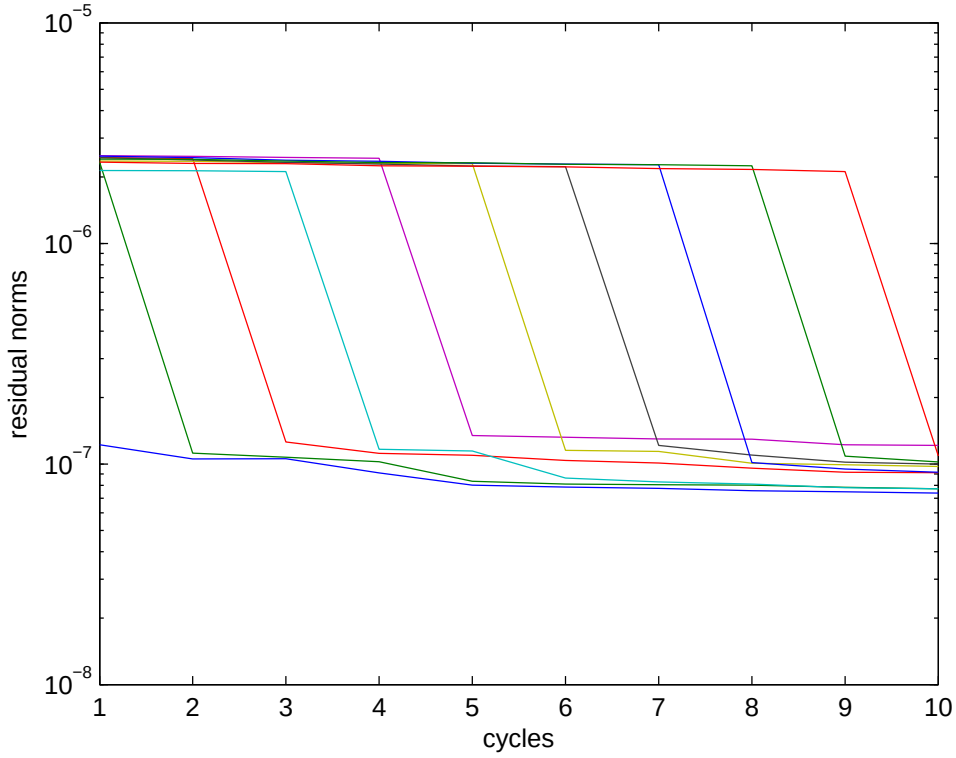

Figure 5.4: Arnoldi-E, using perturbed eigenvectors. Alternate starting vectors.

5.3 Parallel Property Helps Convergence

Theorem 2.3 explains why all eigenvectors can converge at the same time for restarted Arnoldi methods (Algorithm 2.6 and 2.7). The key is the parallel property. We can extend it to a more general setting by using the concept of Krylov decomposition We can prove it by induction. Suppose we have (5.2), so we have

$$Ay_i \in span\{y_i, u\}.$$

$$\text{Then } A^2 y_i \in span\{Ay_i, Au\} \subset span\{y_i, u, Au\}.$$

Now we use induction. Suppose

$$A^j y_i \in span\{y_i, u, Au, \cdots, A^{j-1}u\},$$

$$\begin{aligned}\text{then } A^{j+1} y_i &\in span\{Ay_i, Au, A^2u, \cdots, A^j u\} \\ &\subset span\{y_i, u, Au, A^2u, \cdots, A^j u\}.\end{aligned}$$

So for any $i = 1, \cdots, k$,

$$\begin{aligned}\mathcal{K} &= span\{y_1, y_2, \cdots, y_k, Ay_i, A^2y_i, \cdots, A^{m-k}y_i\} \\ &= span\{y_1, y_2, \cdots, y_k, u, Au, \cdots, A^{m-k-1}u\}. \end{aligned} \tag{5.3}$$

The above says that no matter which vector y_i is used to generate the subspace, it will be equivalent to (5.3). The reason that all eigenvectors can be improved is that

$$Span\{y_i, Ay_i, A^2y_i, \cdots, A^{m-k}y_i\} \subset \mathcal{K}. \tag{5.4}$$

5.4 Near Parallel Property and Near Krylov Property

We have discussed that the parallel property helps convergence of Implicited Restarted Arnoldi in last section. In our new method the parallel property is not satisfied completely on the fine grid, since there is a loss of accuracy when the vectors are moved from a coarser grid to a fine grid. But the idea motivates us to propose the following near parallel property and near Krylov decomposition.

Definition 5.2. Suppose there is a vector r such that

$$Ay_i = \theta_i y_i + a_i r + f_i, \tag{5.5}$$

with f_i to be small, we say the residuals of y_i are nearly parallel.

Let $Y = [y_1, y_2, \cdots, y_k]$, and Θ be a diagonal matrix with corresponding θ_i on the diagonal. We can write the near parallel property in the matrix form:

$$AY = Y\Theta + ra^T + F. \tag{5.6}$$

As shown in last section, the parallel property is induced from the Krylov decomposition, so we also want to define near Krylov decomposition and see its relation with the near parallel property. For further purpose, we give the most general definition of Krylov decomposition, as well as some special Krylov decompositions which satisfy more conditions.

Definition 5.3. For the following three conditions:

(1)

$$AU_m = U_m B_m + u_{m+1} b_{m+1}^T + R, \tag{5.7}$$

where the columns of (U_m, u_{m+1}) are linear independent;

(2)

$$U_m^T u_{m+1} = 0 \text{ and } U_m^T R = 0, \tag{5.8}$$

(3) U_m is orthonormal,

we say there is a general near Krylov decomposition if condition (1) is satisfied. The columns of (U_m, u_{m+1}) are called the basis for the general near Krylov decomposition. R is called the Krylov residual. If condition (3) is also satisfied, which means the basis is orthonormal, we say the decomposition is orthonormal.

Sometimes we may not have condition (3) satisfied, but if condition (2) holds, we can get useful results from the near Krylov decomposition. We may not have an orthonormal basis in (5.7), but the following lemma shows that we can obtain the same Ritz values as if we had an orthonormal basis, if condition (2) holds.

Lemma 5.4. *Let $AU = UB + ub^T + R$ be a general near Krylov decomposition, the columns of $\begin{bmatrix} U & u \end{bmatrix}$ are linearly independent. Suppose (5.8) is satisfied. Assume Q has orthonormal columns, and columns of Q and U span the same subspace. Then B is similar to $Q^T AQ$.*

Proof. Let $U = QR_1$ be the QR decomposition of U, then

$$\begin{aligned} AQR_1 &= QR_1 B + ub^T + R, \\ AQ &= QR_1 BR_1^{-1} + ub^T R_1^{-1} + RR_1^{-1}. \end{aligned} \tag{5.9}$$

Since $U^T u = 0$ and $U^T R = 0$,

$$Q^T(ub^T R_1^{-1}) = (UR_1^{-1})^T(ub^T R_1^{-1}) = (R_1^{-1})^T(U^T u)b^T R_1^{-1} = 0,$$
$$Q^T(RR_1^{-1}) = (UR_1^{-1})^T(RR_1^{-1}) = (R_1^{-1})^T(U^T R)R_1^{-1} = 0.$$

Using the above relations and multiplying Q^T on both sides of (5.9),

$$Q^T AQ = Q^T QR_1 BR_1^{-1} + Q^T ub^T R_1^{-1} + Q^T RR_1^{-1} = R_1 BR_1^{-1}.$$

This means that B is similar to $Q^T AQ$. □

So if (5.8) is satisfied, even if U is not an orthogonal matrix, we can still get the same Ritz values and hence Ritz vectors from the near Krylov decomposition $AU = UB + ub^T + R$.

We are interested in the relation between the near parallel property and the near Krylov property. It is obvious that (5.6) is a special case of (5.7), which means that near parallel property of residuals of k Ritz vectors implies a near Krylov decomposition of dimension k with independent basis. Theorem 5.5 shows that near Krylov decomposition implies the near parallel property.

Theorem 5.5. *Let $AU_m = U_m B + u_{m+1} b^T + R$, where columns of (U_m, u_{m+1}) are linearly independent. Suppose $(\theta_i, g_i), i = 1, \cdots, k$ are eigenpairs of B, denote it by $BG = G\Theta$. Let $y_i = Ug_i$ and $Y = [y_1, \cdots, y_k]$, then $AY_k = Y_k\Theta + ua^T + F$ with $\|F\| \leq \|R\|\|G\|$. If A is symmetric, then $\|F\| \leq \|R\|$.*

Proof.

$$AU = UB + ub^T + R \text{ and } BG = G\Theta,$$
$$AUG = UBG + ub^T G + RG,$$
$$AY = UG\Theta + ub^T G + RG.$$

Let $a^T = u^T G$ and $F = RG$, then

$$AY = Y\Theta + ua^T + F,$$

$$\text{and } \|F\| = \|RG\| \leq \|R\|\|G\|.$$

If A is symmetric, and G has orthonormal columns, then $\|G\| = 1$ and $\|F\| \leq \|R\|$. □

In some cases we may want U to have orthonormal columns in (5.7), and in fact any near Krylov decomposition, including (5.6) can have a near Krylov decomposition with orthonormal basis.

Theorem 5.6. *Suppose there is a near Krylov decomposition*

$$AU = UB + ub^T + R,$$

where columns of (U, u) are linearly independent. Let $U = QR_1$ be the QR decomposition of U, then there is a near Krylov decomposition

$$AQ = QW + qw^T + P,$$

where the columns of $[Q, q]$ are orthonormal and $\|P\| \leq \|R\|\|R_1^{-1}\|$.

Proof.

$$AU = UB + ub^T + R,$$

$$AQR_1 = QR_1B + ub^T + R,$$

$$AQ = QR_1BR_1^{-1} + ub^TR_1^{-1} + RR_1^{-1}.$$

Orthogonalize u against columns of Q and get $u = q + Qg$ where $Q^Tq = 0$. Then

$$AQ = QR_1BR_1^{-1} + (q + Qg)b^TR_1^{-1} + RR_1^{-1},$$

$$AQ = QR_1BR_1^{-1} + qb^TR_1^{-1} + Qgb^TR_1^{-1} + RR_1^{-1},$$

$$AQ = Q(R_1BR_1^{-1} + gb^TR_1^{-1}) + qb^TR_1^{-1} + RR_1^{-1}.$$

Let $W = R_1 B R_1^{-1} + g b^T R_1^{-1}$, $w^T = b^T R_1^{-1}$ and $P = R R_1^{-1}$, we have

$$AQ = QW + uw^T + P,$$

and $\|P\| = \|R R_1^{-1}\| \leq \|P\| \|R_1^{-1}\|$. □

5.5 Maintaining Near Krylov and Near Parallel Property

In Section 5.2, we see that because of the parallel property of all residuals, a Krylov decomposition can be constructed at the end of each restarted Arnoldi cycle. Then the residuals of updated eigenvectors are parallel to each other again, and the algorithm continues. In our new method, we start with a near Krylov subspace $\mathcal{S}$ which contains approximations of eigenvectors, and generate a Krylov subspace $\mathcal{K}$. Let $\mathcal{W}$ to be the overall subspace, then we have

$$\begin{aligned} \mathcal{W} &= \mathcal{S} + \mathcal{K}, \\ \text{where } \mathcal{S} &= span\{y_1, y_2, \cdots, y_k\}, \\ \text{and } \mathcal{K} &= span\{y_j, Ay_j, \cdots, A^{m-k} y_j\} \text{ for some } j. \end{aligned} \tag{5.10}$$

Our goal in this section is to explore how the near Krylov decomposition of $\mathcal{W}$ is constructed, and when the near parallel property of residuals of y_i's in $\mathcal{S}$ can be maintained.

Theorem 5.7 proves that the Krylov residual of the whole subspace $\mathcal{W}$ will not be greater than the Krylov residual of $\mathcal{S}$, if a certain basis is used. Then Theorem 5.8 shows that the Krylov residual of $\mathcal{S}$ will not increase during one cycle. Finally, Corollary 5.9 indicates that if the matrix is symmetric, the near parallel property of residuals will be maintained. Let us conduct a similar analysis for the Arnoldi-E in the new method. At each cycle of Arnoldi-E, there is a certain index j such that

$$\begin{aligned} \mathcal{W} &= \mathcal{S} + \mathcal{K} \\ &= span\{y_1, y_2, \cdots, y_k, Ay_j, A^2 y_j, \cdots A^{m-k} y_j\} \\ &= span\{y_1, y_2, \cdots, y_k, r_j, Ar_j, \cdots A^{m-k-1} r_j\} \text{ for fixed } j, \end{aligned} \tag{5.11}$$

where $r_j = Ay_j - \theta_j y_j$. Let

$$u = \frac{r_j}{\|r_j\|},$$

then u can be considered as the starting vector of $\mathcal{K}$. Although u is not parallel to residuals of all other Ritz eigenvectors, there could be a near Krylov decomposition of $\mathcal{S}$

$$AU_{n\times k} = U_{n\times k}B + ub^T + R_{n\times k}, \tag{5.12}$$

(5.11) and (5.12) play important role in the analysis of Arnoldi-E in the new method.

In the following theorem, we use the general definition of near Krylov decomposition, which means the basis does not have to be orthonormal.

Theorem 5.7. *(The Krylov residual of the whole subspace will not be greater than the Krylov residual of its subspace spanned by approximate eigenvectors) Suppose there is a near Krylov decomposition of a dimension k subspace:*

$$AU_{n\times k} = U_{n\times k}B + ub^T + R_{n\times k}, \tag{5.13}$$

where the columns of $(U_{n\times k}, u)$ *are independent, and*

$$\left[U_{n\times k}, u\right]^T R = 0. \tag{5.14}$$

Suppose there is an Arnoldi decomposition of a dimension p subspace:

$$AV_{n\times p} = V_{n\times p}H + hv_{p+1}e_p^T, \tag{5.15}$$

and u can be written as

$$u = Vd. \tag{5.16}$$

Assume columns of (U, V) *are linear independent, then there is a near Krylov decomposition of dimension* $p + k$

$$A\hat{U}_{n\times(p+k)} = \hat{U}_{n\times(p+k)}\hat{B} + \hat{u}\hat{b}^T + \hat{R}_{n\times(p+k)}, \tag{5.17}$$

where

$$\hat{U}_{n\times(p+k)} = [V, U], \tag{5.18}$$

whose columns are independent. Furthermore,

$$\hat{U}^T_{n\times(p+k)}\hat{u} = 0 \text{ and } \hat{U}^T_{n\times(p+k)}\hat{R}_{n\times(p+k)} = 0, \tag{5.19}$$

$$\|\hat{R}\| \leq \|R\|. \tag{5.20}$$

Proof. Combine (5.13) and (5.15)

$$A\begin{bmatrix} V, U \end{bmatrix} = \begin{bmatrix} V, U \end{bmatrix}\begin{bmatrix} H & \\ & B \end{bmatrix} + \begin{bmatrix} hv_{p+1}e_p^T & 0 \end{bmatrix} + \begin{bmatrix} 0 & ub^T \end{bmatrix} + \begin{bmatrix} 0 & R \end{bmatrix}.$$

Since $u = Vd$ from (5.16),

$$\begin{aligned} A\begin{bmatrix} V, U \end{bmatrix} &= \begin{bmatrix} V, U \end{bmatrix}\begin{bmatrix} H & \\ & B \end{bmatrix} + \begin{bmatrix} hv_{p+1}e_p^T & 0 \end{bmatrix} + \begin{bmatrix} 0 & Vdb^T \end{bmatrix} + \begin{bmatrix} 0 & R \end{bmatrix} \\ &= \begin{bmatrix} V, U \end{bmatrix}\begin{bmatrix} H & db^T \\ & B \end{bmatrix} + \begin{bmatrix} hv_{p+1}e_p^T & 0 \end{bmatrix} + \begin{bmatrix} 0 & R \end{bmatrix}. \end{aligned}$$

Let

$$\begin{aligned} v_{p+1} &= v_0 + \begin{bmatrix} V & U \end{bmatrix} c, \\ \text{and } R &= R_0 + \begin{bmatrix} V & U \end{bmatrix} K, \end{aligned}$$

such that v_0 and columns of R_0 are orthogonal to the columns of V and U.

$$U^T v_0 = 0, V^T v_0 = 0, \tag{5.21}$$

$$U^T R_0 = 0, V^T R_0 = 0. \tag{5.22}$$

Then

$$A\begin{bmatrix} V, U \end{bmatrix} = \begin{bmatrix} V, U \end{bmatrix}\begin{bmatrix} H & db^T \\ & B \end{bmatrix} + \begin{bmatrix} h(v_0 + \begin{bmatrix} V & U \end{bmatrix} c)e_p^T & 0 \end{bmatrix} + \begin{bmatrix} 0 & (R_0 + \begin{bmatrix} V & U \end{bmatrix} K) \end{bmatrix},$$

$$A\begin{bmatrix} V, U \end{bmatrix} = \begin{bmatrix} V, U \end{bmatrix}(\begin{bmatrix} H & db^T \\ & B \end{bmatrix} + hce_p^T + K) + \begin{bmatrix} hv_0e_p^T & 0 \end{bmatrix} + \begin{bmatrix} 0 & R_0 \end{bmatrix}.$$

Let $\hat{U}_{n\times(p+k)} = \begin{bmatrix} V & U \end{bmatrix}$, $\hat{B}_{n\times}(p+k) = \begin{bmatrix} H & db^T \\ & B \end{bmatrix} + hce^T + K$, $\hat{u} = hv_0$, $\hat{b} = e_p$, $\hat{R} = \begin{bmatrix} 0 & R_0 \end{bmatrix}$, then we have

$$A\hat{U}_{n\times(p+k)} = \hat{U}_{n\times(p+k)}\hat{B} + \hat{u}\hat{b}^T + \hat{R}_{n\times(p+k)}.$$

From the construction of $\hat{U}$, $\hat{u}$ and $\hat{R}$. Use (5.21) and (5.22), we have

$$\hat{U}^T\hat{u} = \begin{bmatrix} V & U \end{bmatrix}^T hv_0 = 0,$$
$$\hat{U}^T\hat{R} = \begin{bmatrix} V & U \end{bmatrix}^T \begin{bmatrix} 0 & R_0 \end{bmatrix} = 0.$$

And

$$\|\hat{R}\| = \| \begin{bmatrix} 0 & R_0 \end{bmatrix} \| = \|R_0\| \leq \|R\|. \tag{5.23}$$

□

From the proof of Theorem 5.7, (5.23) tells us that in order to make $\|\hat{R}\|$ to be small, we need $\|R_0\|$ to be small. Since $R = R_0 + \begin{bmatrix} V & U \end{bmatrix} K$, this means if the Krylov residual R of the near Krylov subspace portion $\mathcal{S}$ can be expanded in terms of the vectors of the Krylov subspace portion $\mathcal{K}$ as $\begin{bmatrix} V & U \end{bmatrix} K$, then the Krylov residual of the overall subspace $\mathcal{W}$ can be reduced. Increasing the dimension of the Krylov subspace portion $\mathcal{K}$ may be one way to do it.

Theorem 5.8. *(Krylov residual of eigenvector subspace would not increase during one cycle) Assume there is a near Krylov decomposition*

$$AU_{n\times k} = U_{n\times k}B + ub^T + R_{n\times k}$$

corresponding to the basis $\{y_1, y_2, \cdots, y_k\}$, *and* $\begin{bmatrix} U_{n\times k}, u \end{bmatrix}^T R = 0$. *Suppose the subspace we generate for Arnoldi-E procedure is*

$$span\{y_1, y_2, \cdots, y_k, u, Au, A^2u, \cdots, A^{m-k-1}u\},$$

and the new k Ritz vectors $\{y_1^{new}, y_2^{new}, \cdots, y_k^{new}\}$ *are obtained. There is a near Krylov decomposition*

$$AU_{n\times k}^{new} = U_{n\times k}^{new} B^{new} + u^{new}(b^{new})^T + R_{n\times k}^{new},$$

where the columns of $U_{n\times k}^{new}$ *span the same subspace as* $\{y_1^{new}, y_2^{new}, \cdots, y_k^{new}\}$*, and*

$$\|R^{new}\| \leq \|R\|.$$

Proof. For the subspace $\{y_1, y_2, \cdots, y_k\}$, there is a near Krylov decomposition from the assumption

$$AU_{n\times k} = U_{n\times k} B + ub^T + R_{n\times k},$$

For the subspace $span\{u, Au, A^2u, \cdots, A^{m-k-1}u\}$, there is an Arnoldi decomposition

$$AV_{n\times(m-k)} = V_{n\times(m-k)} H + ve_{n\times(m-k)}^T.$$

And $u = Ve_1$ since it is the starting vector of the Krylov subspace portion. According to Theorem 5.7, there is a near Krylov decomposion

$$A\hat{U}_{n\times m} = \hat{U}_{n\times m}\hat{B} + \hat{u}\hat{b}^T + \hat{R}_{n\times m}, \tag{5.24}$$

$$\text{where } \hat{U}_{n\times m} = \begin{bmatrix} V & U \end{bmatrix}, \tag{5.25}$$

and we also have

$$\|\hat{R}_{n\times m}\| \leq \|R\|, \tag{5.26}$$

$$\hat{U}^T\hat{u} = 0, \hat{U}^T\hat{R} = 0. \tag{5.27}$$

According Lemma 5.4, $\hat{B}$ is similar to the matrix Q^TAQ where columns of Q are orthonormal basis of

$$span\{y_1, y_2, \cdots, y_k, u, Au, A^2u, \cdots, A^{m-k-1}u\}.$$

Hence eigenvalues of B are Ritz values corresponding to the subspace.

Here we assume the k Ritz values of $\hat{B}$ that we want are separated from the other $m-k$ unwanted Ritz values. Which means $\{\theta_1, \cdots, \theta_k\} \cap \{\theta_{k+1}, \cdots, \theta_m\} = \emptyset$. Then according Theorem 2.10, we can write the Shur decomposition of $\hat{B}$ as

$$\hat{B}[G_1, G_2] = [G_1, G_2] \begin{bmatrix} T_{11} & T_{12} \\ 0 & T_{22} \end{bmatrix},$$

where the eigenvalues of T_{11} are the new k Ritz values we want. And hence

$$\hat{B}G_1 = G_1 T_{11}. \tag{5.28}$$

Multiply both sides of (5.24) by G_1, we get

$$\begin{aligned} A\hat{U}_{n\times m}G_1 &= \hat{U}_{n\times m}\hat{B}G_1 + \hat{u}\hat{b}^T G_1 + \hat{R}_{n\times m}G_1, \\ &= \hat{U}_{n\times m}G_1 T_{11} + \hat{u}\hat{b}^T G_1 + \hat{R}_{n\times m}G_1. \end{aligned} \tag{5.29}$$

Let $U^{new} = \hat{U}_{n\times m}G_1$, $B^{new} = T_{11}$, $u^{new} = \hat{u}$, $(b^{new})^T = \hat{b}^T G_1$ and $R^{new} = \hat{R}_{n\times m}G_1$, then

$$AU^{new} = U^{new}B^{new} + u^{new}(b^{new})^T + R^{new}.$$

The subspace spanned by the columns of U^{new} is $span\{y_1^{new}, y_2^{new}, \cdots, y_k^{new}\}$.
Use (5.26) and $\|G_1\| = 1$,

$$\|R^{new}\| = \|\hat{R}_{n\times(k+m)}G_1\| \leq \|\hat{R}_{n\times(k+m)}\|\|G_1\| \leq \|R\|.$$

□

If $U_{n\times k}$ has orthonormal columns in the assumption of Theorem 5.8, then

$$U_{n\times k}^{new} = \hat{U}_{n\times(k+m)}G_1 = [V, U]G_1$$

will be nearly orthonormal. This can happen when A is symmetric and $U_{n\times k}$ has Ritz vectors as its columns.

Corollary 5.9. *(Maintaining near parallel property) If A is symmetric, and the residuals of $\{y_1, y_2, \cdots, y_k\}$ are parallel,*

$$AY_{n\times k} = Y_{n\times k}\Theta + ra^T + F_{n\times k}.$$

After one cycle of Arnoldi-E with the subspace $\mathcal{K}$ generated as (5.11), we can get (5.24) as in the proof of Theorem 5.8. the residuals of updated Ritz vectors of $\{y_1^{new}, y_2^{new}, \cdots, y_k^{new}\}$ are near parallel,

$$AY_{n\times k}^{new} = Y_{n\times k}^{new}\Theta^{new} + r^{new}(a^{new})^T + F_{n\times k}^{new}.$$
$$\text{and } \|F_{n\times k}^{new}\| \le \|F_{n\times k}\|\|R^{-1}\|, \text{ where } QR = \hat{U}_{n\times m} \ (\hat{U}_{n\times m} \text{ is from (5.24)}).$$

Proof. We use the same proof as Theorem 5.8, and get

$$A\hat{U}_{n\times m} = \hat{U}_{n\times m}\hat{B} + \hat{u}\hat{b}^T + \hat{R}_{n\times m} \text{ with } \|\hat{R}_{n\times m}\| \le \|F_{n\times k}\|. \tag{5.30}$$

Let $\hat{U}_{n\times m} = QR$, the above equation becomes

$$AQR = QR\hat{B} + \hat{u}\hat{b}^T + \hat{R}_{n\times m},$$
$$AQ = QR\hat{B}R^{-1} + \hat{u}\hat{b}^T R^{-1} + \hat{R}_{n\times m}R^{-1}.$$

Notice since A is symmetric and $R\hat{B}R^{-1} = \hat{U}^T A\hat{U}$, so $R\hat{B}R^{-1}$ is symmetric. Hence (5.28) becomes

$$R\hat{B}R^{-1}G_1 = G_1\Theta,$$

where T_{11} in (5.28) becomes Θ with the desired eigenvalues on the diagonal, and columns of G_1 are eigenvectors of $R\hat{B}R^{-1}$ corresponding to them with $\|G_1\| = 1$. Since $QG_1 = Y^{new}$,

$$AQG_1 = QR\hat{B}R^{-1}G_1 + \hat{u}\hat{b}^T R^{-1}G_1 + \hat{R}_{n\times m}R^{-1}G_1,$$
$$AY_{n\times k}^{new} = Y_{n\times k}^{new}\Theta^{new} + r^{new}(a^{new})^T + F_{n\times k}^{new}.$$

where $r^{new} = \hat{u}$, $(a^{new})^T = \hat{b}^T R^{-1} G_1$, $F^{new}_{n\times k} = \hat{R}_{n\times m} R^{-1} G_1$. And we have

$$\|F^{new}_{n\times k}\| = \|\hat{R}_{n\times m} R^{-1} G_1\| = \|\hat{R}_{n\times m} R^{-1}\| \leq \|\hat{R}_{n\times m} R^{-1}\| \leq \|F_{n\times k}\| \|R^{-1}\|.$$

□

From experiments we observe that the matrix $\hat{U}_{n\times m}$ in (5.30) is almost orthonormal, and $\|R^{-1}\|$ is very close to 1.

5.6 Near Parallel Helps Convergence

In Section 5.3, we saw how the parallel property (5.2) works so that all approximate eigenvectors can be improved at the same time in Arnoldi(m,k). It is because the whole subspace contains Krylov subspaces with each eigenvector as the starting vector (5.4), i.e, $span\{y_i, Ay_i, \cdots, A^{m-k}y_i\}$. In this section we aim to explain the convergence of Arnoldi-E with similar ideas.

We first prove the whole subspace contains Krylov subspaces with each eigenvector as the starting vector, except the matrix is the original matrix with a perturbation E, i.e, $span\{y_i, (A+E)y_i, \cdots, (A+E)^{m-k}y_i\}$. We give two proofs in 5.6.1 and 5.6.2 for it, one is from the near parallel perspective, and the other is from the near Krylov perspective. Then we give a bound on the difference between two vectors from the Krylov subspace $span\{y_i, Ay_i, \cdots, A^{m-k}y_i\}$ and the Krylov subspace $span\{y_i, (A+E)y_i, \cdots, (A+E)^{m-k}y_i\}$ in 5.6.3.

5.6.1 From the Near Parallel Perspective

Let's focus on only two vectors and see how the near parallel property can help them converge together. This proof is motivated by the induction from (5.2) to (5.3) in Section 5.3.

Theorem 5.10. *Suppose*

$$Ay_1 = \theta_1 y_1 + a_1 r \text{ and } Ay_2 = \theta_2 y_2 + a_2 r + f,$$

with $\|y_1\| = \|y_2\| = 1$. *There is a matrix* E *such that*

$$span\{y_2, (A+E)y_2, \cdots, (A+E)^p y_2\} \subset span\{y_1, Ay_1, \cdots, A^p y_1, y_2\}. \tag{5.31}$$

Let

$$y_2 = \alpha y_2^K + \beta y_2^{\perp K}, \tag{5.32}$$

where $\|y_2^K\| = \|y_2^{\perp K}\| = 1$, $y_2^K \in \mathcal{K} = span\{y_1, Ay_1, \cdots, A^p y_1\}$ *and* $y_2^{\perp K} \perp \mathcal{K}$, *then one choice of* E *is:*

$$E = -\frac{1}{\beta} f (y_2^{\perp K})^T \text{ and } \|E\| \leq \frac{\|f\|}{\beta}.$$

Proof. Let $E = -\frac{1}{\beta} f (y_2^{\perp K})^T$, since $y_2^{\perp K} \perp y_1$,

$$(A+E)y_1 = Ay_1 - \frac{1}{\beta} f (y_2^{\perp K})^T y_1 = Ay_1 = \theta_1 y_1 + a_1 r,$$
$$(A+E)y_2 = Ay_2 - \frac{1}{\beta} f (y_2^{\perp K})^T y_2 = Ay_2 - \frac{1}{\beta} f (y_2^{\perp K})^T y_2 = Ay_2 - f = \theta_2 y_2 + a_2 r,$$

So y_1 and y_2 have parallel residuals under the multiplication of $A+E$. Use the same induction from (5.2) to (5.3) in section 5.3, we can get:

$$span\{y_2, (A+E)y_2, \cdots, (A+E)^p y_2\} \subset span\{y_1, (A+E)y_1, \cdots, (A+E)^p y_1, y_2\}.$$

Next we want to show that

$span\{y_1, (A+E)y_1, \cdots, (A+E)^p y_1, y_2\} = span\{y_1, Ay_1, \cdots, A^p y_1, y_2\}$.

We have $(A+E)y_1 = Ay_1$ from above, and suppose

$$\begin{aligned}
(A+E)^j y_1 &= A^j y_1, \\
\text{then } (A+E)^{j+1} y_1 &= (A+E)A^j y_1 \\
&= A^{j+1} y_1 + E A^j y_1 \\
&= A^{j+1} y_1 - \frac{1}{\beta} f (y_2^{\perp K})^T A^j y_1 \\
&= A^{j+1} y_1, \text{ since } y_2^{\perp K} \perp A^j y_1 \text{ for } j = 1, \cdots, p-1.
\end{aligned}$$

So $span\{y_2, (A+E)y_2, \cdots, (A+E)^p y_2\} \subset span\{y_1, (A+E)y_1, \cdots, (A+E)^p y_1, y_2\}$

$$= span\{y_1, Ay_1, \cdots, A^p y_1, y_2\}.$$

And

$$\|E\| = \| - \frac{1}{\beta} f(y_2^{\perp K})^T \| \leq \frac{\|f\| \|(y_2^{\perp K})^T\|}{\|\beta\|} = \frac{\|f\|}{\|\beta\|}.$$

□

It seems when A is symmetric or near symmetric, the projection of y_2 on $\{y_1, Ay_1, \cdots, A^p y_1\}$ is very small. Hence α in (5.32) is small and β is close to 1. $\|E\|$ is mainly determined by $\|f\|$.

5.6.2 From the Near Krylov Perspective

There is another way to prove Theorem 5.10, from the perspective of near Krylov decomposition. However, we get the same result by this different approach. Any Krylov subspace has a corresponding Arnoldi decomposition $AV = VH + ve^T$, where (V, v) is orthonormal and H is an upper Hessenberg. Ve_1, the first column of V, is the starting vector of the Krylov subspace. According to the implicit Q-theorem, it is unique. We are going to prove under the context of Theorem 5.10, there is an Arnoldi decomposition $(A+E)Q = QH + qe^T$ with (Q, q) orthonormal and H upper Hessenberg. Q is constructed so that the eigenvector y_2 is the first column, and hence there is a Krylov subspace with y_2 as the starting vector.

Theorem 5.10 (continuing from p. 69). *Suppose* $Ay_1 = \theta_1 y_1 + a_1 r$ *and* $Ay_2 = \theta_2 y_2 + a_2 r + f$ *with* $\|y_1\| = \|y_2\| = 1$. *Thereis a matrix* E *such that*

$$(A+E)Q_{n\times p} = Q_{n\times p} H_{p\times p} + q e_{p+1}^T \text{ with } Qe_1 = y_2.$$

We will show that

$$span\{y_2, (A+E)y_2, \cdots, (A+E)^p y_2\} = span\{q_1, q_2, \cdots, q_{p+1}\}$$

$$\subset span\{y_1, Ay_1, \cdots, A^p y_1, y_2\}. \tag{5.33}$$

Furthermore, let

$$y_2 = \alpha y_2^K + \beta y_2^{\perp K},$$

as in Theorem 5.10, E will be the same.

$$E = -\frac{1}{\beta} f (y_2^{\perp K})^T \text{ and } \|E\| \leq \frac{\|f\|}{\beta}.$$

Proof. From (5.11), when there are only two Ritz vectors,

$$\mathcal{W} = span\{y_1, y_2, r, Ar, \cdots, A^{p-1}r\}.$$

If we put y_2 as the first vector, we can have

$$\begin{aligned} & A \begin{bmatrix} y_2 & r & \cdots & A^{p-1}y & y_1 \end{bmatrix}_{n\times(p+2)} \\ & = \begin{bmatrix} y_2 & r & \cdots & A^{p-1}y & y_1 \end{bmatrix} \begin{bmatrix} \theta_2 & 0 & & & * \\ a_2 & 0 & & & * \\ 0 & 1 & 0 & & * \\ 0 & 0 & 1 & & * \\ \vdots & & & \ddots & \\ 0 & 0 & \cdots & 1 & * \\ 0 & & \cdots & & * \ \theta_1 \end{bmatrix}_{(p+2)\times(p+2)} + v e_{p+1}^T \\ & + \begin{bmatrix} f & 0 & \cdots & 0 \end{bmatrix}_{n\times(p+2)}, \end{aligned} \tag{5.34}$$

where

$$\begin{bmatrix} y_2 & r & \cdots & A^{p-1}y & y_1 \end{bmatrix}^T v = 0.$$

Let

$$H_0 = \begin{bmatrix} \theta_2 & 0 & & & * \\ a_2 & 0 & & & * \\ 0 & 1 & 0 & & * \\ 0 & 0 & 1 & & * \\ \cdots & & & & \\ 0 & 0 & \cdots & 1 & * \\ & & & & \theta_1 \end{bmatrix}$$

be the upper Henssenberg matrix. (5.34) becomes

$$AQR = QRH_0 + ve_{p+1}^T + \begin{bmatrix} f & 0 & \cdots & 0 \end{bmatrix}.$$

Let

$$\begin{bmatrix} y_2 & r & Ar & \cdots & A^{p-1}y & y_1 \end{bmatrix} = QR \tag{5.35}$$

be the QR decomposition where $Qe_1 = y_2$, then

$$AQ = Q(RH_0R^{-1}) + ve_{p+1}^T R^{-1} + \begin{bmatrix} f & 0 & \cdots & 0 \end{bmatrix} R^{-1}.$$

Let $H = RH_0R^{-1}$. Since H_0 is Upper Hessenberg, R and R^{-1} are upper triangular, so H is upper Hessenberg.

$$AQ = QH + ve_{p+1}^T R^{-1} + \begin{bmatrix} f & 0 & \cdots & 0 \end{bmatrix} R^{-1}. \tag{5.36}$$

Now we move the Krylov residual at the end of (5.36) back to A,

$$AQ - \begin{bmatrix} f & 0 & \cdots & 0 \end{bmatrix} R^{-1} = QH + ve_{p+1}^T R^{-1},$$
$$(A - \begin{bmatrix} f & 0 & \cdots & 0 \end{bmatrix} R^{-1}Q^T)Q = QH + ve_{p+1}^T R^{-1}.$$

And we get

$$(A + E)Q = QH + ve_{p+1}^T R^{-1}, \tag{5.37}$$

where

$$E = - \begin{bmatrix} f & 0 & \cdots & 0 \end{bmatrix} R^{-1}Q^T. \tag{5.38}$$

Since

$$\begin{aligned} e_{p+1}^T R^{-1} &= [0, 0, \cdots, 0, *, *]_{(p+2)\times(p+2)} \\ &= [0, 0, \cdots, 0, R^{-1}_{(p+1)\times(p+1)}, R^{-1}_{(p+2)\times(p+2)}]. \end{aligned}$$

Equating the first p columns on both sides of (5.37), we have

$$(A+E)Q = QH + qe_{p+1}^T, \tag{5.39}$$
$$\text{where } q = vR^{-1}_{(p+1)\times(p+1)}.$$

According to the implicit Q-theorem, (5.39) indicates that the first p columns of Q form a basis of a Krylov subspace with the starting vector y_2 for the matrix $A+E$.

$$span\{q_1, q_2, \cdots, q_{p+1}\} = span\{y_2, (A+E)y_2, \cdots, (A+E)^p y_2\}$$
$$\subset span\{q_1, q_2, \cdots, q_{p+1}, q_{p+2}\} = span\{y_1, Ay_1, \cdots, A^p y_1, y_2\}.$$

This proves (5.33).

Next we will show the bound for E. (5.38) shows that the norm of E is determined by Q and R, where Q and R is from (5.35) and $QR = \begin{bmatrix} y_2 & r & Ar & \cdots & A^{p-1}r & y_1 \end{bmatrix}$. Instead of this matrix, we look at another matrix by changing the order of the columns. Assume

$$\begin{bmatrix} r & Ar & \cdots & A^{p-1}r & y_1 & y_2 \end{bmatrix} = Q_2 R_2, \tag{5.40}$$

where

$$Q_2(:, \text{end}) = Q_2(:, p+2) = y_2^{\perp K}, \tag{5.41}$$
$$\text{and } R_2(\text{end}, \text{end}) = R_2(p+2, p+2) = \beta. \tag{5.42}$$

Notice that

$$\begin{bmatrix} r & Ar & \cdots & A^{p-1}r & y_1 & y_2 \end{bmatrix} \begin{bmatrix} 0 & I_{(p+1)\times(p+1)} \\ 1 & 0 \end{bmatrix} = \begin{bmatrix} y_2 & r & Ar & \cdots & A^{p-1}r & y_1 \end{bmatrix}. \tag{5.43}$$

So

$$
\begin{aligned}
R &= Q^T \begin{bmatrix} y_2 & r & Ar & \cdots & A^{p-1}r & y_1 \end{bmatrix} \\
&= Q^T \begin{bmatrix} r & Ar & \cdots & A^{p-1}r & y_1 & y_2 \end{bmatrix} \begin{bmatrix} 0 & I_{(p+1)\times(p+1)} \\ 1 & 0 \end{bmatrix} \text{(use (5.43))} \\
&= Q^T Q_2 R_2 \begin{bmatrix} 0 & I_{(p+1)\times(p+1)} \\ 1 & 0 \end{bmatrix} .\text{(use (5.40))}
\end{aligned} \tag{5.44}
$$

And then

$$
\begin{aligned}
E &= -\begin{bmatrix} f & 0 & \cdots & 0 \end{bmatrix} R^{-1} Q^T \\
&= -\begin{bmatrix} f & 0 & \cdots & 0 \end{bmatrix} \begin{bmatrix} 0 & I_{(p+1)\times(p+1)} \\ 1 & 0 \end{bmatrix}^T R_2^{-1} Q_2^T Q Q^T \text{(use (5.44))} \\
&= -\begin{bmatrix} f & 0 & \cdots & 0 \end{bmatrix} \begin{bmatrix} 0 & 1 \\ I_{(p+1)\times(p+1)} & 0 \end{bmatrix} R_2^{-1} Q_2^T \\
&= -\begin{bmatrix} 0 & 0 & \cdots & f \end{bmatrix} R_2^{-1} Q_2^T \\
&= -R_2^{-1}(p+2, p+2) \begin{bmatrix} 0 & 0 & \cdots & f \end{bmatrix} Q_2^T \\
&= -R_2^{-1}(p+2, p+2) f Q_2(:, p+2)^T \\
&= -\frac{1}{\beta} f (y_2^{\perp K})^T.
\end{aligned}
$$

The last step uses (5.41) and (5.42). So

$$
|E\| = \| -\frac{1}{\beta} f (y_2^{\perp K})^T \| \leq \frac{\|f\|}{\|\beta\|}.
$$

□

5.6.3 Bound for Vectors in Two Krylov Subspaces

Theorem 5.10 shows that $span\{y_2, (A+E)y_2, \cdots, (A+E)^p y_2\} \subset span\{y_1, Ay_1, \cdots, A^p y_1, y_2\}$. In this subsection we want to discuss how such deviation affects the

convergence of y_2. There are a lot of discussions related to perturbation theory. For the symmetric case or when matrices are diagonalizable, we can do spectral analysis. Here we want to study general cases, and we use the Cauchy integral to express matrix functions. The idea can be found in the reference [12] [13]. We first introduce some background, and then give the theorem for our method.

Any vector in $span\{y, Ay, \cdots, A^p y\}$ can be written as $p(A)y$ with degree p, and any vector in $span\{y_2, (A+E)y_2, \cdots, (A+E)^p y_2\}$ is $p(A+E)y$. $p(A)$ is a matrix function, so by using the Cauchy integral, it would be

$$p(A) = \frac{1}{2\pi i}\int_\Gamma p(z)(zI - A)^{-1}dz.$$

And $p(A + E)$ is

$$p(A + E) = \frac{1}{2\pi i}\int_\Gamma p(z)(zI - A - E)^{-1}dz.$$

In order to bound $\|p(A) - p(A + E)\|$, we look at the bound of $\|(zI - A)^{-1} - (zI - A - E)^{-1}\|$. Since

$$\begin{aligned}&(I - (zI - A)^{-1}E)^{-1}(zI - A)^{-1}(zI - A - E)\\ =&(I - (zI - A)^{-1}E)^{-1}(I - (zI - A)^{-1}E) = I,\end{aligned}$$

so the resolvent $(zI - A - E)^{-1}$ for $p(A + E)$ is

$$(zI - A - E)^{-1} = (I - (zI - A)^{-1}E)^{-1}(zI - A)^{-1}. \tag{5.45}$$

If $\|(zI - A)^{-1}E\| \le \|(zI - A)^{-1}\|\|E\| < 1$, which means $\|E\| < \dfrac{1}{\|(zI - A)^{-1}\|}$, then $(I - (zI - A)^{-1}E)^{-1}$ has a convergent Neumann series, and (5.45) can be expanded as

$$(zI - A - E)^{-1} = \sum_{j=0}^{\infty}((zI - A)^{-1}E)^j(zI - A)^{-1}.$$

Then

$$(zI - A - E)^{-1} - (zI - A)^{-1} = \sum_{j=1}^{\infty}((zI - A)^{-1}E)^j(zI - A)^{-1}.$$

Let $\|E\| = \epsilon$ and $\dfrac{1}{\|(zI-A)^{-1}\|} = \delta$. Then $\|(zI-A)^{-1}E\| \le \|(zI-A)^{-1}\|\|E\| = \dfrac{\epsilon}{\delta}$.

$$\begin{aligned}\text{And } \|(zI-A-E)^{-1} - (zI-A)^{-1}\| &= \|\sum_{j=1}^{\infty}((zI-A)^{-1}E)^j(zI-A)^{-1}\| \\ &\le \sum_{j=1}^{\infty}(\frac{\epsilon}{\delta})^j\frac{1}{\delta} = \frac{\frac{\epsilon}{\delta}}{1-\frac{\epsilon}{\delta}}\frac{1}{\delta} \\ &= \frac{\epsilon/\delta}{\delta-\epsilon}. \end{aligned} \tag{5.46}$$

In the Cauchy integral the curve Γ is a finite union of Jordan curves in the complex plane whose interior contains the spectra of A and $A+E$. To make bounds for such integrals, we choose the curve Γ to be the boundary of the δ-psedospectrum of A. There are several equivalent definitions of δ-psedospectrum, and here are two of them.

$$\sigma_\delta := \{z \in C : \|(zI-A)^{-1}\| > 1/\delta\}.$$

$$\sigma_\delta := \{z \in C : z \in \sigma(A+E) \text{ for some } \|E\| < \delta\}.$$

The following theorem finds the bound of $p(A)y$ and $p(A+E)y$ for our method. It is based on the work of [28].

Theorem 5.11. *Suppose there are two Krylov subspaces $K_1 = span\{y, Ay, \cdots, A^{m-1}y\}$ and $K_2 = span\{y, (A+E)y, \cdots, (A+E)^{m-1}y\}$ with the perturbation matrix $\|E\| = \epsilon$ and $\|y\| = 1$. Let $\delta = \dfrac{1}{\|(zI-A)^{-1}\|} \gg \epsilon$, if the best approximation of an eigenvector z is $\hat{y} = p(A)y$ from K_1, then $\tilde{y} = p(A+E)y$ is an approximation of z in K_2 with $\|\hat{y} - \tilde{y}\| \le O(\epsilon)$.*

Proof.

$$\begin{aligned}
\|\hat{y} - \tilde{y}\| &\leq \|p(A)y - p(A+E)y\| \\
&\leq \|p(A) - p(A+E)\|\|y\| \\
&\leq \frac{1}{2\pi}\| \int_\Gamma p(z)((zI - A - E)^{-1} - (zI - A)^{-1})dz\| \\
&\leq \frac{L_\delta}{2\pi}(\max_{z\in\Gamma}|p(z)|)(\max\|(zI - A - E)^{-1} - (zI - A)^{-1})\|) \text{ (use (5.43))} \\
&\leq (\frac{\epsilon}{\delta - \epsilon})(\frac{L_\delta}{2\pi\delta})\max_{z\in\Gamma}|p(z)| \\
&= O(\epsilon),
\end{aligned}$$

where L_δ denotes the arc length of $\Gamma = \partial\sigma_\delta(A)$. □

5.7 Examples

5.7.1 Fix the Starting Vector

Two examples are shown in this subsection, one has a symmetric matrix, and the other deals with a non-symmetric problem. These experiments aim to verify Theorems 5.7-5.10. In order to make explanations clearer, we fix the starting vector as Arnoldi-E proceeds on the fine grid.

Example 5.12. Problem: $-u'' = \lambda u$. matrix size A is 1023 on the fine grid, and the coarse grid is 256. The convergence tolerance for the smallest 10 eigenpairs on the coarse grid is 1e-3. Then on the fine grid, we use the approximation for the first eigenvector as the starting vector for Arnoldi-E. So instead of cycling through all desired Ritz vectors, y_1 is always the starting vector.

Here are three figures. Figure 5.5 shows that the near Krylov property is maintained in each cycle, and Figures 5.6 and 5.7 show how the near Krylov property can help the convergence of eigenvectors.

Let the whole subspace be $\mathcal{W} = \mathcal{S} + \mathcal{K}$ as described in (5.11). The Krylov decompositions for $\mathcal{S}$ and $\mathcal{W}$ are:

$$AU_{n\times k} = U_{n\times k}B + ub^T + R_{n\times k},$$
$$A\hat{U}_{n\times m} = \hat{U}_{n\times m}\hat{B} + \hat{u}\hat{b}^T + \hat{R}_{n\times m}.$$

In Figure 5.5, stars are Krylov residuals of $\mathcal{S}$ at the beginning of each cycle, which are $\|R_{n\times k}\|$. Dots are Krylov residuals of $\mathcal{W}$ at the same cycle, which are $\|\hat{R}_{n\times m}\|$. We can see dots are always below stars, which verifies the result of Theorem 5.7 that $\|\hat{R}_{n\times m}\| \leq \|R_{n\times k}\|$. Then in the next cycle, $\|R^{new}_{n\times k}\|$ is determined by $\|\hat{R}_{n\times m}\|$, and the Krylov residual does not increase. We have $\|R^{new}_{n\times k}\| \leq \|\hat{R}_{n\times m}\| \leq \|R_{n\times k}\|$ as shown in Theorem 5.8.

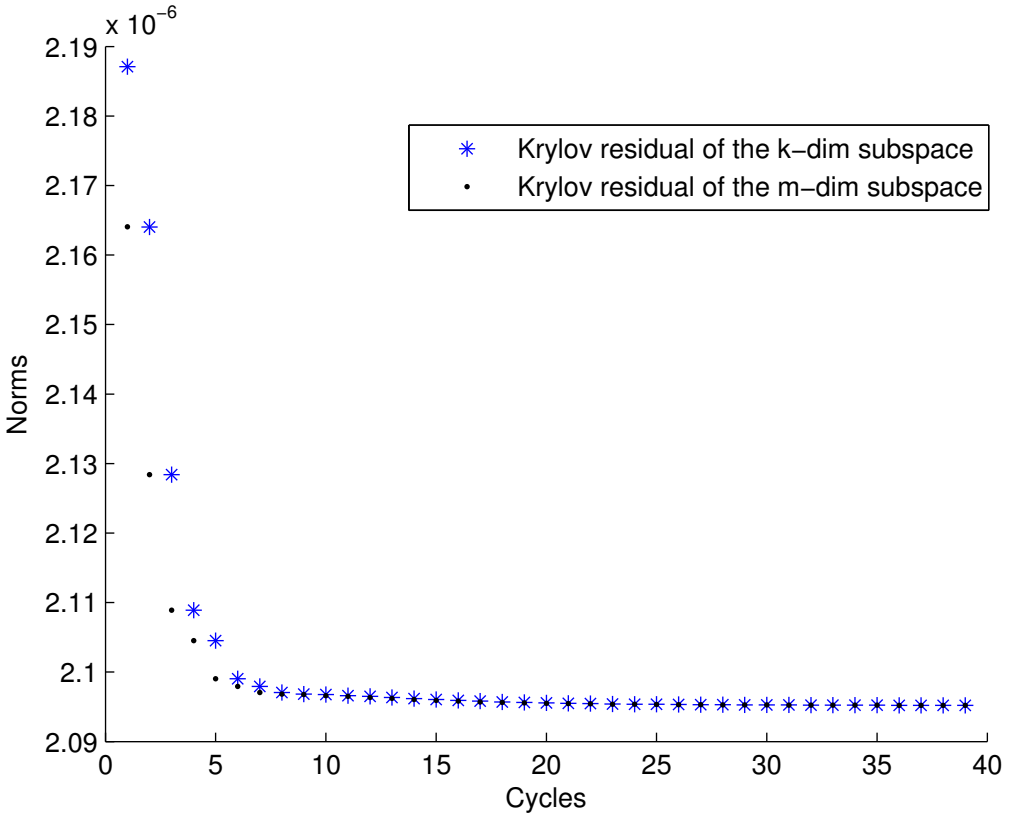

Figure 5.5: Maintain near Krylov property. A is symmetric. Starting vector is fixed as y_1.

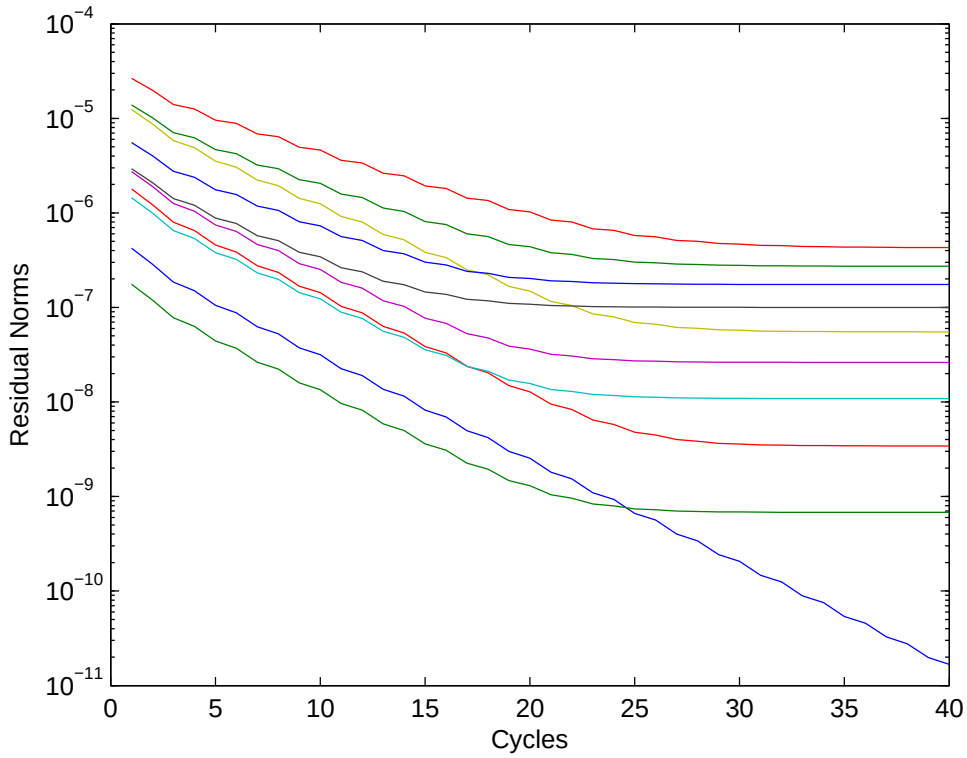

Figure 5.6: Near parallel helps convergence. A is symmetric. Starting vector is fixed as y_1.

Figure 5.6 shows the residual norms of 10 approximate eigenvectors on the fine grid. We restart each cycle with the first Ritz vector in this experiment, but all other eigenvectors converge together for about 20 cycles, then they level off. It seems each vector has a limit and when the residual reaches that limit, the accuracy does not change.

In Figure 5.7 we only plot the residual of two eigenvectors and discuss what the limit is for one specific vector. It shows the residuals of the first and second vectors. Suppose

$$Ay_1 = \theta_1 y_1 + a_1 r_1,$$

$$Ay_2 = \theta_2 y_2 + a_2 r_1 + f_2,$$

where $f_2 \perp r_1$.

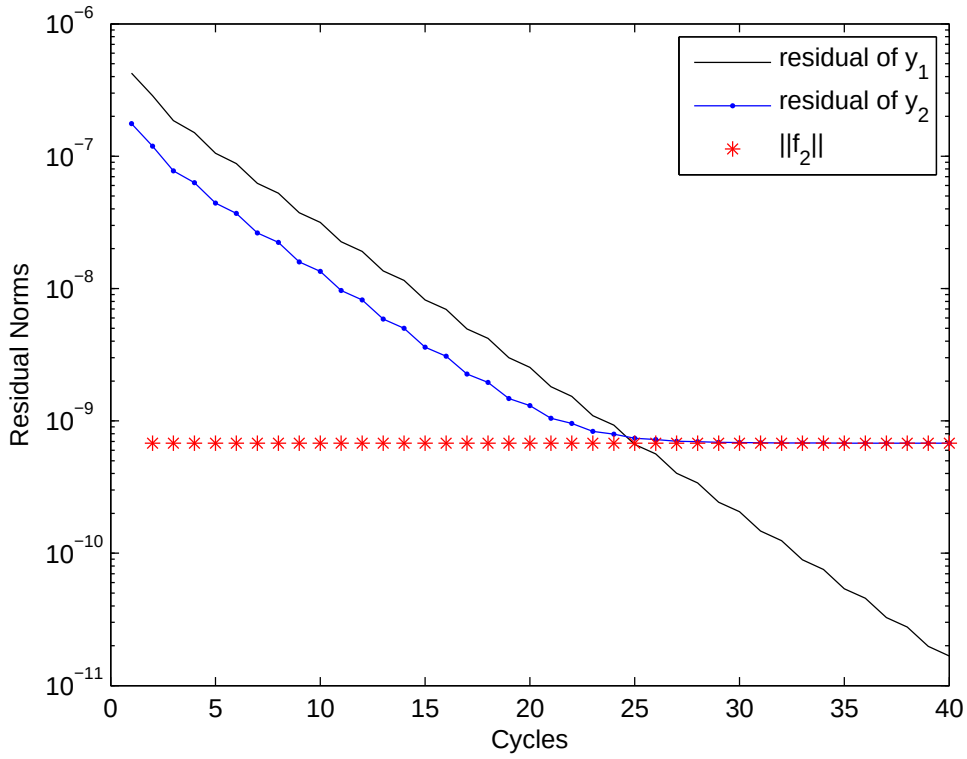

Figure 5.7: Near parallel helps convergence. A is symmetric. Starting vector is fixed as y_1.

In Figure 5.7, red stars represent $\|f_2\|$, which measures how parallel the two vectors are. $\|f_2\|$ does not change much, and it slightly decreases, which illustrates that the near parallel property is maintained. When the residual norm of the second vector is bigger than $\|f_2\|$, the second vector is improved and the residual norm converges down to $\|f_2\|$, which is about 1e-9. When the residual norm reaches the level of $\|f_2\|$, it is not improved. According to Theorem 5.10, we find $p(A+E)y_2$ in the subspace each time, where $\|E\|$ is almost the same as $\|f_2\|$ in the symmetric case. Finally we get the eigenvector of $A+E$ and E has norm about 1e-9.

We can see from Figure 5.6 that other vectors have their own limits of convergence, which should be determined by $\|f_i\|$ where $Ay_i = \theta_i y_i + a_i r_1 + f_i$. So if the residuals of approximate eigenvectors are more parallel to each other, then it is more likely that they will converge together, and then Arnoldi-E is more efficient.

In the next example, we add the coefficient to u' in the differential equation and then the matrix A is non-symmetric.

Example 5.13. Problem: $-u'' + 100u' = \lambda u$. The matrix A has the form (2.11). The size is 1023 on the fine grid, and the coarse grid is 255. We get the accuracy of 1e-3 for the smallest 15 eigenpairs on the coarse grid. Then on the fine grid, we fix the first Ritz vector y_1 as the starting vector.

We show three figures as in Example 5.12, which are supposed to verify the near Krylov property and how it works for convergence. Since A is not symmetric, the results are very different from the above symmetric problem. Figure 5.8 shows again the Krylov residuals of the whole subspace $\mathcal{W}$ are not bigger than the k-dimensional subspace $\mathcal{S}$, but Figure 5.8 is very different from Figure 5.5.

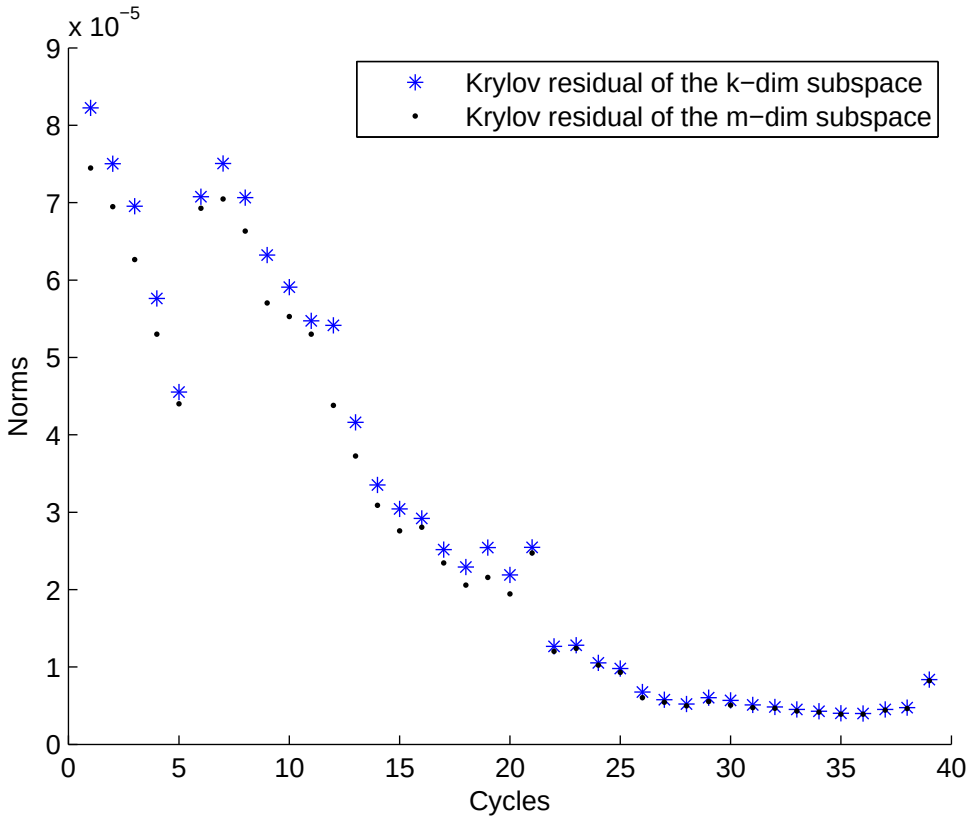

Figure 5.8: Maintain near parallel and near Krylov property. A is non-symmetric. Starting vector is fixed as y_1.

In Figure 5.5, the stars are slightly smaller in magnitude than the dots in the previous cycle, but in Figure 5.8, there are stars larger than the dots in the previous cycle. The reason is that in the figures we plot the norm of $R_{n\times k}$ and $\hat{R}_{n\times m}$, where

$$\begin{aligned} AU_{n\times k} &= U_{n\times k}B + ub^T + R_{n\times k}, \text{ with } u = r_1, \\ A\hat{U}_{n\times m} &= \hat{U}_{n\times m}\hat{B} + \hat{u}\hat{b}^T + \hat{R}_{n\times m}. \end{aligned} \tag{5.47}$$

In theorem 5.8, we show that

$$\begin{aligned} AU^{new}_{n\times k} &= U^{new}_{n\times k}B^{new} + \hat{u}(b^{new})^T + R^{new}_{n\times k}, \\ \text{and } \|R^{new}_{n\times k}\| &\leq \|R_{n\times k}\|. \end{aligned} \tag{5.48}$$

However, in (5.47) the vector u is always taken as r_1. We get (5.48) with $\|R^{new}_{n\times k}\| \leq \|R_{n\times k}\|$ at the end of the cycle, but when we restart the next cycle, the vector u is changed from $\hat{u}$ in (5.48) to r_1. Therefore $\|R_{n\times k}\|$ for the next cycle is not the same as $\|R^{new}_{n\times k}\|$.

We observe from (5.48) that if the norm of the first column of $R^{new}_{n\times k}$ is much smaller than the norm of the first column of $\hat{u}(b^{new})^T$, then the direction of r_1 will be mostly determined by $\hat{u}$. In this case, there will not be much difference from (5.48) to (5.47). This is one possible reason that why when A is symmetric, stars do not get bigger than dots of the previous cycle in Figure 5.5.

Another difference between the symmetric and non-symmetric cases is that in Figure 5.8, we see a greater decrease of the near Krylov residual.

Figure 5.9 shows the residual norms of 10 approximate eigenvectors on the fine grid. We see that all eigenvectors are improved at the same time as we restart each cycle with the first eigenvector. There are no limits as we see in Figure 5.6.

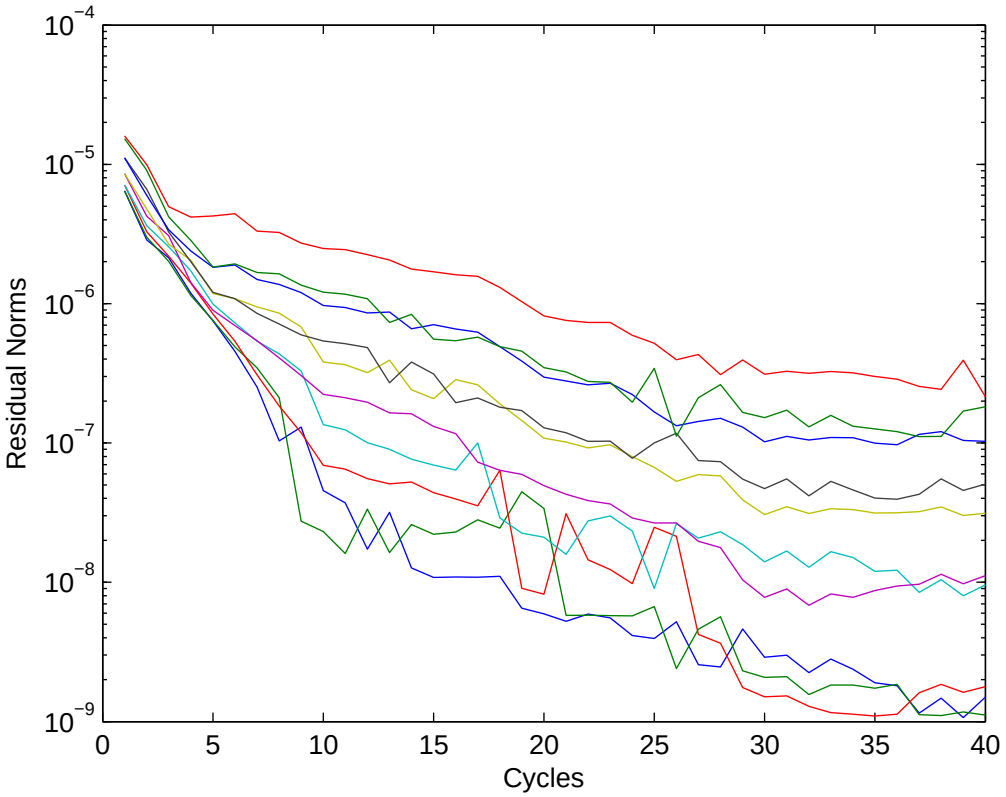

Figure 5.9: Near parallel helps convergence. A is non-symmetric. Starting vector is fixed as y_1.

In Figure 5.10, the line shows the convergence of the second eigenvector. Dots show the norm of f_2, and stars are norms of $\hat{f}_2$, which are defined below.

$$\begin{aligned} Ay_1 &= \theta_1 y_1 + a_1 r_1, \\ Ay_2 &= \theta_2 y_2 + a_2 r_1 + f_2 \\ &= \hat{\theta}_2 y_2 + \hat{a}_2 r_1 + \Sigma \alpha_i y_i + \hat{f}_2, \end{aligned}$$

where $f_2 \perp r_1$ and $\hat{f}_2 \perp span\{y_1, \cdots, y_k, r_1\}$.

The residual norm of y_2 is roughly determined by $\|\hat{f}_2\|$, which is compatible with the results of Theorem 5.10 and 5.11.

Figure 5.10 shows that when A is non-symmetric, f_2 and $\hat{f}_2$ can be very different. They are almost the same when A is symmetric, hence in Figure 5.7 we only

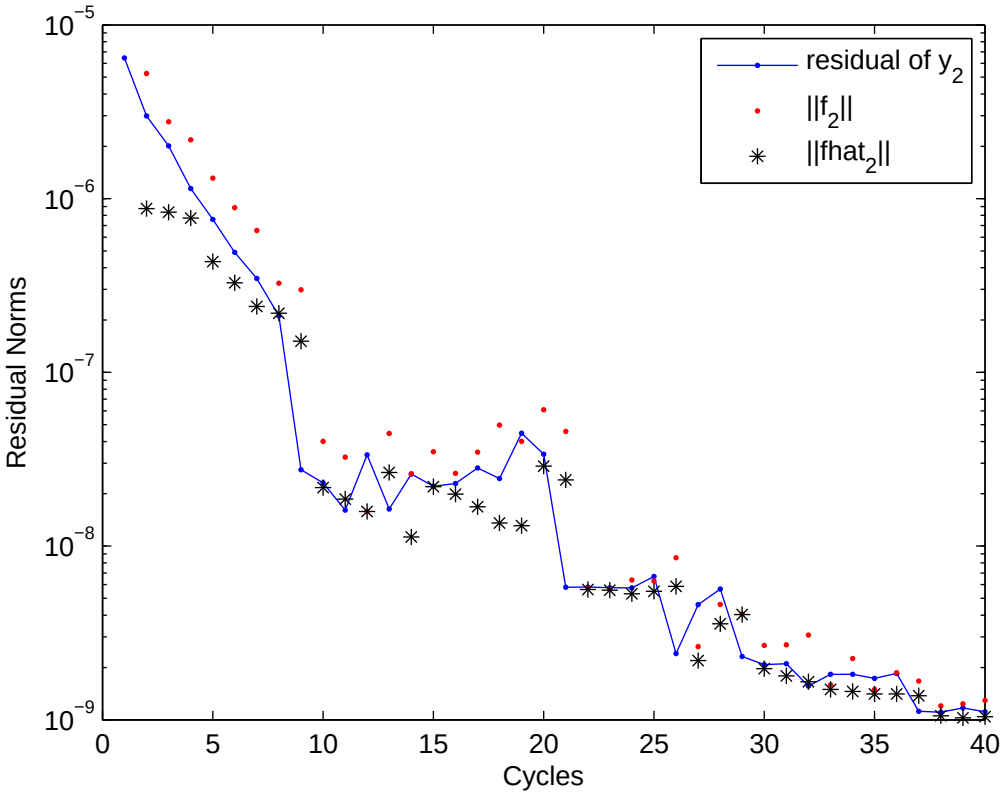

Figure 5.10: Near parallel helps convergence. A is non-symmetric. Starting vector is fixed as y_1.

plot $\|f_2\|$ at each cycle. But for non-symmetric case, the example shows that f_i have components in the subspace $\mathcal{S} = span\{y_1, y_2, \cdots, y_k\}$.

The norm of $\hat{f}_2$ decreases significantly unlike for f_2 in Figure 5.7. This results in the decrease of the Krylov residual, and hence it helps the convergence of eigenvectors.

5.7.2 Change the Starting Vector

In practice, we alternate through all desired Ritz vectors to speed up the convergence. The following experiment deals with the same problem in Example 5.12, but we change the starting vector at each cycle. We are interested in the near Krylov property and convergence behaviour.

Example 5.12 (continuing from p. 78). Problem: $-u'' = \lambda u$. Matrix size of A is 1023 on the fine grid, and the coarse grid is 255. We get accuracy of 1e-3 for the smallest 10 eigenpairs on the coarse grid. On the fine grid, we alternate through all desired approximate eigenvectors as starting vectors for Arnoldi-E.

Figure 5.11 shows the convergence of all desired eigenvectors.

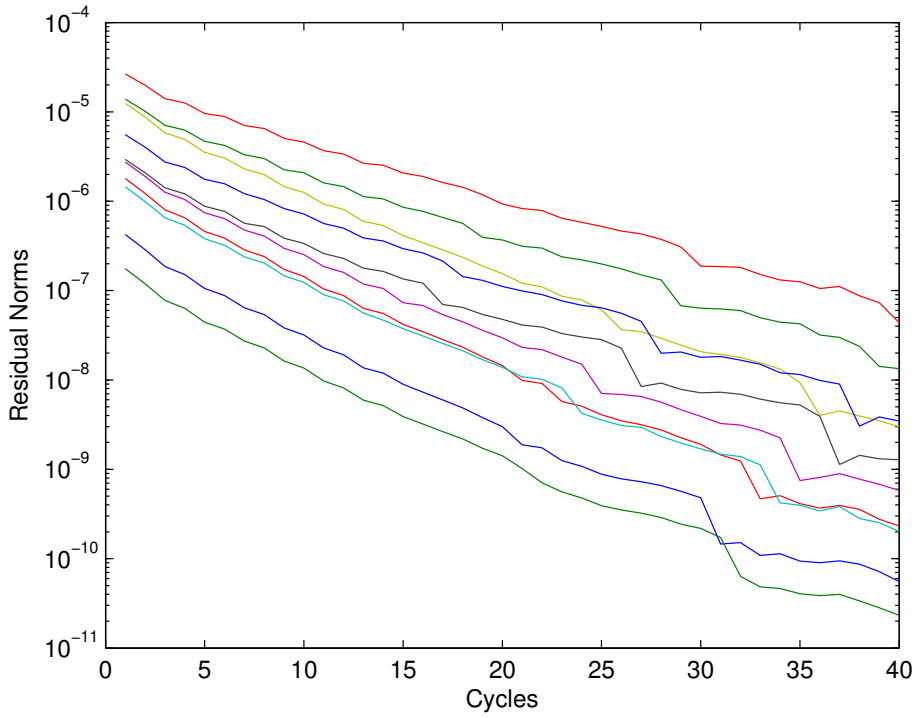

Figure 5.11: Near parallel helps convergence. A is symmetric. Alternate starting vectors.

Figure 5.12 shows the residual of the second vector and the norm of f_2, where f_2 is defined below. Suppose at cycle j, y_j is the starting vector, and

$$Ay_j = \theta_j y_j + a_j r_j,$$

$$Ay_2 = \theta_2 y_2 + a_2 r_j + f_2,$$

where $f_2 \perp r_j$.

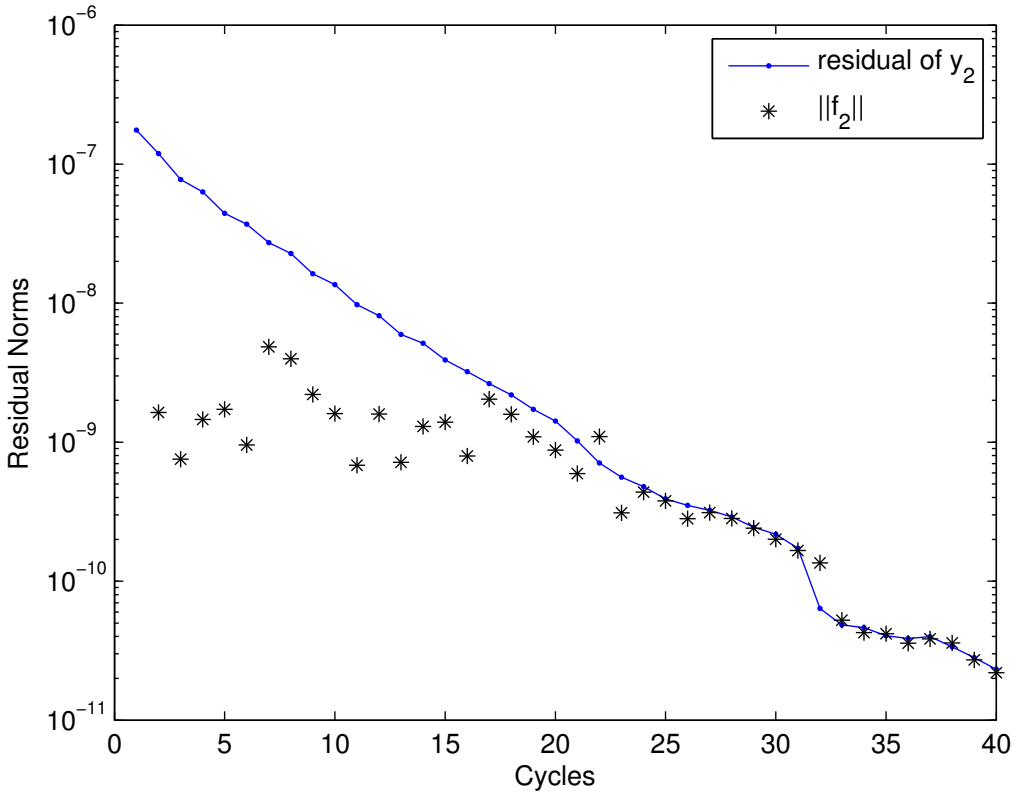

Figure 5.12: Near parallel helps convergence. A is symmetric. Alternate starting vector.

Compare Figure 5.12 with Figure 5.7, $\|f_2\|$ is changing all the time. Next is some analysis about it. Suppose after a cycle we have

$$Ay_j = \theta_j y_j + \gamma_j = \theta_j y_j + a_j u + f_j,$$
$$Ay_2 = \theta_2 y_2 + \gamma_2 = \theta_2 y_2 + a_2 u + f_2.$$

with f_2 and f_j small. Let y_j be the starting vector of the Krylov subspace portion for the next cycle. Then in fact we use the following parallel relation.

$$Ay_j = \theta_j y_j + \tilde{a}_j r,$$
$$Ay_2 = \theta_2 y_2 + \tilde{a}_2 r + \tilde{f}_2,$$
$$\text{where } \tilde{a}_j r = a_j u + f_j. \tag{5.49}$$

Equation (5.49) means that the vector r is the combination of u and f_j, then $\tilde{a}_2$ may decrease, since γ_2, the residual of y_2, may not be so parallel to r, and $\|\tilde{f}_2\|$ may increase. Although the stars jump up and down in Figure 5.12, Example 5.12 still shows that the approximate eigenvectors will converge to norms of $\|f_i\|$'s. Since all desired eigenvectors improve by alternating, $\|f_i\|$'s will decrease and hence residuals will converge.

CHAPTER SIX

Multiple Grids for Arnoldi

In this Chapter, we extend the Two-grid Arnoldi to Multiple-grid Arnoldi. We give the Algorithm and two examples.

As before, the problem size is n^f. We let p be the number of grid levels used, with grid level 1 being the coarsest and grid level p being the finest one corresponding to matrix size n^f. We now give the algorithm. Basically it is the Two-grid Arnoldi method, except we repeat Steps 2 and 3 for each of grid levels 2 through p, from second coarsest up to finest grid.

Algorithm 6.1 Multiple-Grids Arnoldi

0. Initial Setup: Let the problem size be n^f. Choose the grid levels. Let p be the number of grids ordered from coarsest to finest. Choose m = the maximum subspace size, k = the number of Ritz vectors retained at the restart, nev = the number of desired eigenpairs, $rtol$ = the residual norm tolerance.
1. Coarsest Grid Computation: Run restarted Arnoldi(m,k) on the coarsest grid until the nev smallest magnitude eigenvalues have converged to $rtol$.
2. For $grid\ level = 2 \ldots p$:
   A. Move to next finer grid: Move the k coarser grid Ritz vectors to the next finer grid (we use spline interpolation). Apply Rayleigh-Ritz procedure on the finer grid to these vectors. This gives the initial k finer grid approximate eigenvectors.
   B. Finer grid computation: Improve the approximate eigenvectors on the finer grid with the Arnoldi-E [18] method. As starting vector for the Krylov portion in the first cycle, we use the the Ritz vector correspond-

ing to the smallest Ritz value in magnitude. Then for starting vectors of subsequent cycles, we alternate through the nev smallest Ritz vectors. However, converged Ritz pairs are skipped.

In the examples that follow, we are in 1-D, and we let the decreasing sizes of the matrices be n^f, $\frac{n^f+1}{2} - 1$, $\frac{n^f+1}{2^2} - 1$, ..., $\frac{n^f+1}{2^p} - 1$. Other choices are possible, such as skipping some levels.

Example 6.1. We return to a matrix from the 1-D convection-diffusion equation, but now with convection of $\beta = 51.2$. The size is again $n^f = 4095$. Standard Arnoldi(30,15) takes 1574 cycles for 10 Ritz pairs to converge to residual norm below 10^{-8}. Table 6.1 has the results with different choices of coarsest grid and increasing the number of subintervals in the grid by a factor of 2 at each new phase. The Multiple-grid Arnoldi result with coarsest grid of 2047 uses only two grids, while with coarsest of 31, there are eight grid levels. The best Two-grid Arnoldi(30,15) result is 50.75 fine-grid-equivalent cycles with $n^c = 1023$. With Multiple-grid Arnoldi, we can get below 10 fine-grid-equivalents. So while Two-grid improves by a factor of 30 compared to regular Arnoldi, Multiple-grid is over 150 times better than regular Arnoldi. Here we are getting the significant speedup that is characteristic of multigrid methods for linear equations on problems with less convection. Multiple-grid Arnoldi also is very consistent for the choice of smallest matrix from size 31 up to 255. Two-grid is consistent for smallest matrix of size 255 up to 1023, but struggles with smaller ones.

We next give an example for which Multiple-Grid Arnoldi does not work as well.

Example 6.2. As in the previous example, we have a matrix from the 1-D convection-diffusion equation, but the convection is increased to $\beta = 102.4$ and the size of the matrix is reduced to $n^f = 1023$. We use Arnoldi(30,16) since the matrix is more

non-normal. Standard Arnoldi(30,16) takes 109 cycles for 10 Ritz pairs to converge to residual norm below 10^{-8}. Table 6.2 has the results with different choices of coarsest grid and increasing the number of subintervals in the grid by a factor of 2 at each new phase. Multiple-grid Arnoldi beats the two-grid on some of the choices, but not by as much as in the previous example. The important thing to note is that using too small of a coarsest grid can make things worse. For coarsest grid of size 31, the Multiple-grid method takes over twice as long as regular Arnoldi. The method is not as effective as in the previous example, because approximations from a coarse grid to the next are not as accurate with the increased convection. Also, there is not the same opportunity versus regular Arnoldi, because the finer grids are missing which are difficult for regular Arnoldi and for which approximations from the next coarser grid are particularly accurate.

Table 6.1: Two-grid Arnoldi vs. Multiple-grid Arnoldi. Matrix is dimension $n = 4095$ from 1-D Conv-diff with $\beta = 51.2$.

Coarsest grid matrix size	2047	1023	511	255	127	63	31
Two-grid Arnoldi cycle equiv's	227	50.8	56.4	55.7	108	728	514
Multiple-grid Arn. cycle equiv's	227	41.8	15.6	9.56	11.9	9.86	10.1

Table 6.2: Two-grid Arnoldi vs. Multiple-grid Arnoldi. Matrix is dimension $n = 1023$ from 1-D Conv-diff with $\beta = 102.4$.

Coarsest grid matrix size	511	255	127	63	31
Two-grid Arnoldi cycle equiv's	47	34.8	71.9	73.6	513
Multiple-grid Arnoldi cycle equiv's	47	39.8	55.9	72.1	264

CHAPTER SEVEN

Future Work

In order to improve multigrid Arnoldi methods both experimentally and theoretically, we have things to do in the future.

1 We have explored Multiple-grid Arnoldi in Chapter Six, but more work needs to be done. Especially needed are more experiments to determine when multiple grids are worthwhile and how many grids levels work best.

2 One challenge for the method is to reduce the Krylov residual when we apply Arnoldi-E on the fine grid. Combing all Ritz vectors into one starting vector and generating a Krylov subspace is one idea. This eliminates the Krylov residual. It may also be easier to extend the method on more grids by constructing a single vector on each grid. Then the most important question is how to form such vector in a robust and cheap way because there are stability issues. There may be other approaches to reducing the Krylov residual.

3 More research about highly non-symmetric matrices is needed. Such matrices are derived from convection-diffusion equations with big convection coefficients. Our method works well for such problems compared to some other methods in our experiments, but more general theory needs to be developed. Multigrid Arnoldi should be tested on finite element problems. Often a generalized eigenvalue problem needs to be solved.

4 We need to work on understanding the effectiveness of splitting complex Ritz vectors into real and imaginary parts as starting vectors.

5 We plan to adapt the methods in this work for deflating eigenvalues in the solution of large systems of linear equations.

6 Development of an algebraic multigrid version would significantly extend the applicability of Multigrid Arnoldi.

BIBLIOGRAPHY

[1] D. Arnoldi, *Lecture notes on numerical analysis of partial differential equations,* University of Minnesota (2011).

[2] W. E. Arnoldi, *The principle of minimized iterations in the solution of the matrix eigenvalue problem,* Quarterly of Applied Mathematics, volume 9, pages 1729, (1951).

[3] A. Brandt, *Multi-level adaptive solutions to boundary-value problems,* Mathematics of Computation 31.138 (1977): 333-90.

[4] R. P. Fedorenko, *The speed of convergence of one iterative process,* USSR Computational Mathematics and Mathematical Physics 4.3 (1964): 227-35.

[5] E. Anderson, Z. Bai, C. Bischof, S. Blackford, J. Demmel, J. Dongarra, J. Du Croz, A. Greenbaum, S. Hammarling, A. McKenney, D. Sorensen, *Lapack User's Guide,(Third ed.),* Philadelphia, PA: Society for Industrial and Applied Mathematics. ISBN 0-89871-447-8.

[6] J. W. Demmel, *Numerical Linear Algebra,* (1993).

[7] W. L. Briggs, V. E. Henson, and S. F. McCormick, *A multigrid tutorial,* SIAM. Philadelphia, PA (2000).

[8] Jasper van den Eshof and Gerard LG Sleijpen, *Inexact Krylov subspace methods for linear systems,* SIAM Journal on Matrix Analysis and Applications 26.1 (2005; 2004): 125-53.

[9] G. H. Golub and C. F. Van Loan, *Matrix Computations,* Johns Hopkins, second edition (1989)

[10] G. H. Golub, Z. Zhang and H. Zha, *Large sparse symmetric eigencalue problems with homogeneous linear constraints: the lanczos process with inner-outer iterations,* Linear Algebra Appl., 309 (2000), pp.289-306

[11] Douglas R. Hundley, *Cubic Splines and Matlab, course notes,* Whitman College (2009)

[12] N. J. Higham, *Functions of Matrices: Theory and Computation,* SIAM, Philadelphia (2008).

[13] T. Kato, *Perturbation Theory for Linear Operators,* 2nd ed., Springer-Verlag, Berlin, 1980.

[14] C. Lanczos, *an iteration method for the solution of the eigenvalue problem of linear differential and integral operators,* journal of research of the national bureau of standards 45.4 (1950): 255-82.

[15] R. B. Lehoucq, *Analysis and implementation of an implicitly restarted Arnoldi iteratio,* Ph.D, thesis, Rice University, Houston, TX (1995).

[16] R. B. Lehoucq, D. C. Sorensen, C. Yang, *ARPACK Users Guide: Solution of Large-Scale Eigenvalue Problems with Implicitly Restarted Arnoldi Methods,* Philadelphia: SIAM. ISBN 978-0-89871-407-4.

[17] R. B. Morgan, *Computing interior eigenvalues of large matrices*, Linear Algebra Appl. (1991): 154-156:289-309.

[18] R. B. Morgan, *On restarting the Arnoldi method for large nonsymmetric eigenvalue problems*, Mathematics of Computation of the American Mathematical Society 65.215 (1996): 1213-30.

[19] R. B. Morgan, M. Zeng, *Harmonic projection methods for large non-symmetric eigenvalue problems,* Numerical Linear Algebra with Applications 5.1 (1998): 33-55.

[20] R. B. Morgan, M. Zeng, *A harmonic restarted Arnoldi algorithm for calculating eigenvalues and determining multiplicity,* Linear Algebra Appl (2006): 415:96-113

[21] R. B. Morgan, *Implicitly restarted GMREs and Arnoldi methods for nonsymmetric systems of equations,* SIAM Journal on Matrix Analysis and Applications 21.4 (2000): 1112-35.

[22] K. Neymeyr, *Solving mesh eigenproblems with multigrid efficiency,* Numerical Methods for Scientific Computing. Variational problems and applications. CIMNE, Barcelona (2003).

[23] C. C. Paige, B. N. Parlett, and H. A. van der Vorst, *Approximate solutions and eigenvalue bounds from Krylov subspaces,* Num. Lin. Alg. with Appl. (1995): 2:115-133.

[24] B. Parlett, *The symmetric eigenvalue problems,* Prentice-Hall, Englewood Cliffs, NJ (1980).

[25] D. C. Sorensen, *Implicit application of polynomial filters in a k-step Arnoldi method,* SIAM Journal on Matrix Analysis and Applications 13.1 (1992): 357-85.

[26] G. W. Stewart, *A Krylov-Schur Algorithm for large eigenproblems,* SIAM Journal on Matrix Analysis and Applications 23.3 (2002): 601-14.

[27] G. W. Stewart, *Backward error bounds for approximate Krylov subspaces,* Linear Algebra and Its Applications 340.1 (2002): 81-6.

[28] J. A. Sifusentes, M. Embree, and R. B. Morgan, *Gmres convergence for perturbed coefficient matrices, with application to approximate deflation preconditioning,* SIAM Journal on Matrix Analysis and Applications 34.3 (2013): 1066-88.

[29] Y. Saad, *Numerical methods for large eigenvalue problems,* SIAM, Philadelpha, PA (2011).

[30] Y. Saad, *Iterative methods for sparse linear systems,* PWS Publishing, Boston, MA (1996).

[31] V. Simoncini and D. B. Szyld, *Theory of inexact Krylov subspace methods and applications to scientific computing,* SIAM Journal on Scientific Computing 25.2 (2003): 454-77.

[32] J. Xu and A. Zhou, *A two-grid discretization scheme for eigenvalue problems,* Mathematics of Computation of the American Mathematical Society 70.233 (2001; 1999): 17-25.

[33] D. S. Watkins, *The Matrix Eigenvalue Problem; GR and Krylov Subspace Methods,* 32 Vol. Portland: Ringgold Inc (2008).